Southampton Solent University

School of Maritime Science and Engineering

BEng (Hons) Yacht & Powercraft Design

Marin Lauber

PRELIMINARY DESIGN OF A MINI 6.50 WITH A FOIL CFD INVESTIGATION

May 2017

This project is submitted in part fulfilment of the Degree of

Bachelor of Engineering with Honours in Yacht & Powercraft Design

Southampton Solent University

May 2017

This Page Intentionally Left Blank

Acknowledgements

I wish to express my sincere gratitude to all the people who helped, one way of another, to the fulfilment of this project.

I would like to express my deepest gratitude to my project supervisor, Jean-Baptiste R. G. Souppez for his excellent guidance throughout this project and his many valuable advices.

I would like to thank Jonathan Ridley for helping me with the CFD part of this project and for running my cases on his personal computer. I would like to thank Yves Courvoisier, Giorgio Provinciali, Paolo Motta and the rest of the Hydros team for providing me with their VPP software and for helping me to run the cases. I would also like to tank Giles Barkley, course leader of Yacht and Powercraft Design for letting me use the University's towing tank.

I would like to thank Simon Koster for the information he provided me about the building, design and sailing aspect of his Mini 6.50. I would also like to thanks Nicolas Groux for his information about the sails and the interest he showed in my project.

Finally, I would like to thank all my friends who help me during this project, especially Otto Villani, Aladin Montel, Joan Civera, Bryan Matiba for their help in the towing tank and Christelle Rochat for the proof reading, any mistake however remains my entire responsibility.

This Page Intentionally Left Blank

Abstract

The aim of this project is to produce the preliminary design of a prototype Mini 6.50 taking full advantage of the latest changes in the rule allowing for foils to be used. A towing tank procedure was undertaken to assess the resistance of a scow hull shape and was compared to resistance of a standard hull shape obtained using the Delft systematic yacht series regression method. A first principle approach as well as an advanced velocity prediction program were used to finalise the choice of hull shape which favoured the scow hull shape. A basic computational fluid dynamic approach was used to select a suitable foil section and analyse different foil geometry. Structural and stability calculation were developed and checked against common classification society rules. This resulted in the forthcoming preliminary design report.

This Page Intentionally Left Blank

Table of Contents

List of Figures

List of Equations

List of Tables

Nomenclature

Through this report and drawings, the following abbreviation will be used:

Abbreviation	Description	Units
L_{WL}	Length waterline	m
L_{OA}	Length overall	m
B_{WL}	Beam waterline	m
B_{OA}	Beam overall	m
Δ	Displacement	kg
∇	Volume displaced	m^3
AWP	Area waterplane	m^2
C_P	Prismatic coefficient	-
LCB	Longitudinal centre of buoyancy	-
LCF	Longitudinal centre of flotation	-
GM	Metacentric height	m
GZ	Righting arm	m
RM	Righting moment	Nm
HM	Heeling moment	Nm
TWA	True wind angle	degrees
TWS	True wind speed	Knots
CLR	Centre of lateral resistance	-
CE	Centre of effort	-
ε_a	Aerodynamic drag angle	Degrees
ε_h	Hydrodynamic drag angle	Degrees
F_X	Force on the X axis, drag	N
F_Y	Force on the Y axis, sideforce	N
F_Z	Force on the Z axis, lift	N
M_X	Moment about the X axis, righting moment	Nm
M_Y	Moment about the Y axis, pitching moment	Nm
M_Z	Moment about the Z axis, yawing moment	Nm
Re	Reynold’s number	-
Fn	Froude number	-
ρ	Density	Kg/m^3
μ	Dynamic viscosity	$kg/(s \cdot m)$
σ	Direct stress	N/m^2
E	Modulus of elasticity	N/m^2
G	Modulus of rigidity	N/m^2
ε	Poison’s ratio	-
τ	Shear stress	N/m^2
ψ	Fibre weight fraction	-
φ	Fibre volume fraction	-
AoA	Angle of attack	Degrees
Amps	Amperes	A
AR_G	Geometric aspect ratio	-
C_L	Lift coefficient	-
C_D	Drag coefficient	-
C_{Di}	Induced drag coefficient	-
C_V	Viscous drag coefficient	-
v, U	Velocity	m/s
Oz	Ounce per sailmaker yard	Oz
1E6	$1*10^6$=1’000’000 (1 million)	-

This Page Intentionally Left Blank

1. Introduction

"The Mini Rules are designed to encourage offshore racing on small, moderately-priced monohull racing boats with short-handed crews. The rules are intended to promote the research and development of security and performance of these sailboats in offshore racing." (Mini, 2017).

This project aims to produce the preliminary design of a prototype Mini 6.50 with emphasis on the performance aspect of the design. Therefore, a computational fluid dynamic investigation of the foils will be performed. The design process will follow the basic design spiral but will adapt it to the requirements of a racing yacht to finally produce the intended preliminary design.

In the past years, the Mini 6.50 class has been a laboratory for most of the innovations present nowadays on offshore racing yachts. This freedom in the design comes from very simple rules. The length, beam, draft, air draft are fixed but other than this the designer has the right to create whatever he wants in this box. More recently, with the arrival of the scow bow, the class has been yet again the source of interesting designs. The last evolution of the rules allows even more freedom to the appendages by allowing them to extend outside of the maximum beam once the starting line has been crossed. The later described project will focus on the latest innovation of the class, the scow bow hull shape and foils. It will try to bring an answer to the gains obtained on foiling yachts compared to non-foiling designs. This will be done by the mean of velocity prediction program (VPP) and a computational fluid dynamic (CFD) analysis of the foils.

The foil arrangement will be inspired of what has been done in one of the major classes of offshore racing yachts: the IMOCA with their so-called Dali moustache foils, in reference to the shape of the famous painter's moustache.

Particular attention will be put on the structural design of the yacht as well as its stability as this yacht could end up facing severe conditions during the Transat. A preliminary scantling calculation was undertaken against the ISO 12215-5 scantling rule with a special regard to the overall weight.

The conclusion will try to underline areas of the project which seem to require more work before the boat could reach a more advanced design phase as well as proposing a critical analysis of the work undertaken.

2. Design Brief

The aim of this project is to produce the preliminary design of a Mini 6.50 prototype class yacht. The yacht will be design to race the Mini circuit with a focus on the Mini Transat, which occurs every two years (2017 and 2019). The two next editions will start in La Rochelle, stop in Las Palmas before crossing to Le Marin, Martinique. The boat will be designed with this race in mind, and especially the second leg of the Transat.

The objective of this preliminary design is to produce a boat which would be able to win this Transat. This project will not try to fit in any pre-defined budget or use any alternative construction materials or methods. The choice of the materials will therefore be governed only by the Mini 6.50 rules and their mechanical properties. The seaworthiness and the structural integrity of the vessel will also be of first concern.

2.1. Rules and Regulations

The major rule to what this design needs to comply to is the Mini 6.50 class rule. This box rule, is relatively open and gives a lot of freedom to the designer in terms of hull shape, appendages configuration, sail plan, etc. It defines the major dimensions of the boat but also refers to other rules and regulations that the yacht must comply to to be accepted in the class. These additional rules are:

- Racing Rules of Sailing (RRS, 2017)
- Offshore Special Regulations (OSR, 2017)
- Equipment Rules of Sailing (ERS, 2017)
- ISO 12215 for design category C
- ISO 12217 for design category C

These five additional rules, which are all derived of requirements of the Mini 6.50 class rule, bring requirements in terms of mandatory safety equipment, structural design of the yacht, stability regulations, man overboard prevention, etc.

Throughout the project, effort will be made to check the yacht against the major requirements. But because of the preliminary nature of this work, some of them will be intentionally omitted.

3. Parametric Study

The parametric undertaken for this project focused on winning designs of the last editions of the Transat and on designs which seems of interest to the author. Because these parameters are closely linked to the performance of the yacht, it can be difficult to find information which matches between the different sources. In addition to the major dimensions of the boat, the parametric study was also used to collect information about the different sail sets used on the yachts and, when available, the different structural arrangements.

3.1. Design Dimensions

3.1.1. Displacement

In terms of displacement, all the boats are within 50 kilograms of each other (lightship displacement), which usually comes from the difference in the weight of the keel. As the displacement is key in performance, the boats are pushed to be as light as possible, the large angle stability test of the Mini 6.50 rule being the limiting factor for the weight of the bulb, which represents a fair amount of the total weight.

3.1.2. Beam

With the maximum beam overall (B_{OA}) being 3 meters, as imposed by the class rule, there is very few, to none advantages to go for less than the maximum because of the small angle stability test, which required a certain waterline beam to pass the maximum value of angle of list (10°). There are however differences in the waterline beam for the boats which are lighter. Refer to Appendix A for the full parametric study.

3.1.3. Length

The following figure shows the variation in sail area displacement ratio for different waterline lengths. It is interesting to note that even if the waterline length changes between the boats, the sail area displacement ratio stays very similar. This can be explained because the sail area is maximised and the weight is kept to a minimum on all the studied designs.

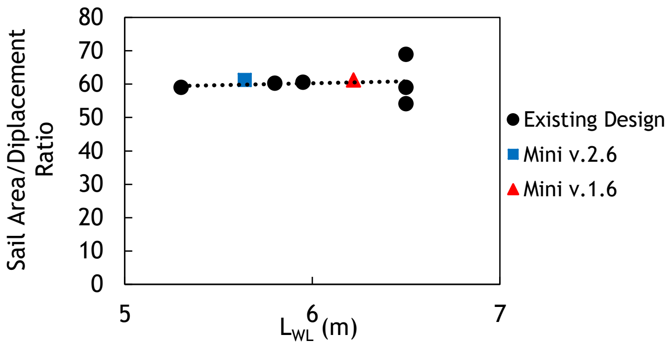

Figure 1: Sail area displacement ratio for different waterline length.

3.1.4. Sail Area and Sail Plan

The only limitation in the sail design being the number allowed on board for the Transat, the sail area varies between the different designs. A tendency can be seen for the heavier boats to have more sail area, at least upwind, but for the downwind sail area, all are within the same values. The following table shows a typical sail set and sail area for a Mini 6.50 prototype.

Table 1: Sail set and sail area for a Mini 6.50.

Sail	*Area (m^2)*	*Features*
Main	27-32	3-4 Reefs
Jib	18-20	1 Reef
Storm Jib	4-2.5	Mandatory, 1 Reef
Gennaker	22-35	Upwind
Light Kite	~90	
Medium Kite	~75	
Code 5	~45	1 Reef

3.2. Weather Study

To determine the typical sailing condition the yacht will encounter during the race, a weather study was performed. The Mini Transat being a transatlantic crossing, at a period of the year where the weather systems are well known and have been recorded for many years, defining the typical weather conditions is somewhat facilitated.

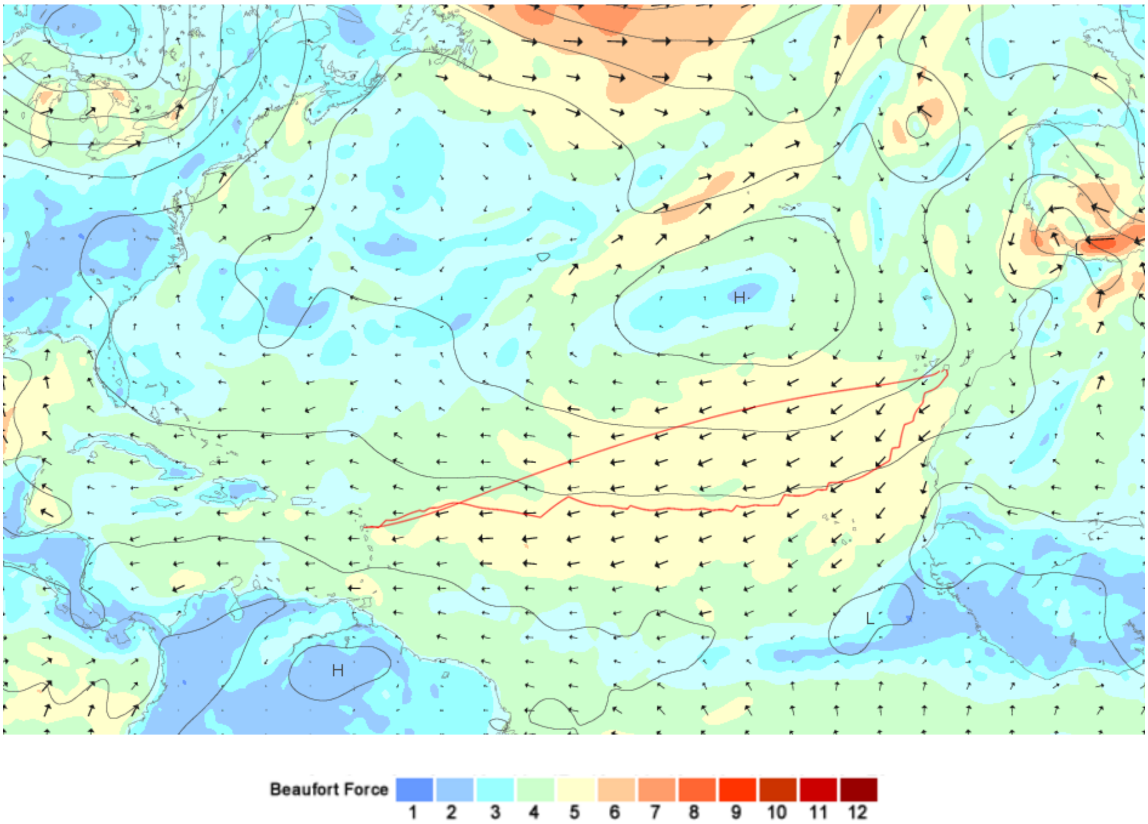

Figure 2: Atlantic Ocean on the 1st of November 2015 (Magicseaweed, 2016).

Figure 2 shows a typical Atlantic Ocean weather situation in early November, date of the start of the second leg of the 2015 edition of the Mini Transat. With the Azores high quite active, the trade winds are encouraged to settle in the south of this high pressure providing the typical Atlantic crossing conditions. By interpolating the track of the winner of this edition of the race on this weather map, it starts to be clear that the weather which will be faced during the crossing is most likely to be downwind, with true wind angles (TWA) between 120-150° and typical true wind speeds (TWS) of 12-18 knots. One can also note that, even if this is not represented on the map, the weather for the first leg will be similar, at least in terms of TWA.

This will be the conditions for what the yacht will be optimised in terms of hull shape, appendages configuration and sail plan.

4. Preliminary Weight Estimate

This project being aimed to design a racing yacht, weight is critical, especially as there is now weight limit in the rules. Early in the design spiral, a detailed weight estimate was performed to find the target design displacement. It was performed using the research done in the parametric study and known data about existing yachts for the scantlings.

Consumables were calculated for a race duration of 15 days, with 3.5 litres of water per person per day, resulting in a total of 52.5 litres, which was rounded up to 60 litres. Food was included based on the weight of freeze dried food for the duration of the second leg. Care was taken to have a precise weight estimate by including the clothes, the weight of the skipper, etc. Different margins were used depending on the confidence the author had on the various weights.

To define the design displacement, an average of the weight of the boat at the start and at the end of the Transat was calculated. This resulted in a design displacement of 960 kg. The breakdown of the weight of the boat can be seen on the following table:

Table 2: Preliminary weight estimate.

Preliminary Weight Estimate	
Item	Weight (kg)
Group 1- Hull, Deck & Appendages	583.00
Group 2- Mast & Sails	86.14
Group 3- Deck Hardware & Running Rigging	17.23
Group 4- Navigation/Communication & Power	10.36
Group 5- Safety Equipment	126.99
Group 7- Other & Consumables	165.29
Total with Margin (Transat Start)	989.00
Total with Margin (Transat Finish)	936.00
Design Displacement (Average Transat)	962.50

This weight estimate was refined during the design process each time a new element was defined in terms of weight and position in the boat.

The hull and structure being the major contributors to the weight of the yacht, the easiest way to decrease the total displacement is to reduce the weight of either the structure or the bulb.

The weight estimate was adapted to the loading conditions required for the stability test. Following this, a preliminary stability check was performed for each hull shape to get a feel of how close to the requirements each hull was. This basic study showed that the waterline beam is the most important factor to pass the stability test.

Refer to Appendix B for a full break down of the weight estimate.

5. Hull Design

They are many parameters which must be taken into consideration when designing a hull shape. The following will describe the choices undertaken for the major ones and the specificity of the different hull shapes which will be compared: scow bow and standard.

5.1. Prismatic Coefficient

The prismatic coefficient defines the distribution of the volume along the hull length. It has major influence on the performance of the yacht, especially downwind, where wave drag will represent the major component of the resistance. Graph of the optimum prismatic coefficient against Froude number can be found in (Fossati, 2009). For Froude number, above 0.35, which normally correspond to an upwind speed for a sailing yacht, the recommended value is around 0.55. For higher values, the prismatic coefficient increases up to 0.6.

With the usual hull shape of Mini 6.50 being very wide and flat, and because the boats are primarily design to sail downwind, at high Froude number, high prismatic coefficient values are usually preferred. A target design prismatic coefficient of around 0.6 was chosen.

5.2. Beam Waterline

The beam waterline has a direct influence on the wetted surface area and therefore the viscous resistance. A balance must be found between the wetted surface area and the righting moment. This ratio can be optimised by the addition of a chine on the side of the hull, which will have the effect of shifting the centre of buoyancy rapidly athwartships and therefore rapidly increasing the righting moment while reducing the wetted surface area by introducing deeper sections in the water. The chine will also add some directional stability to the boat and remove the load on the rudder.

Another consideration of the beam waterline is the small angle stability. By reducing it, the weight of the bulb must also be reduced, which is not a bad thing as it will reduce the overall weight of the boat. This can be done up to the point where the large angle stability test cannot be passed anymore. A balance needs to be found for these requirements. A quick hand calculation can be done to find the minimum required metacentric height (GM) for the yacht:

$$GM = \frac{m \times d}{\sin(10°) \times \Delta}$$

Equation 1: Required metacentric height.

This equation has the advantage of taking into account only the transverse shift of the centre of gravity. In this case, the keel has been assumed to weigh 300 kg, with a centre of gravity 1.8 m below waterline and the ballast is assumed to feature the maximum 200 kg offset of 1 m off the centreline. The resulting minimum GM to pass the angle of list is 2.71 m. This was not expressed as a required B_{WL} because the two different hull shapes will feature different L_{WL}, which is also a variable of the metacentric height.

5.3. Longitudinal Centre of Buoyancy

The longitudinal centre of buoyancy (LCB) defines the position of the centre of the immersed volume. For beating upwind, at low speed it should be at 3% of L_{WL} behind midship (L. Larson, R. E. Eliasson, M. Orych, 2014) but for downwind, at high speed it should be moved aft to 6-8%

of L_{WL}. On normal sailing yacht this is hard to achieve because it requires a large transom which is not compatible with the required upwind LCB. Luckily on a small and light boat like this, it can be dynamically adjusted by stacking weights on the boat and by filling the water ballast.

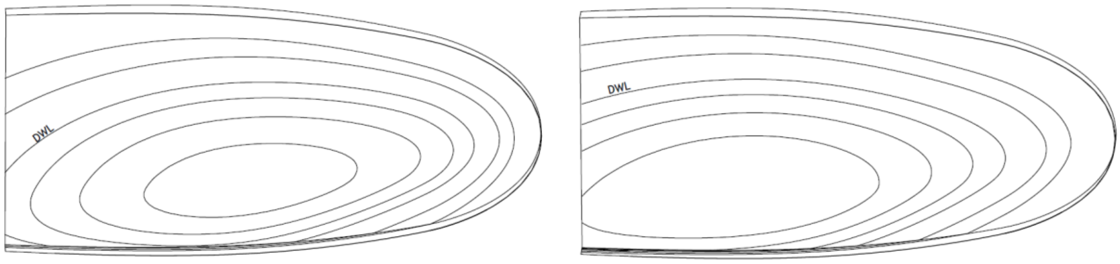

Figure 3: Heeled waterlines (10°) for the un-ballasted and ballasted case.

The yacht will therefore be designed with the LCB at around 3% of L_{WL} aft of midship to optimise upwind performance while the ballast tank and stacking will be used to virtually shift it backwards for downwind sailing. Trimming the boat on its transom will also have the desirable effect of straightening the waterlines as the transom is immersed, thus reducing the pressure gradient and the wave drag (See Figure 2). Immersing the transom will also increase the dynamic waterline when sailing at high speed. It will also move the centre of lateral resistance of the hull back, which should unload the rudder.

5.4. Heeled Properties

All the aforementioned hull design parameters are not only valid in the upright case but also in heeled conditions. According to (Verdier, 2015) it is also very important that: "*the centre of the section area curve doesn't invert itself when heeled*". This usually happens with boats which have a very squeezed bow (beaver tail shape) and this results in an increase in wetted surface area without an increase in righting moment, which doesn't help improve the performances. To avoid this, the bow sections have to be made fuller.

Since the yacht is equipped with foils, the bow down trim when heeled will affect the performance. This bow down trim will be increased by the sail trimming moment. For the scow bow hull with the important volume forward this should not be a problem but, for the standard hull shape, this could be an issue.

5.5. Scow Bow Hull

Refer to drawing: Lines Plan v2.6

Once the basic design parameters had been defined, the design process of the scow hull shape took place. It was decided to use a chine as an effective mean of increasing the righting moment/wetted surface area ratio when heeled. To do so, the chine must be lowered in the aft part of the hull while kept at a sensible height in the forward region, where the typical rounded hull shape will be present. Immersing the transom would mean an increase in wetted surface area in the upright condition, although being beneficial at high speed, it heavily penalises the yacht in light airs. While efforts were made to try to accommodate the desired LCB position without immersing the transom too much, the resulting LCB position is almost on midship. Obviously, the increased volume in the bow will shift the LCB forward and tends to balance it at midship since the canoe body is almost symmetrical about this point.

The position of the LCB may not be as crucial on a scow bow hull shape, and the absence of research led to the decision to carry on with this LCB.

To accommodate the foils alongside the topside, the maximum beam of the yacht must be located aft of midship, which inevitably shifts the maximum waterline beam aft. The design target for the prismatic coefficient of 0.6 could be respected without too much adjustments required, albeit featuring a lower prismatic coefficient may have caused some issues.

Because of the particular shape of the bow, the waterline length was not considered as one of the driving design parameters but was kept to a sensible value while being reduced compared to a standard hull shape.

5.6. Standard Hull

Refer to drawing: Lines Plan v1.6

As stated before, heeled sectional area is important for the performance of the yacht. To avoid designing a yacht with a beaver tail bow, it was decided to add volume in the bow of the standard hull shape, as it is the trend nowadays on Pogo 3 (Verdier) and Ofcet 6.50 (Betrand). Again, the chine was kept all the way around the boat but this time it is risen in the aft section and lowered in the front to lower the volume as much as possible. This will also help to introduce volume early when the boat is heeled, which will help keeping the section area curves straight in this bow (see 5.4.).

The maximum beam is also located aft of midship to accommodate the foils but this time, because the chine is risen in the aft part, the maximum beam waterline is located at midship. With this more usual hull shape, the chosen LCB position could be respected without too much difficulties, however, this still requires the transom to be immersed.

It is interesting to note that the wetted surface area of both the scow hull shape and this hull shape are not very different, because of the low length beam ratio and the similar volume repartition, one could expect this result.

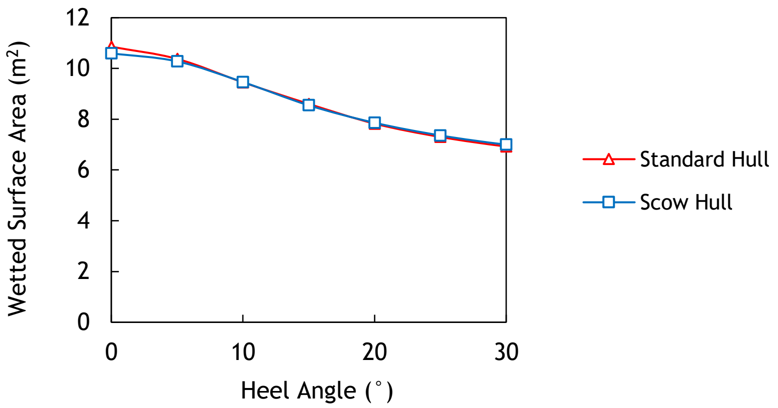

Figure 4: Wetted surface area for different heel angles.

5.7. Sheer Line and Profile

With the Mini 6.50 Rules limiting the average minimum freeboard to 0.75 meters and the need of more freeboard at midship to help pass the 90° stability test, an inverted freeboard design was chosen. Care was taken to minimise the freeboard to pass the two requirements by the smallest margin. This enables the deck to be kept as low as possible thus lowering the vertical centre of gravity as well as reducing the amount of materials used in the boat. The mast also finds itself lower on the deck, which results in more sail area and a lower centre of effort.

Having an inverted sheer line also gives a bit more room inside the yacht, especially at midship, where the skipper will spend most of his time downstairs. The inverted sheer line also gives a more modern look to the yacht even if this was not a criteria.

5.8. Dallenbaugh Angle

Dallenbaugh angle is a measure of how much a yacht heels under the action of a certain wind pressure. It doesn't give the actual heel the yacht will experience as it doesn't account for the reduction in heeling moment due to the sails being inclined. It can be used to compare different designs when the basic upright hydrostatic characteristics are known. Even if this measure of the stiffness or tenderness of a sailing yacht is crude, it was calculated during the preliminary design phase. It is important to note that this doesn't account for the canting keel, water ballast and foils, which will increase the righting moment.

$$Dallenbaugh\ Angle = \frac{279 \times Sail\ Area \times Heeling\ Arm}{\Delta \times \mathrm{GM}}$$

Equation 2: Dallenbaugh angle equation.

The results for the two hull types, the scow hull and the standard hull are respectively:

- Scow: 18.27°
- Standard: 19.75°

6. Preliminary VPP

Velocity prediction programs (VPP) are used during the design process to evaluate and compare the performance of different types of hulls. They can also be used to study the changes of a parameter of the sail plan, or the appendages, to the performance of the yacht.

6.1. WinDesign VPP Results

A preliminary VPP hull comparison was performed using Wolfson's unit VPP program WinDesign 4. To better isolate the performance differences emanating from the hull shape, a standard appendages package was defined, including: a canting keel, a pair of daggerboards (to replicate the sideforce and drag of the tip of the foil) and twin rudders. To simplify the set-up of all the hulls, three conditions will be considered for the canting keel: on the centreline, canted at 20 degrees and fully canted to 40 degrees. As the keel extension was not known at this stage of the design, it was neglected. A standard rig and sail plan were also used. The water ballasts were also ignored in this study.

The six boats were run on a course against a trial horse (v1.4). Based on the weather study, the race was divided in 12 legs and each leg was given a TWS and TWA. The following graph presents the results of this VPP comparison (see Appendix C for the full results):

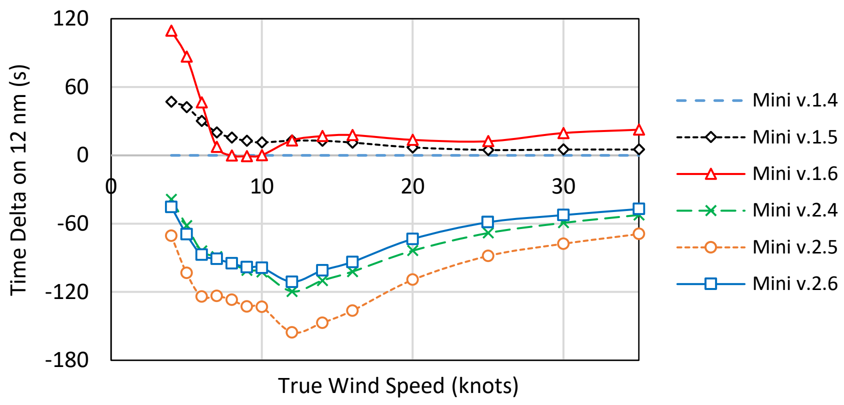

Figure 5: WinDesign VPP results for the different hull shapes. Positive means the yacht is faster than the trailhorse.

The v.1 of the yacht corresponds to the standard hull shape and the v.2 corresponds to the scow hull shapes. For the course considered, WinDesign fails to predict the expected performance increase of a scow over a standard hull shape.

An explanation of this perhaps lies in the hydrodynamic model of the VPP, which relies on regression methods to estimate the residuary resistance of the yacht. With the available models in the program based on old style hull shape where planing was not a major variable in the performance, or was simply not happening, the resistance is overestimated at high Froude number and the dependency on the waterline length, which the scow is lacking, results in a yacht performing poorly.

Examples are available in the literature comparing WinDesign prediction to actual polar measured on the boat. These data can be seen on figure 3. The red line interpolated on the graph is the VPP results for the scow bow hull shape, which is similar to the one presented but vastly differs to the measured one. Also, note that the sail plan used for this comparison features only three sails and not the full set.

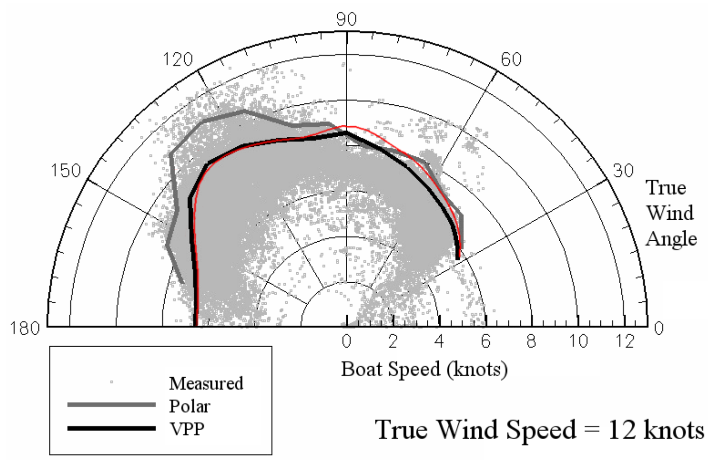

Figure 6: Mini 6.50 WinDesign VPP against measured data from (Raymond, 2009) with Mini v.2.6 ploted on top (red curve).

The major differences in these predictions to actual performances of the yacht led to the decision to compare the hull shape using a different approach.

With most of the other method used to predict hull performance such as ORC VPP or panel code being limited by the maximum speed and the scow not fitting in the Delft series because of a too small length/beam ratio, the only option left was to tank test the hull.

7. Hull Comparison

At this point of the project, the opportunity to use a Velocity Prediction Program more refined than WinDesign presented itself. As the author has interest in the prediction of performance of sailing yachts, it was decided to follow this path. The VPP itself was written by Giorgio Provinciali and belongs to Hydros Innovation (Hydros-Innovation, 2017) . This VPP program has the advantage of solving for the six degrees of freedom (DOF) as opposed to only three for WinDesign. The drawback of this is that a large amount of data is required to produce a good fitting of the resistance surface through the measured points. The results from the towing tank will thus be extended to three displacement, due to the need of having the immersion of the hull shape as a parameter for the resistance. The result of this VPP will however not be used as the primary mean of comparing the hull shapes as the small amount of data which will be collected doesn't guaranty any valuable results.

The primary mean of comparing the hull shape will be to assume that in a given sailing condition, the hulls will be sailing at the same righting moment. The resistance measured in the tank at certain heel and leeway angle will be compared to the resistance of the standard hull, at the same righting moment, estimated using a Delft spreadsheet written by the author.

7.1. Towing Tank Model

With towing speed as well as building weight in mind a scale of 1:5 was chosen for the model. This allows for a relatively big model, which is easier to build accurately and still permits measurable forces to be recorded. It was decided to test the model with the keel and the bulb to replicate the interaction drag of the keel with the hull. The foils were not included in this experiment because of two major reasons: first, building scaled foils is relatively difficult as they usually feature asymmetric sections which are concave and are therefore very difficult to replicate if not made in female moulds. The other reason is that the different foils geometry will be analysed using computational fluid dynamic and the final shape of the foil was therefore not known at this stage of the design. The following summarise the model dimensions:

Table 3: Towing tank model dimensions.

Tank Testing Model		
Scale	1/5	-
L_{WL}	1.128	m
B_{WL}	0.47	m
Displacement 100%	7.5	kg
Built Weight	3.75	kg

The model was laminated on a male foam plug of the hull milled by Southampton Solent University. It was coated with a layer of glass fibres and epoxy. Filler and paint were then applied to smoothen the surface. The keel fin was made of a balsa wood core laminated with carbon fibres to give it stiffness and prevent it from bending during the towing procedure. The bulb was built in wood and faired using the same technique as the hull.

7.2. Towing Tank Matrix

To determine the upright and heeled/yawed resistance of the yacht, a consequent number of runs had to be performed. They start by an assessment of the form factor of the yacht with low speed runs. Once these low speed runs were made, the test was carried on with increased speed to plot an upright resistance curve.

Once the upright resistance is known, the heeled and yawed resistance can be measured. The following table summarises the tank testing matrix performed. A breakdown of each run is presented in Appendix D.

Table 4: Tank testing matrix.

ID	Configuration	Test	Heel (°)	Fn	Description
M_100_1	100% Displacement	Upright Resistance	0	0.175-1	Basic resistance test & form factor investigation.
M_100_2		Heel with yaw	5	0.55-1	Change of leeway for the hull with the Keel and Bulb.
M_100_3		Heel with yaw	10	0.55-1	
M_100_4		Heel with yaw	15	0.55-1	
M_75_1	75% Displacement	Upright Resistance	0	0.175-1	Basic resistance test & form factor investigation.
M_75_2		Heel with yaw	5	0.55-1	Change of leeway for the hull with the Keel and Bulb.
M_75_3		Heel with yaw	10	0.55-1	
M_75_4		Heel with yaw	15	0.55-1	
M_50_1	50% Displacement	Upright Resistance	0	0.175-1	Basic resistance test & form factor investigation.
M_50_2		Heel with yaw	5	0.55-1	Change of leeway for the hull with the Keel and Bulb.
M_50_3		Heel with yaw	10	0.55-1	
M_50_4		Heel with yaw	15	0.55-1	

The form factor will be determined for each displacement in the upright condition. This value may differ from the actual heeled form factor but even if the model was tested at the particular heel without any sideforce (by changing the yaw angle until no sideforce is produced), we cannot be sure that this is not the result of a balance of the sideforce distribution along the hull which sums up to zero, which will mean that the induced drag is not zero (J. A: Keuning, U.B. Sonnenberg, n.d.). Another consideration is that at high speed, the form factor doesn't have as much influence as at low speed, especially for planing yachts. The following shows the Prohaska plot for the 100% and 80% displacement conditions:

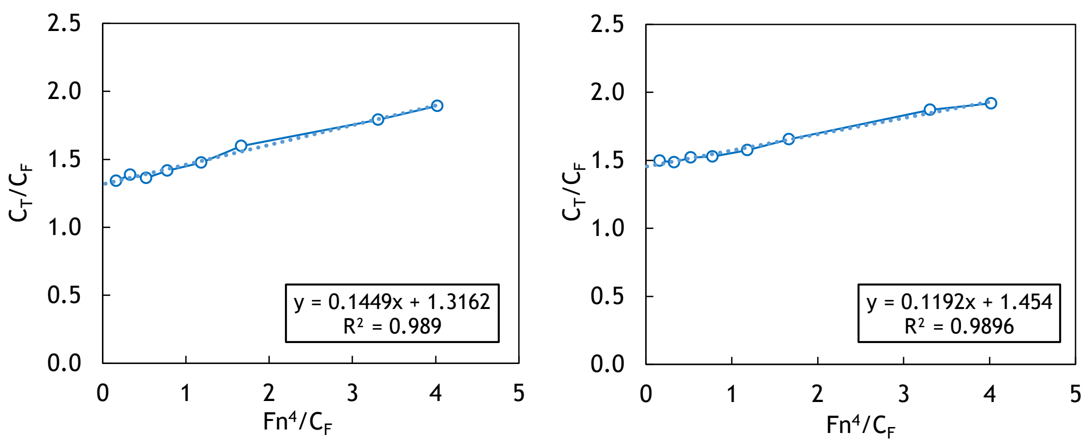

Figure 7: Prohaska plot for the 100% and 80% displacement.

Because the yacht was tested with the keel, the form factor is greatly increased when the displacement is changed.

7.3. Results Analysis

Even if the scow hull shape doesn't fit in the Delft systematic series, a basic upright resistance comparison was performed. This in shown on the following graph:

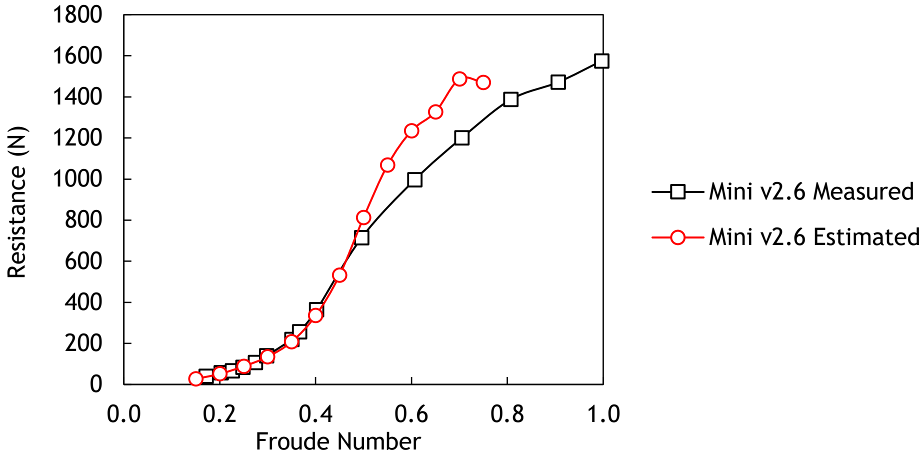

Figure 8: Upright measured and estimated resistance for different Froude number.

The resistance predicted by the Delft spreadsheet shows a good agreement with the towing tank data up to Froude number of 0.5. After this, the hull goes in the planing mode and the resistance predictions differ. In the higher end of the prediction, the resistance starts to be affected by yacht not fitting the systematic series. As the yacht is more likely to operate in the higher end of the Froude number, this will lead to very big inaccuracy in the results.

The scaling of the resistance to the full-size yacht showed some interesting behaviour. For the lightest displacement, 50%, at high Froude number, because the lift produced by the hull is significant compared to its weight, the dynamic wetted surface area is much smaller than the static. This results in too much viscous resistance being stripped out of the model and therefore a too low wave coefficient is scaled to the full-size. This results in the resistance dropping after a certain Froude number as show on the following graph:

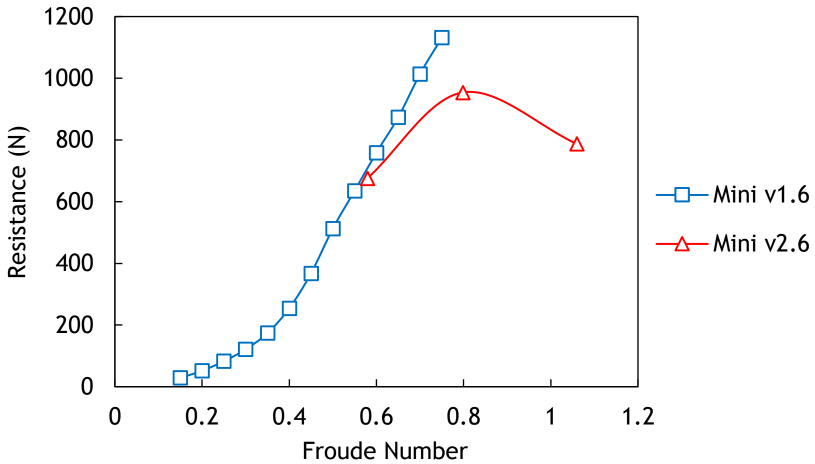

Figure 9: Resistance for the 50% displacement, 5° of heel, 1° of yaw case.

Regarding sideforce, results showed that in the upright condition, a significant amount of sideforce was produced after a Froude number of 0.5. This could be the result of a misalignment of the model or the speed being too high and with the canting keel fully canted, a yaw moment is induced, which increase the leeway angle on the keel. This will also have the effect of increasing the induced drag. For the full result of the towing tank, refer to Appendix E.

7.4. Delft Systematic Series Comparison

The spreadsheet written to calculate the total resistance of the yacht is derived from (J. A. Keuning, M. Katgert, 2008), which is the most recent version of the delft series regression method and is extended to Froude Number of 0.75.

With the scow bow hull producing more righting moment, the standard hull will have to be tested at a higher heel angles. The following shows the differences in heel angles for the same righting moment.

Table 5: Heel angle for same righting moment.

Yacht	100%		81%		50%	
	GZ (m)	Heel (°)	GZ (m)	Heel (°)	GZ (m)	Heel (°)
Mini v1.6	0.32	5.5	0.33	5.3	0.35	5.1
	0.58	11.8	0.60	11.7	0.63	11.4
	0.76	18.7	0.78	18.8	0.81	19.3
Mini v2.6	0.32	5	0.33	5	0.35	5
	0.58	10	0.60	10	0.63	10
	0.76	15	0.78	15	0.81	15

The yacht was therefore tested at these heel angles using the spreadsheet and the resistance was compared to the same case for the towing tank results. The following shows a typical result.

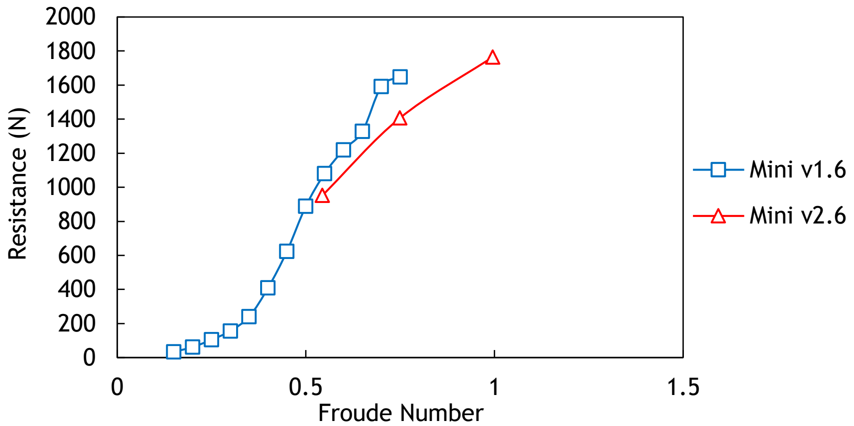

Figure 10: Resistance at 100% displacement, 5° of heel and 1° of yaw for different Froude number.

As see on the previous graph, the scow hull feature less resistance in this condition. The difference follow the same trends as for the upright case. When comparing the resistance for cases with more heel, the differences in resistance start to be significant. Up to the point where Delft predict almost two times the resistance, see graph 6. The differences in shape between the Delft hull shape on what the regression method is based and the standard hull shape can explain this differences.

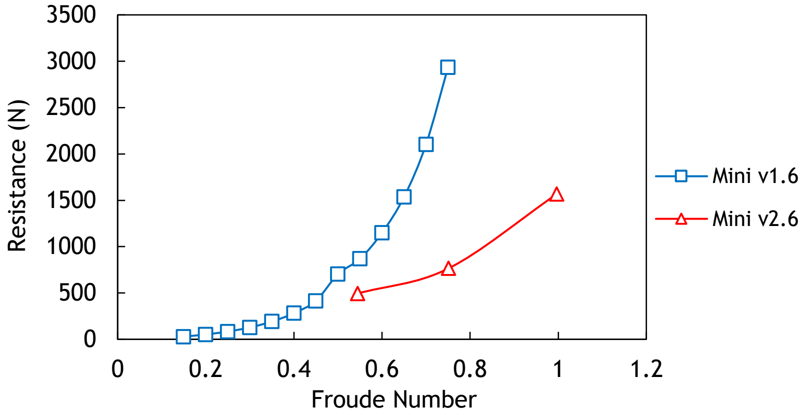

Figure 11: Resistance at 50% displacement, 15° of heel and 3° of yaw for different Froude number.

All the case compared showed a lower resistance for the scow hull shape (see Appendix F). This led to the decision of carrying on the project using the scow hull shape.

7.5. Advanced VPP Analysis

The towing tank results were used as a part of the hydrodynamic model. The foil results from the CFD analysis completed it. To reduce the number of runs which had to be made, it was decided to favour the downwind speeds and heel angles using preliminary results obtained from WinDesign (see Appendix C). Because of the foils, the resistance of the yacht had to be measured for different displacements. The displacements which will be tested are 100%, 75% and 50%. Later during the test the 75% displacement was changed to 80% as it corresponds to the lightship displacement of the yacht and was also easier to achieve in terms of weight of the model than the 75% case.

Because of the limitation in terms of measurements equipment in the tank the following assumptions had to be made:

- The vertical force (F_Z) produced by the hull is assumed to be only a result of the buoyancy force acting on the hull. The lift generated by the hull when planing is ignored.
- The trim of the yacht was kept to 0° (free to trim dynamically) for the whole set of tank testing mainly to reduce the number of runs required. The static trim of the yacht could have been altered but the towing mechanism doesn't allow for the trim to be locked, therefor the yacht could not have been tested at a particular trim angle.
- The keel is assumed to be always canted to its maximum (40°).

The aerodynamic model uses the ORC VPP method to define the drive and sideforce of the rig.

The fitting and the VPP solving were performed by Yves Courvoisier and Paolo Motta from Hydros, using the provided forces matrix for the hulls, foils and rudders. Unfortunately, the VPP didn't find any equilibrium for the defined sailing condition. The solver was trying to reduce the leeway as much as possible, but even in this condition, the foils were still producing too much sideforce. They are many factors which could lead to such a result:

- An error could be present in the set-up of the VPP or in the definition of the sail plan and sail area.
- The assumption made regarding the trim of the yacht don't represent the equilibrium case well enough. This leads to the tip producing too much sideforce and therefore the solver trying to reduce the leeway as much as possible, which also reduces the vertical lift. This result in the yacht trying to avoid sailing on the foils. By varying the trim of the yacht, the shaft could produce more lift, which would result in a decrease of the

total sideforce which will now match the sail sideforce while still producing enough vertical lift to lighten the yacht.

Because of time constrain and the huge amount of data required to solve this problem it was decided to stop here. In further iteration of the design, the hull and foils could be measured at different trim angle to try to balance the sidefroce. For the Hydros report on the VPP results refer to Appendix G.

8. Sail Plan

The rig being the only mean of propulsion of the yacht, it must be carefully designed. In box rules like the Mini 6.50 rule, a lot of freedom is given to the designer to maximise the potential of the rig. This is also one of the critical part of the yacht as a failure of the rig often means a withdrawal of the race.

8.1. Rig Structural Design.

As the air draft is limited to 12 meters by the rule (as well as the minimum freeboard), the P value is highly constrained. To maximise the sail area and lower the centre of effort, the boom has to be taken as low as possible and the height of the rig maximised.

Standard carbon rig is the preferred option amongst the fleet due to its light weight an ease of use. A small number of yachts are however fitted with wing mast, trading weight for windage. With the large beam, those wing mast don't require deck spreaders to be supported and can simply be attached straight to the deck. The following will describe a comparison in terms of weight and windage for a standard single spreader rig and a wing mast.

The most common way of dimensioning a rig is to treat it as a 2D framework. 3/7 of the load of the jib are assumed to be acting on the head, while the remaining 4/7 are assumed to act on the clew. The mainsail is assumed to act as a uniformly distributed load (UDL) along the mast length. A wind pressure is then applied to the yacht until the generated heeling moment is equal to a chosen righting moment. The chosen righting moment is equal to 1.5 times the righting moment of the yacht at 30° of heel with the keel canted to account for the added dynamic righting moment produced by the foils. The forces are then resolved in each member of the rig and a factor of safety is applied. The resulting mat compression is then used to determine the required transverse mast flexural rigidity (EI_{XX}) based on Euler's buckling theory.

The required longitudinal flexural rigidity (EI_{YY}) is specified by defining an acceptable forestay sag ($\delta_{forestay}$). The required forestay tension and backstay tension to match this sag are then calculated using a simplified catenary equation relating sag and tension of a rope under a UDL (equ. 3). The load of the jib is assumed to act uniformly along the length of the forestay. The generated mast compression in then used to define the mast longitudinal flexural rigidity based on Euler's buckling theory.

$$T = \frac{qL^2}{8\delta_{forestay}}$$

Equation 3: Sag and tension in a catenary equation from (Eng-tips, 2012) .

The chosen allowable forestay sag of 2.0% resulted in a forestay tension of 4720N. The same method was used for the wing mast.

To determine the required transverse mast flexural rigidity of the wing mast, the same method previously explained was used, adapting it to a wing mast with a diamond. Refer to Appendix H and I for the full framework analysis.

Knowing the required flexural rigidity for both the rigs, a basic mast laminate could be specified. From knowledge of the author, a prepreg laminate was specified with a fibre distribution of 80% at 0°, 10% at ±45° and the remaining 10% at 90°. With the very few layers used for the standard rig, the chosen distribution is not respected. Refer to Appendix J for the full calculations.

This study yield a linear weight for the standard mast of 1.11 kg/m for the tube itself and a weight of 2.0 kg/m for the wing mast. Due the major gain in weight, the windage was not calculated for the rigs and the standard rig was chosen for the yacht. Note that this weight is likely to increase because it doesn't account for the local reinforcements for the fittings.

The specified standing rigging will be made of Ultra high molecular weight polyethylene fibres (UHMPE). Many types are available on the market and the main one are presented in the following table:

Table 6: Ultra high molecular weight polyethylene fibre comparison with PBO.

UHMWPE Fibre Type	**Tensile Strength** GPa	**Tensile Modulus** GPa	**Elongation** at break %	**Creep** %/Day
SK99	4.1	155	3.0-4.0	0.006
DM20	3.1	94		0.00007
SK75	3.3-3.9	109-132		0.02
SK78				0.006
PBO (Zylon)	5.8	180	3.5	0.00032

For standing rigging, one of the most important aspect is creep (permanent elongation under long term load). In this field, DM 20 has a serious advantage over its competitor with a creep more than 5 times smaller than standard modulus PBO. Despite being less rigid, DM 20 was chosen as the standing rigging material.

8.2. Preliminary Sail Configuration

With the class rule limiting the number of sails to seven, including a storm jib, choices have to be made regarding the sails configurations and range. From the weather study, one remember that the race is going to be mostly VMG downwind in wind strengths of around 12-17 knots. The sailset will therefore be designed for those conditions.

A fractional rig was specified for this design. Fractional rigs have become more and more popular nowadays due to the increase performance the bring. Their ability to control the bend of the mast more effectively than masthead rig give it a significant gain in performance. The top of the jib being lower than the top of the main, the tip vortex generated by the jib is reduced, which will reflect on the performance of the sail plan (T. Whiden, M. Levitt, 2016).

As presented in the parametric study, a typical Mini 6.50 sailset for the Transat consist of: A main, a jib, a storm jib, a gennaker and three spinnakers. They are however small variations between the boats, which are trying to maximise the range of each sails. The following will describe the preliminary considerations when designing such a sail plan. This area of the design is very likely to be changed if the boat is raced, mostly because of the tastes and choices of the skipper on the sails.

- The mainsail will feature a powerful square top to maximise the sail area. It will be controlled by five full length batten and made of 7.5 Oz polyester cloth. Three reefs will be installed in the main. The final area of the main is 29 m^2.
- The jib will be made of 4.6 Oz polyester cloth with a full length top batten and two leech battens. It is attached to the forestay via loops. It can be reduced to 70% of the

original area with a reef. This enable its wind range to be broaden. The area of the jib is 19 m^2. By having the clew of the sail high relatively to the deck will reduce the upwind performance (due to the loses of the endplate provided by the deck) but once upwind is passed, the sail will be easier to trim. With regards to the Transat, it was decided to go for the second option.

- The mandatory storm jib, of a maximum area of 4 m^2 can be reefed to 2.5 m^2 and will be made of 9.8 Oz (340 g/m^2) polyester cloth as per the Mini 6.50 rule (J-29-a-1).
- A gennaker is specified for light wind upwind/reaching conditions, as these boats often lack power in front. It will be fractionally rigged to lower as much as possible the centre of effort. Adjustments of its position on the pole is possible to broaden its range. From the parametric, an area of 30 m^2 was chosen. It will be deployed via a furler. Polyester cloth of 1.5 Oz was specified for this sail.
- The three kites will all be made of polyester cloth. Polyester was specified over nylon because the latter is weakened when wet. Their fabric weight range from 1.5 Oz for the heavy weather runner, the Code 5 to .75 Oz for the A2, the light wind runner. They enable wind speed from 0-25+ to be covered. It was chosen to run them on the same sheeting circuit to simplify the deck plan. A reaching strut will be used to virtually lengthen the yacht and control the shape of the kite more effectively.

8.3. Balance

The longitudinal distance between the point of application of the side force in the sail and the point of lateral resistance from the appendages defines the balance of the yacht. If those two points are aligned, the boat would be balanced and no rudder required to keep her on the track. This is rarely the case as the more the boat heels, the more the two centre move.

A usually method used to determine where to place the rig relative to the keel, or the opposite, is to simplify the case to the static upwind case. The centre of effort is then taken as the centre of area of the combined sails and the same of done for the appendages, taking the ¼ chord length of each of the appendages. The longitudinal distance difference is then expressed as a percentage of L_{WL}. Example in the literature (L. Larson, R. E. Eliasson, M. Orych, 2014) give a range of values for different rig types. A more advanced approach can be used to estimate the amount the CLR shifts with the changes in heel angles (A. Claughton, R. Pemberton, M. Prince, 2012), with the following formula:

$$\delta CLR = \frac{HA \times \sin(\emptyset)}{\tan(90 - \epsilon_h)}$$

Equation 4: Centre of lateral resistance shift.

The displacement of the CLR can then be calculated for a range of heel angles and hydrodynamic lift angles. A condition must then be chosen, at which the yacht will be in equilibrium.

All these considerations work well for boats with a standard appendage set, where the keel and the sail plan are both on the centreline. For other cases, where the point of application of the side force (KSF) is not well known, these considerations are of little use. In the case of a canting keel and foils, they are many variables which influence the position of the CLR: the heel, the leeway, the heave, the speed, the keel cant, the keel yaw, etc. With foils, because they are used to produce vertical lift, they also require to be positioned forward of the centre of gravity of the yacht, this could have an influence on the balance as they cannot be moved backwards. The foils were therefore placed in front of the centre of gravity as to cover 90% of the vertical lift with the rudder takin the last 10%. To accurately measure the centre of lateral resistance of the yacht, a full CFD analysis of the yacht would be required in further stages of the design. This would be the most accurate solution and will also be able to give a detailed analysis of the contribution of each of the appendages to the sidefrorce as well as the side force and munk moment (M. Prince, A.R. Claughton, n.d.) generated by the hull. Towing tank could also be used but this will be subject to many assumptions for the foils and will only give the final CLR and not a breakdown of the forces.

A simplistic approach was used to determine the balance of the yacht. A light wind scenario was considered, where the keel would be on the centreline. Both the keel and the rudder will take part in the generation of the sideforce in these conditions. A lead value of 3% of L_{WL} was chosen, this is a relatively low value but remembering that in more breeze, the foil would be used, this is acceptable.

9. Stability

It is a requirement from the Mini 6.50 rule for the boat to comply with the ISO 12217-2 for design category C. In addition to this requirement, the Mini 6.50 rule also define two stability test the boat must pass to take part in the Transat.

9.1. Mini 6.50 Stability Test

The required stability tests are, the small and large angle stability. Each yacht must demonstrate that she passes both requirements before taking part in the Transat. The following table summarizes those requirements extracted from the Mini 6.50 rule:

Table 7: Mini 6.50 required stability test.

Rules	Requirements
J-21-a	As for angles of vanishing stability, the boat must have positive stability with a 45 kg weight (not including Archimedes' effect) at the upper halyard exit and the boat in the most unfavourable configuration regarding the ballasts, movable weight and mast(s). The boat must not have flooding water.
J-21-b	As for small angle of stability, the boat must not exceed a 10 degrees heel angle with the most unfavourable ballast, movable keel and mas(s)t configuration.

The loading condition required for these stability tests includes the whole boat, empty of all external equipment, except for the liferaft. The sails do not require to be onboard as well as all the mandatory safety equipment. In these conditions, the weight of the yacht is reduced drastically compared to the sailing conditions.

The weight estimate was adjusted to account for these changes and this yield the following displacement and position of the centre of gravity in the worst case:

Table 8: Stability test loading condition.

Displacement	930	kg
LCG	-0.538	m
VCG	-0.23	m
TCG	-0.622	m

To define the minimum allowed weight for the bulb, and the maximum keel extension, several iterations where done by varying the two parameters and checking for the two requirements in Maxsurf Stability. This yield a weight of the bulb of 300 kg and an extension when fully canted of 200mm.

This set-up result in an angle of list of 8.7° and a righting moment at masthead of 48.5 kg. The tests are therefore successfully passed. The results of the full stability analysis are presented in Appendix K.

9.2. ISO 12217-2

In addition to its own two stability test, the Mini 6.50 class rule requires all the yachts to be designed and built in accordance with the ISO 12217-2. Although the yachts are taking part in race of category 1 (OSR), which would mean that they must be designed for category A, they only required to be designed for category C.

The different criteria were checked using the built-in criteria function in Maxsurf Stability. Three load cases had to be considered: departure, 50% load and arrival. All those are based on the worst case loading the boat will experience, the start of the Transat, and reduced accordingly. These load cases requires the upwind sails to be ready to be set and the canting keel on the centre line. Water ballast don't require to be filled. The following shows the results of the stability test and the departure condition for the ISO 12217-2. The two red dotted lines represent the two stability criteria described earlier.

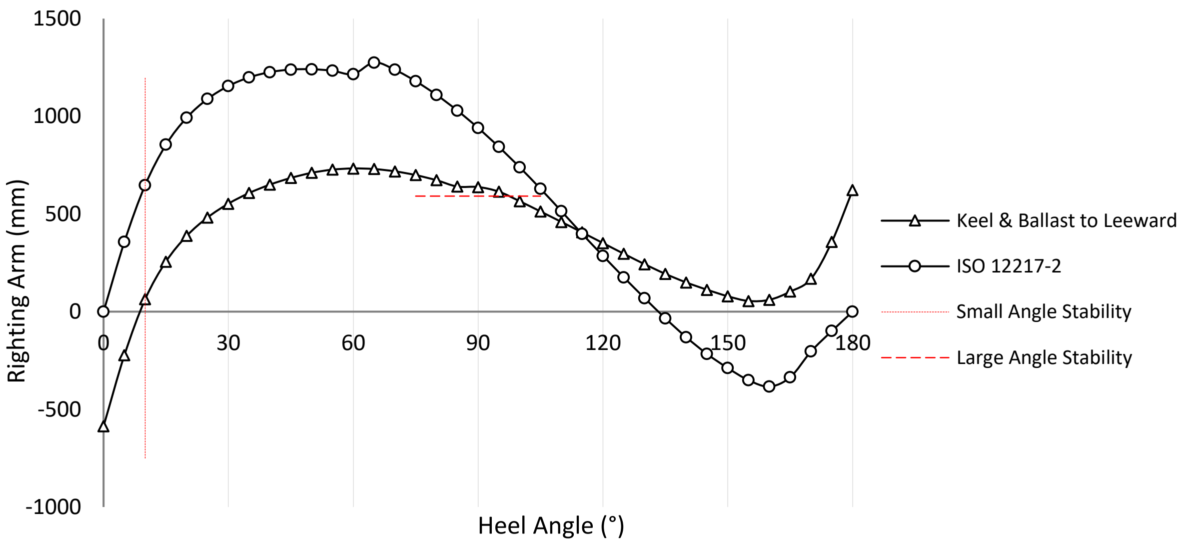

Figure 12: Righting arm for different heel angles.

All the requirements are passed with a significant margin, except for the wind stiffness test, which fails. However, as stated in the ISO 12217-2, the boat complies if: "*these requirements are satisfied when the sail is reefed provided that the reefed sail area is not less than 2/3 of A_S.*" (ISO, 2015). When the sail area is reduced from 49 to 32.6 m^2, the yacht now passes the requirement. Because it was unclear in this part of the ISO if the reef in the sail also meant a reduction of the heeling arm, the same heeling arm as for the full sail was kept. In further stage of the design, if this requirement is not met anymore, the owner manual would need to feature a warning about the maximum wind speed before a reef must be taken.

The STIX requirements, which is a method of obtaining the full stability assessment of a sailing yacht, is also passed for all the conditions. A breakdown of all the STIX parameters as well as a summary of all the criteria for both the ISO 12217-2 and the Mini 6.50 stability test is presented in Appendix K.

10. Appendages Design

10.1. Rudders

Regarding rudder arrangement, they are two possibilities: single or twin rudders. They are several benefits of having either arrangements but because of the wide beam at the transom and the nature of the race the boat will take part in, a twin rudder arrangement was specified.

Because of its offset from the centre line and its toe out angle, the rudder can work more effectively than when on the centreline of the boat. The heeled waterlines are used to find the point at which the hull is immersed most of the time. The toe out angle of the rudder will have a significant influence on the performance of the yacht and its balance but finding the centre of effort of the sail plan and the appendages is relatively complicated so a first principle approach will be used: the rudder will be placed perpendicular to the hull at the desired offset from the centreline. With a twin rudder arrangement, being able to lift the windward rudder clear of the water is serious advantage, because it removes some drag but more importantly the alignment of the rudder doesn't need to be changed during racing as it is the case with fixed twin rudder.

Two sections were compared for their lift and drag using XFoil. XFoil combine a high order panel code with a viscous/inviscid boundary layer analysis. The two sections which were analysed are the NACA 0010 and NACA 63-010. The first being a common appendage section for cruising yachts, and the latter being more effective at low angle of attack as it can be seen on the following graph (Appendix L).

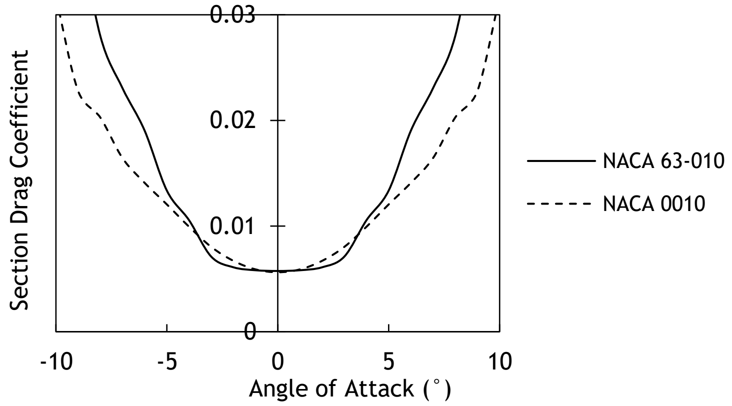

Figure 13: Section drag coefficient for different angle of attack.

At low angle of attack the 63-010 shows better L/D ratios, except at zero angle of attack, where the NACA 0010 performs better. Ideally the rudder should be kept at minimum angle of attack most of the time but, in reality, small adjustments are required, which have a range of 2-3 degrees. This will favour the 63 series as it's drag bucket as a range of around 6 degrees. As the boat is intended to be sailed by experimented sailors, large rudder angles are not very likely to be seen, especially because offshore single handed boats tend to be equilibrated to remove all loads of the rudder, which implies that it will operate most of the time at low angle of attack, where the NACA 63-010 shows better performance. The later section was therefore chosen.

The actual dimension of the rudder was defined by allocating a portion of the side force to the rudder. The upwind case was considered, and the rudder was assumed to take 5% of the total side force of the yacht. This number is relatively low but it should also be remembered that in the upwind case, the chine is likely to be immersed and will produce a fair amount of sideforce (Kouyoumdjian, 2014) and, as said previously, the aim is to minimise the load on the rudder.

Because the rudder is the downwash of the keel, it experiences a lower angle of attack than the leeway (J. A. Keuning, M. Katgert, K. J. Vemeulen, 2006) which in this case will result in a higher rudder angle relatively to the yacht.

Knowing the sail sideforce, we can express the required lift coefficient for the rudder as:

$$C_L = \frac{L}{\frac{1}{2}\rho v^2 A}$$

Equation 5: Lift coefficient.

And by knowing the required lift coefficient, the required angle of attack of the rudder can be found.

$$\frac{\partial C_L}{\partial \alpha} = \frac{2\pi}{1 + \frac{2}{AR_e}}$$

Equation 6: Lift curve slope.

These considerations yield a rudder spacing of 1 meter from the centreline with a tow out angle of 16°. The area was kept low, 0.18 m^2 to reduce the wetted surface area and by choosing a relatively large span of 0.86 meter, the aspect ratio is relatively high, therefore achieving good lift generation. The required rudder angle to produce the necessary side force is 1.31°, which falls within the drag bucket of the NACA 63-010 series.

The same approach was used to dimension the elevator of the rudder. A fraction of the displacement of the yacht was allocated to the rudder and the required angle of attack calculated. This yield an elevator dimension of 0.5 metre span and 0.1 metre chord.

10.2. Keel

With the yacht being fitted with a canting keel, it doesn't rely on it to produce the sideforce but on the foils. This implies that the major goal of the keel is to hold the bulb without creating too much drag. A number of sections are available for keels, typical cruiser keel sections with feature a more forgiving NACA 00 section, which is more tolerant to high angle of attack than for example a NACA 63. As this yacht will be skippered by experienced sailors, the section investigation will be carried out in the later type of sections. A NACA 63 was compared to a NACA 64 and a NACA 66.

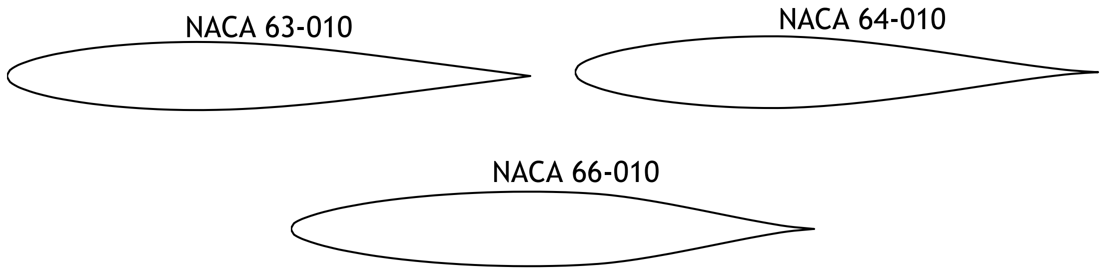

Figure 14: Keel sections (Thickness/Chord ratio not at scale).

The major difference between those three sections is the position of the maximum thickness. The 63 having the thickness at 30% of the chord and so one. The aim of moving the maximum thickness aft is to delay the point where an adverse pressure gradient occurs and therefore the point where the flow will change from laminar to transitional thus reducing drag. The three sections were normalised to a 10% thickness chord ratio for this comparison. The analysis was performed using XFoil as for the rudder section (Appendix L).

The following graph shows the section drag coefficient as a function of the section lift coefficient. All the section features a drag bucket at low angles of attack and a serious increase in drag passes a certain point. The 63 and 64 are very close in terms of drag with the 66 being a bit penalised at very low angle of attack. The NACA 63 series showed the best properties both in terms of lift drag ratio but also in terms of polyvalence. This section was therefore chosen as the keel section.

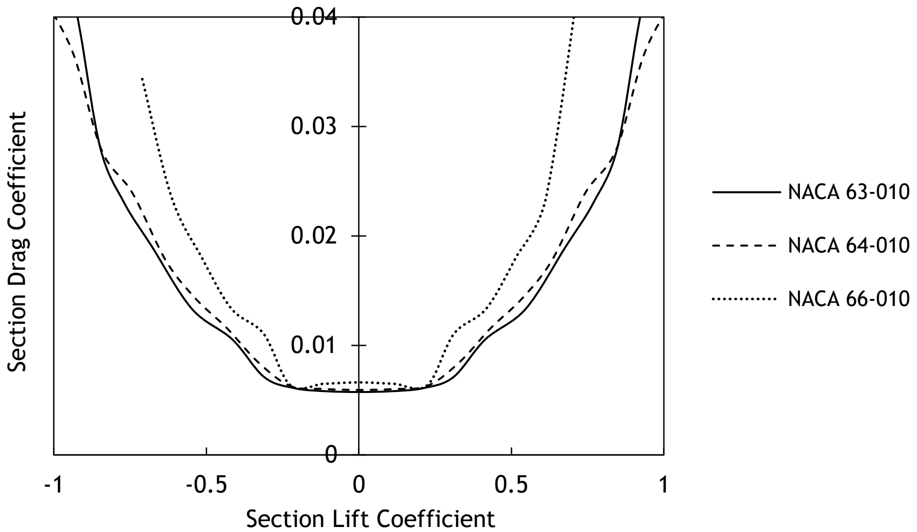

Figure 15: Section Drag Coefficient for different Lift Coefficient.

The keel area itself is derived from structural calculations which yield the minimum chord length of the section.

10.3. Bulb

They are many aspects to consider when designing a bulb shape for a yacht: its drag, position of the centre of gravity, its interaction with the keel and more specifically, the reduction of the tip vortex of the keel. Many of these aspects have only a small influence in the final performance of the boat, therefore only the drag and the position of the centre of gravity of the bulb will be considered.

The following investigation will be based on a first principle approach where a set of bulbs will be compared in terms of their viscous resistance and position of the centre of gravity. Three different bulb shapes will be compared based on commonly used sections, a NACA 63 section, a NACA 66 section and finally a bulb section based on a NACA 66 but modified to be flatter. The thickness chord ratio of these bulbs was altered keeping the same volume and the viscous drag was calculated using Hoerner's (Hoerner, 1965) form factor for bulb shaped appendages and the ITTC 1957 friction drag formula:

$$(1+k) = 1 + 1.5\left(\frac{t}{c}\right)$$

Equation 7: Form factor for bulb shaped appendages.

The following graph shows the results for the three appendages varying the thickness chord ratio for the same total bulb volume. They were tested at a Froude number of 0.35, simulating the upwind case.

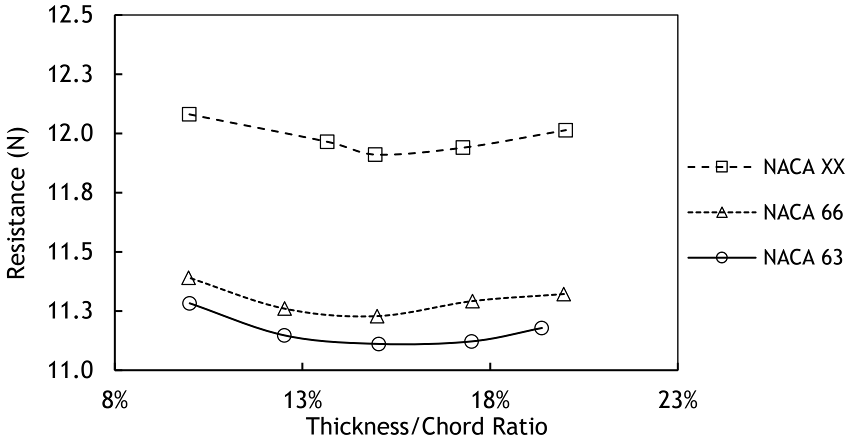

Figure 16: Bulb viscous resistance for different thickness/chord ratio.

Because of its flatter section and especially its flatter tail, the modified bulb (NACA XX) features a greater wetted surface area. It can also be noted that all the bulbs have the minimum viscous resistance at thickness chord ratio of around 15%. Under this values, the bulbs are too long and have a wetted surface area that is too big as is the form factor which also leads to an increase in viscous resistance. For this study, the chosen bulb thickness chord ratio that will be used is 15%.

The main advantage of the modified bulb is to lower the centre of gravity of the bulb but this comes with a higher viscous resistance (due to the increased wetted surface area). Balancing the importance of the drag against the position of the VCG is no easy task because their influence over the final yacht performance are hard to quantify. It was therefore chosen to select the modified bulb which is similar to what other boats have. This factor could be addressed in a later stage of the design by proceeding to a full CFD analysis of the appendages, which will also have the advantage of being able to give the centre of lateral resistance of the yacht, which is difficult to predict when the appendages are not in line with each other. See Appendix M for the full calculations.

11. Foil Design

The aim of this project was to incorporate to a Mini 6.50. The gain brought by the lift generated by those foils which in turn reduced the immersed volume of the yacht and therefore increases its speed. It is potentially the area of the boat where the biggest gains can be made. The result of the last Vendee Globe, which saw the first four boats to cross the finishing line being equipped with Dali moustache foils, can be taken as a real-life example of the performance gained with such a set-up. It can however be argued that the foils are not the only factor influencing the performance of the boat, as proved by Alex Thompson who raced more than half the way without one of his foils. The following part will describe the design process undertaken to design the aforementioned foils.

11.1. Dali Moustache Foil

They are many possible variations in the foils which can be designed for an offshore racing yacht like a Mini 6.50. A basic comparison of the available design was performed at the beginning of the design phase to establish which path will be followed. The following table shows the pros and cons of the possible design variations.

Table 9: Foil design variations pros and cons.

Design	Added Righting Moment	Sideforce	Other
DSS	Yes	No	Foil reduces sideforce
IMOCA Dali Moustache	Yes	Yes	Sideforce produces RM
Quant 23	Yes	No	Foil reduces sideforce

If the foils weren't required to produce any sideforce, any of the studied arrangements could be used, but as the yacht relies on them for reaching and upwind conditions, the only possibility is to use the so called "Dali Moustache option", which is what is also used, and was invented for the IMOCA class.

The arrangement will however be different from the one of the IMOCA because the foils must fit in the maximum beam of the yacht defined by the Mini 6.50 rule (3m) when retracted. This led to choosing a curved shaft, which puts the tip more horizontal when extended.

To dimension the foils, a fraction of the weight of the boat was allocated to them and a sailing scenario was defined. It was decided that the foil tip must produce 30% of the weight of the boat at a speed of 13 knots. With the keel and the rudder also contributing to the vertical lift generation, a greater part of the displacement of the boat will be carried by the appendages, the buoyancy providing the remains. This yields a tip span of 1 meter with a chord of 0.25 meters.

11.2. Computational Fluid Dynamic Analysis

The opportunity to analyse the foil using a Computational Fluid Dynamic (CFD) package (ANSYS CFX) arose early in the design stage. The aim was to use this program to help with the choice of the foil section and give a refined flow analysis of the foil.

Ansys CFX solves fluid flow problem using the Reynold's Averaged Navier-Stockes (RANS) equations. These four partial differential equations (PDE's) describe the continuity, the x, y, and z momentum and the energy present in the flow. They focus on solving for the mean values of the flow and not the fluctuations.

The K-epsilon (*k-ε)* turbulent model is used to simulate the values of the mean flow for a turbulent flow. This is the most commonly used turbulent model in engineering simulations because of the relatively low computational requirements. It adds two more partial differential equations to the four already defined by the Navier-Stokes equations: one for the turbulent kinetic energy (k) and one for the turbulent dissipation *(ε)* (H. Versteeg, W. Malalasrka, 2007).

$$\frac{\partial(\rho k)}{\partial t} + div(\rho k U) = div\left[\frac{\mu_t}{\sigma_k} grad\ k\right] + 2\mu_t S_{ij}.S_{ij} - \rho\epsilon$$

Equation 8: Turbulent kinetic energy k.

$$\frac{\partial(\rho\epsilon)}{\partial t} + div(\rho\epsilon U) = div\left[\frac{\mu_t}{\sigma_k} grad\ \epsilon\right] + C_{1\epsilon}\frac{\epsilon}{k}2\mu_t S_{ij}.S_{ij} - C_{2\epsilon}\rho\frac{\epsilon^2}{k}$$

Equation 9: Turbulent dissipation ε.

One of the most time consuming and important part of all computer simulation (CFD, FEA, etc.) is the meshing, where the domain is divided in several cells. This number, being too small, can lead to inaccuracy in the results or, if being too big, requires a large amount of computational time which can be very costly. Designing a mesh which lies in-between the two is important to achieve valuable results without the need of a lot of computational time.

One way to evaluate if the number of cells in a domain gives an accurate result can be found in: *Procedure for Estimation and Reporting of Uncertainty Due to Discretization in CFD Applications* (I.B. Celik, 2008). The method given here enables the results from the same simulation but with different mesh sizes to be compared to determine if the problem is mesh independent, i.e., that the solution doesn't depend on the size of the mesh or if the problem is mesh dependent, where the size of the mesh influences the results. Three different meshes were run with the same foil section and set up and the results were used to determine the grid convergence index (GCI).

$$GCI_{fine}^{21} = \frac{1.25e_a^{21}}{r_{21}^p - 1}$$

Equation 10: Fine grid convergence index.

A test case was setup with the Eppler 214 section at an angle of attack of 4° and a Reynolds number of 1E6. The mesh used can be seen on Figure 18: Detail of the Eppler 214 fine mesh used for the grid dependency study. It is made of a swept method with a refinement in the mesh upwind of the foil and in its wake. The surface of the section is further refined and an inflation layer is present to increase the mesh resolution on the surface of the section, where the boundary layer will occur.

To define the thickness of this boundary layer, a suitable y^+ value was specified. The y^+ (y plus) value is a normalised distance from the wall and is used to describe the distance from the wall to the first node of the mesh (LEAP, 2017). The k-ε turbulence model used a scalable wall function to calculate the viscous sublayer and the buffer layer at y+ values under 11.06 (ANSYS, 2011). This y^+ value yields a boundary layer thickness of about 0.26 mm. The model was therefore meshed to have cells at least this thickness on the surface of the foil.

$$y = \frac{y^+\mu}{\rho u_*}$$

Equation 11: Wall distance equation.

The results for the finer mesh gave a GCI of 0.14% and 2.2% for the lift and drag respectively as presented in the following table.

Table 10: Grid dependence study for the 2D case.

Value	Φ= Lift Force	Φ= Drag Force
N_1, N_2, N_3	164000, 89000, 36000	164000, 89000, 36000
r_{21}	1.35	1.35
r_{32}	1.57	1.57
Φ_1	63.001	0.961
Φ_2	62.973	0.968
Φ_3	62.551	1.046
p	1.106	1.106
Φ_{ext}^{21}	63.07	0.94
e^{21}_a	0.04%	0.69%
e^{21}_{ext}	0.11%	2%
GCI^{21}_{fine}	0.14%	2.2%

This study showed that the solution was grid independent for the considered grid size, the finer mesh will therefore be used as such for the foil section analysis. The the forces obtained as well as the calculations of the CGI are presented in Appendix N.

11.3. 2D Section Selection

With the required size of the grid now determined, the 2D section analysis started. The different sections will be analysed as infinite span foils (2D). The sections will be compared for the lift and drag properties as well as their pressure distribution.

The first step was to compare four different foil sections at different angles of attack for a same operating Reynold's number. The four sections which were selected are: a NACA 63-412, Eppler 214, Eppler 387 and Eppler 817. The different sections are presented in the following figure:

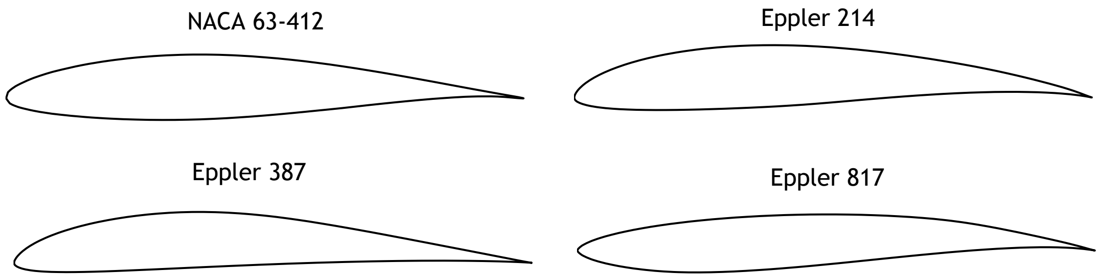

Figure 17: Foil sections compared (Thickness/Chord ratio not at scale).

These sections were meshed using the same method as the one described earlier and featuring the same number of elements. The inflation layer was designed to respect the chosen y^+ value. The following shows a detail of the mesh used. The refined area around the foil and the inflation layer can be seen. Note that the trailing edge has been cut to a sensible thickness.

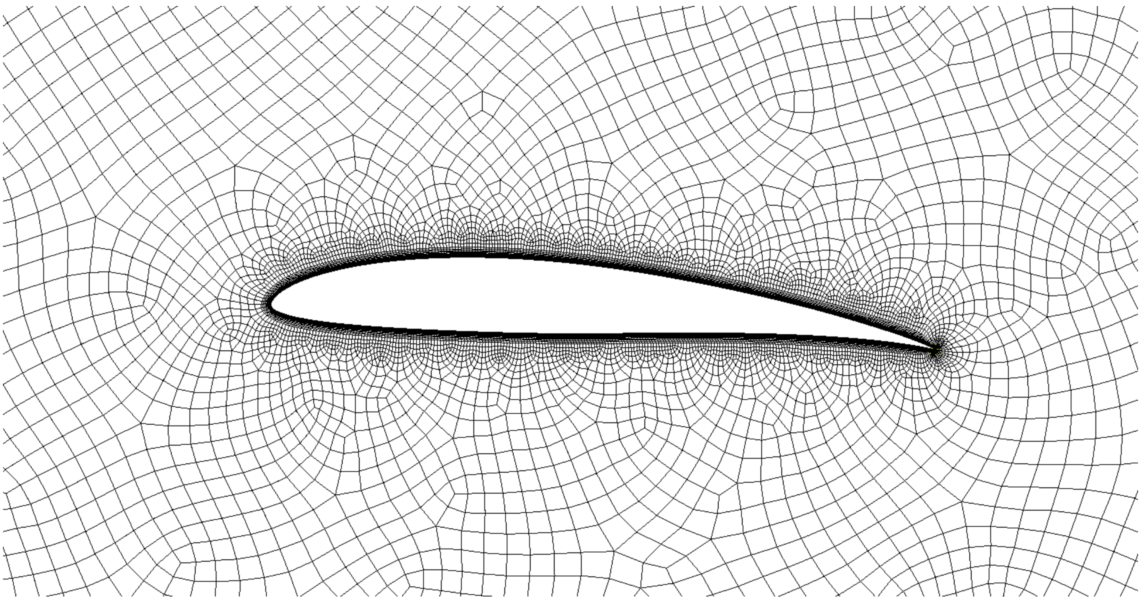

Figure 18: Detail of the Eppler 214 fine mesh used for the grid dependency study.

The main advantage of performing a RANS investigation of the section is that a panel code doesn't consider viscous effect and the boundary layer when computing the lift and drag of the section.

The four sections will be tested at the same Reynold's number, 1E6, which is the operating Reynold's number that the foil itself will experience. The following graph shows the lift/drag ratio as a function of the angle of attack for the different sections. Refer to Appendix O for the full 2D section results.

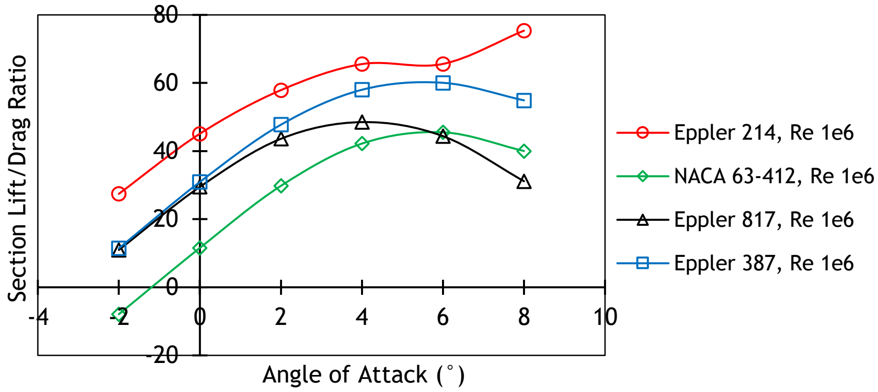

Figure 19: Section Lift/Drag ratio for different angle of attack.

The Eppler 214 showed to be the most efficient section at the chosen Reynold's number and operating conditions. This is important for a preliminary foil design because the final speed of the yacht is not well known, so a foil which is polyvalent is required. Having a good lift to drag ratio for a wide range of angle of attack results in a foil which will perform in all conditions (leeway and pitch of the boat).

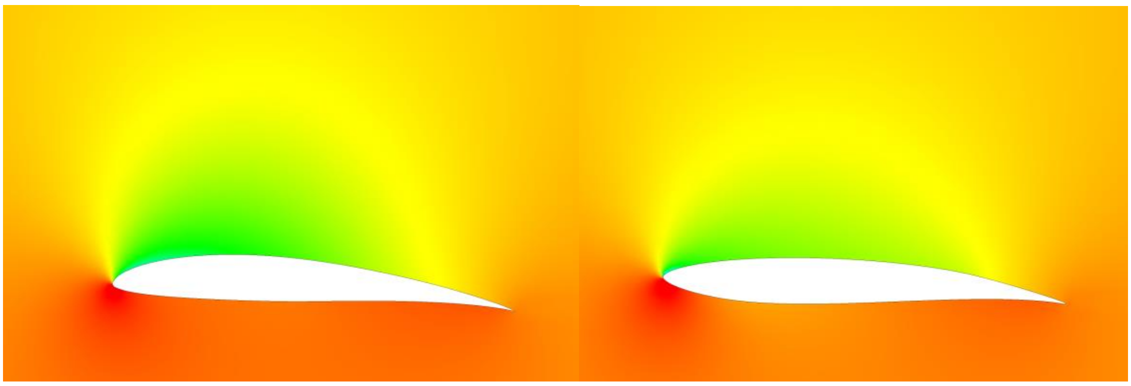

Figure 20: Eppler 214 and Eppler 817 pressure distribution in identical pressure scale.

The previous figure shows the pressure distribution for the two sections, the Eppler 817 shows a smaller peak pressure and a more uniformly distributed pressure along its chord length whereas the Eppler 214 shows a higher peak pressure at the front but still a good overall pressure distribution. The Eppler 817 shows the best pressure distribution due to its flatter top and thus lower pressure gradient. The Eppler 214 is the second best, with a pressure distribution similar to the other two sections.

Considering the pressure distribution and the lift drag properties of the different sections, the Eppler 214 was chosen as the section which will be used for the foil design.

11.4. 3D Foil Comparison

Because the 3D foil will be analysed at the same Reynold's number and using the same turbulent model (*k-ε*) as the sections, the same y^+ value and corresponding first node distance can be used as for the 2D section. This time an unstructured mesh will be used. Unstructured meshes are usually coarser than structured meshes but far easier to produce and refine in critical areas. The method used here is tetrahedral patch conforming with a refined mesh in way of the foil and its wake. The inflation on the surface of the mesh with a first node distance of 0.26 mm to respect the chosen y^+ value of 11.06.

To reduce the complexity of solving for the free surface, the foils will be analysed fully immersed, in a single phase flow. The results produced will therefore not reflect the actual forced produced by the foils in its operating conditions but hopefully the better foil in reality will still be the best one under these assumptions. Again, to reduce the number of simulations, the range of operating angle of attack was reduced. The foils will be analysed for angle of attack (leeway) between 0 and 6 degrees, which is the typical range of angle of attack that the yacht should experience while sailing. The pitching motion of the yacht will also be ignored as this is a very dynamic value and will highly depend on the sea.

Due to the complexity of the mesh created and the capability of the student version of CFX, the runs were solved on a computer owned by Jonathan Ridley (Ridley, 2017) which enable problems with meshes bigger than 512k elements to be run.

The convergence criteria for the runs was defined to be at a Root Man Square (RMS) of less than 1E-4, this is a high value (usual RMS for research work are around 1E-6) but remembering the preliminary nature of this work, these values are acceptable. This will have the effect of reducing the computational time without sacrificing too much accuracy.

Again, a grid dependency study was undertaken. The case used is “Mk iii AoA 2 and Re 1E6”. The result of the study is presented in the following table. Refer to appendix P for the full calculations.

Table 11: Grid dependency study for the 3D case.

Values	Φ= Lift Force	Φ= Drag Force
N_1, N_2, N_3	2.57E6, 1.45E6, 1.16E6	2.57E6, 1.45E6, 1.16E6
r_{21}	1.33	1.33
r_{32}	1.12	1.12
Φ_1	132.5	1198.1
Φ_2	133.3	1196.2
Φ_3	133.3	1195.7
p	4.0	4.0
Φ_{ext}^{21}	132.1	1199.1
e^{21}_{a}	0.62%	0.16%
e^{21}_{ext}	0.30%	0.08%
$\boldsymbol{GCI^{21}_{fine}}$	0.37%	0.10%

The simulation was thus considered as grid independent and the mesh size of 2.57E6 elements will be used throughout the study of the foils.

The different design variations which will be tested are as follows:

- Mk ii: Larger tip chord, same tip span, same elbow radius.
- Mk iii: Normal tip chord, same tip span, same elbow radius.
- Mk iv: Normal tip chord, same tip span, same elbow radius, different shaft.
- Mk v: Normal tip chord, same tip span, smaller elbow radius.

Figure 21: Mk ii, Mk iii and Mk v foils, Mk iv omitted.

Because of the difference in the geometry itslef and the results produced, the Mk iv version was omitted in this study. The probleme being that the more vertical shaft created a sideforce oposed to the sideforce of the tip but with a greater magnitude, which meant that the foil was producing negative sideforce, wich would lead to a large leeway angle. The results are however presented in Appendix Q. The following shows the three tested designs at a range of angle of attack:

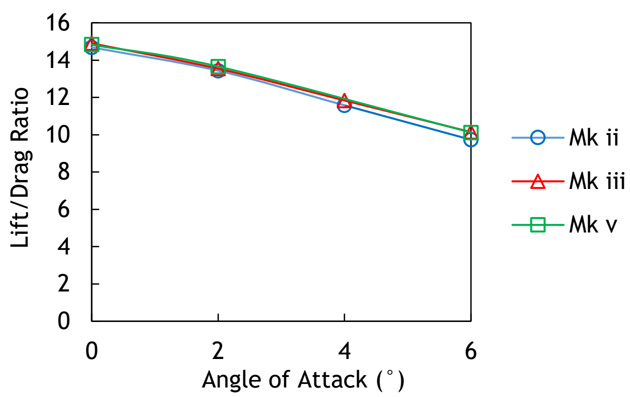

Figure 22: Foils Lift/Drag ratio for different angle of attack.

From the previous graph, one can note that the design variations made between the foils have very little influence on the overall forces produced. The lift drag ratio, are within the same range. The Mk iii shows better lift/drag performances than its opponents. Creating more lift near the tip of the foil will also modify the pressure distribution at this point and the tip vortex generated will therefore be exaggerated.

On the following graph, increasing the size of the tip results in the foil producing less drag for the same sideforce, especially at high angle of attack. This mean that the yacht will be subject to less resistance for the same heeling moment (if we assume that the speed doesn't influence the heeling moment). In a similar way, the bigger tip also produces more lift for the same the drag (see appendix).

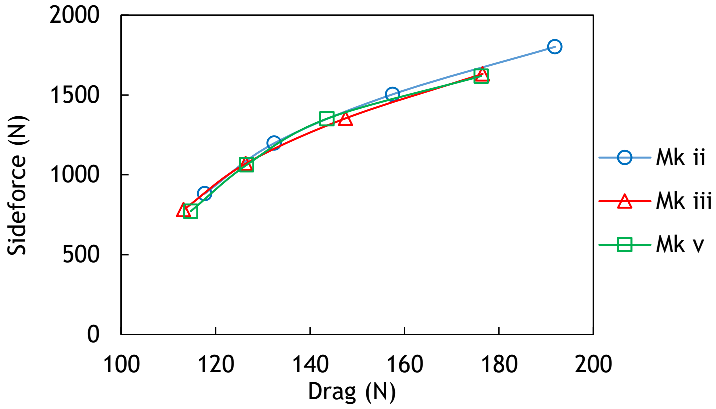

Figure 23: Foil sideforce against drag.

When designing any kind of hydrofoils, a fair amount of time is spend trying to generate a pressure distribution which is as close as possible as being elliptical. This will result in a smaller pressure differential near the tip, therefore reducing induced drag.

The following shows the difference in the flow at the tip. With the bigger tip, more sideforce is produced and an important pressure differential is maintained close to the tip of the foil. This leads to a bigger tip vortex being generated. The other version of the foil produces less sideforce and therefore a not as big tip vortex. From the results shown in **Error! Reference source not found.** We can conclude that even if the tip vortex and therefore the drag is bigger, it is largely compensated by the increased sideforce generated.

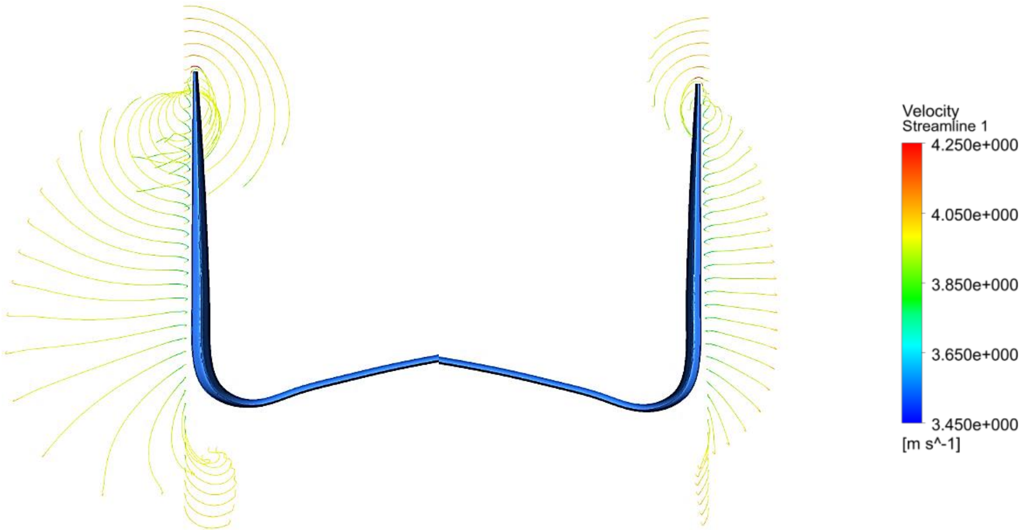

Figure 24: Streamlines showing tip velocity for Mk ii and Mk iii foil at AoA: 4° and Re: 1e6.

It can also be noted that a vortex is not only resent at the tip of the foil, but the elbow also generates a vortex. With the relatively large leeway angle of this case, the pressure gradient crated in the elbow will be relatively big and the generated tip vortex will have a significant impact on the drag. All these assumptions are valid until the foil is piercing the surface, after this, wave drag will become an important factor in the drag of the foil. With a bigger tip vortex, the Mk ii version is more likely to generate more wave drag due to a bigger pressure differential.

Despite this consideration, as it showed better lift/drag ratio and is generating more sideforce, the Mk ii version of this foil will be used on the yacht.

12. Structure

Refer to drawings: Structural Arrangement, Bulkhead and Frames and Structural Details.

The structural design of this yacht must be in accordance with the ISO 12215-5, for design category C, as stated in the class rules. The following will describe the preliminary structural calculations undertaken for this design. The emphasis will be put on the keel and foil structure as a failure of this part would mean a withdrawal of the race. When scantling cannot be obtained from classification society, a first principle approach will be used. The production method will also be looked after due to its influence on the chosen materials and the lamination sequence.

12.1. Construction Method and Materials

Because of the high stiffness to weight ratio required, a carbon epoxy sandwich laminate was specified as it fulfils all the above requirements. With regards to building method, both female and male moulding are attractive. Female moulds usually required less or even no surfacing of the hull, but considering the round shape of the bow of the yacht, bonding the core to the outside skin could be an issue. Using a male mould will be a cheaper solution, as the finish of the mould is not as important like in a female mould. However, a fair amount of fairing will take place to achieve a good surface finish of the hull. Bonding the core to the inside skin could be facilitated. Knowledge of the author on the build technic used on other scow bow mini 6.50 led to the decision to use the latter described building method. Vacuum assistance will help improve the properties of the laminate and ensure a good bonding of the layers together.

12.2. Structural Layout

The structural layout arose from practical considerations and rule driven choices. The Offshore Special Regulations (OSR) requires a forward watertight bulkhead in the first 5 to 15% of the length of the boat. To minimise the size of the forward panels while still providing efficient protection, the bulkhead was placed on the forward perpendicular. To carry the high compressive load, a mast bulkhead was placed under it, amidships. The long panels between those primary stiffeners was broken down with another frame. An aft frame was added 0.6 meters from the transom, to serve as a water ballast side and a cockpit end. The remaining space between this frame and the mast bulkhead was broken down with two additional frames.

A centreline girder is run from the aft frame up to the forward watertight bulkhead. An additional girder, running parallel to the centreline aft of the mast then tappers to the forward watertight bulkhead.

12.3. Panel Hydrostatic Scantling

When designing a hull laminate for a typical yacht, the weight requirement for the skins of the laminate is the driving factor, a symmetric laminate is produced to pass this requirement and then the bending moment requirements are met with addition of unidirectional reinforcements. The following equation express the minimum required dry fibre weight of the outside skin. Note that a care factor (k_6) of 0.9 was taken.

$$w_{OS} = k_{DC} \times k_4 \times k_5 \times k_6 \times (0.1L_{WL} + 0.15)\ kg/m^2$$

Equation 12: Minimum sandwich skin fibre mass requirements (ISO, 2008).

Because of the very light required weight for the outside skin of this yacht (300 g/m^2), another element came into play: the watertightness of the laminate. With common layers used being

200 g/m^2 (it can be argued that lighter fabrics are available but most suppliers don't produce fabric under this weight and they are very hard to hand laminate) and the high fibre volume fraction associated with vacuum assisted lamination, the skin cannot be made watertight under 400 g/m^2.With this in mind, a basic laminate was specified based on knowledge of the author on typical laminate for this type of yachts.

Table 12: Typical bottom laminate.

Layer	Weight (g/m^2)	Orientation
RC-200T	200	±45°
UTC-200	200	0°
M80 CORCELL 15mm	-	-
UTC-200	200	0°
RC-200T	200	±45°

It was decided to use a layer of twill (RC-200T) on the outside of the laminate to give a better surface finish as well as protecting the unidirectional from peeling away if damaged. The required weight of the inside skin could have been reduced to 70% of the weight of the outside skin, but, to prevent the skins from leaking, the same laminate was used.

Because of the high anisotropy of this laminate, care must be taken to design a structure with panel with a high aspect ratio. If not, the panels will not be able to take the bending moment at 90° of the unidirectional fibres. Other laminate sequences have been investigated but none of them gave better results and this was therefore chosen as the basic hull bottom laminate.

Because of its high shear elongation and its good mechanical properties, a SAN foam core (Corcell M) was specified for this yacht. As she will be built on a male mould, the thickness of the core in the hull must be kept to a constant thickness throughout the yacht. As the volume of core used in the hull can be included in the mandatory 1200 litres of buoyancy foam, a core thickness of 15 mm was specified. There is almost no advantages to go for a thinner core as this may require more fibre to cope with the bending moment and the gain in weight would be minimal. The limiting factor for the core is the shear force requirements, which is a function of the core density. Even if those requirements are passed with a significant margin in the slamming region, it was decided to keep the core density to 85 kg/m^3. Because of the addition of foils and the increased speed that the yacht should experience, the slamming loads could be higher than predicted by ISO and the actual margin therefore reduced. The core density was however reduced at the back of the hull and in the topsides, due to the reduced pressure.

With the reduced hydrostatic pressure acting on the topside, the unidirectional layer of the inside skin was removed. It was however kept on the outside skin for watertightness reasons. Refer to Appendix R for ISO 12215-2 panels results.

12.4. Stiffeners

For bulkheads and frame, a basic laminate was specified as per the ISO requirements for the thickness of the skin and the core of sandwich bulkheads.

$$t_s \times t_c \geq \frac{t_b^2}{6}\left(\frac{25}{\sigma_d}\right)\ mm \qquad\qquad t_s \times \frac{t_c^2}{2} \geq \frac{t_b^3}{12}\left(\frac{4000}{E_{io}}\right)\ mm$$

Equation 13: Minimum skin and core thickness for sandwich bulkhead (ISO, 2008).

This yields the following bulkhead laminate:

Table 13: Basic frame and bulkhead laminate.

Layer	Weight (g/m^2)	Orientation
XC-305	305	±45°
M60 CORCELL 15mm	-	-
XC-305	305	±45°

Based on this, each frame and stiffener was reinforced and its high adjusted to pass each requirement by the mean of a unidirectional capping. When the capping was to stiff and therefore attracting the neutral axis of the stiffener, a unidirectional pad was laid underneath the stiffener to bring the neutral axis down and thus increasing the allowable bending moment. It was preferred to extend the frames and stiffeners up, which reduces the size of the cut-out and the amount of capping needed. This results in a lighter frame. Structural depth was not considered an issue in this project.

The height of most of the stiffeners was extended to be able to fit the required 1200 litres of buoyancy foam in the yacht. This results in some stiffeners passing the requirement with a significant margin (see Appendix S).

The forward watertight bulkhead and the aft bulkhead were dimensioned by defining a water head. Both use the same laminate as the frames and no additional stiffener is required.

Where possible, stiffeners have been used for another purpose than supporting a panel. This was achieved by carefully consideration of the structural arrangement of the yacht. Natural stiffeners have been used in area with rapid curvature changes as the chine, the cockpit edge, the toe rails etc. This leads to very few structural members in the yacht and reduces the overall weight.

12.5. Keel Structure

The keel structure being one of the critical part of the yacht, it must be treated with care. The ISO 12215-9 gives guidance on how to proceed to calculate the required bending moment and sheer force which must be taken by the keel floors. It considers four load cases: longitudinal grounding, transverse knock-down, vertical pounding and a special case for canting keels. The maximum shear force and bending moment of these requirements are then used and allocated to each of the keel floor depending on their stiffness. The following assumptions have been made for the keel structure:

- The mast bulkhead is fully fixed between the two floors.
- The aft keel floor is simply supported.
- The centreline girder is omitted for the structural calculations.
- The load is fully transmitted from the keel bearing to the floors.

The keel fin was dimensioned using a first principle approach. A 90° knock-down was assumed as a worst-case scenario. The fin was assumed as a cantilever beam with a point load. Both stress and deflection were checked. As for the foils, the keel fin will be built out of prepreg carbon fibre in a female mould. This will greatly improve the mechanical properties of the fin. Shear boxes will be used to deal with the shear force and the shell of the keel will deal with the bending stress.

The aft keel floor, which will incorporate the yawing axis must be reinforced using first principle approach. The bearing will be made of Vesconite Hilube thermopolymer (Vesconite, 2017), which is a self-lubricating plastic. It can be machined to the required shape and is not affected by salt water. This bearing will be glued inside the frame. Both bearing strength and shear were checked using the loads defined in the ISO 12215-9.

In further iteration of the design the load path of the forward and aft keel bearing would require extra attention. Grillage theory of finite element analysis could be used.

Refer to Appendix T and U for the full calculations.

12.6. Foil Structure

Refer to drawings: Foil Structure.

With the specified section having a thickness chord ratio of 10%, and a chord of 250mm, this yield a foil thickness of 25mm. From preliminary hand calculations using basic carbon fibre properties, it was decided to increase this thickness to 12.5%, to limit deflection and reduce weight, before proceeding to the full 3D analysis of the foils.

The loads were taken from the CFD analysis of the foil in the worst-case scenario and a factor of safety of 5 was added, accounting for the uncertainty in the real loads acting on the foils. The structure of the foil will be check for both stress and deflection. With forces and moments about each axis calculated in CFX, the lever of each force can be calculated by simply dividing each moment with its corresponding force. These forces and levers are then used to calculate the deflection and stress in the foil.

The structure of the foil itself is very dependent on the available building method and materials. As this pieces are usually high-tech and required high strength they are built in carbon prepreg. It was chosen to build them using low temperature carbon prepreg using female mould to give the best possible surface finish. It was then defined that the intrados and extrados of the foil will be made of carbon unidirectional fabric, to take the bending load, with and twill outer layer to give the better possible surface finish and protect the unidirectional from peeling if damaged. Two sheer box, made of double-bias at ±45° will be laminated around CNC shaped non-structural foam plugs. They will have the task of dealing with the shear force and torsion in the foil.

A first principle approach was used to calculate both the stress and the deflection in the foil. It was approximated as a cantilever with a point load. For sack a simplicity, only the bending stress due to on moment will be calculated. The deflection due to shear will also be neglected as the shear force distribution in the foil is known. As with most composite structure, stress requirements are passed before deflection is acceptable. In this case, effort had to be made to keep the deflection and twist angle to sensible figures.

$$\varphi = \frac{Tl}{J_z G}$$

Equation 14: Twist angle equation.

To determine the mechanical properties of the composite laminate classical laminate theory was used. Values provided by prepreg manufacturer (Gurit, 2017) were used instead of ISO standard values as these will result in a very heavy foil. The following shows the final values for the stresses and deflection of the foil.

Table 14: Foil stresses and displacements results.

Variable	Value	Units
Bending Stress max	710	N/mm^2
Shear Stress max	41.12	N/mm^2
Deflection at Tip	28.5	mm
Twist Angle at tip	1.23	°

The given deflection and twist angles will have an influence on the forced produced by the foil. To account for this, a hydro-elastic analysis of the foil would be necessary in further stage of the design. Refer to Appendix V or the full CLA analysis of the laminate and the calculations.

12.7. Foil Support

The supporting structure of the foil will consist of a foil case, between the two foil bearings. A longitudinal frame will be used to take the compressive load of the foil and spread it into the mast and the forward frame. Local reinforcement on the mast bulkhead were calculated using first principle approach. The bearing will be made of the same material as the aft keel bearing.

13. Deck Arrangement

Refer to drawing: Deck Plan

The deck arrangement was design with knowledge of the author on typical deck design and with the help of the parametric study. The major governing rules in this section are the Offshore Special Regulations and the Mini 6.50 rule. The major requirements are highlighted in the following table:

Table 15: Requirements applicable to the deck layout.

Rules	Requirements
Mini 6.50 rule, J-7	The overall volume of the coach roof in cubic meters must be of at least the maximum beam in meters divided by 6.
Mini 6.50 rule, J-8	The deck camber must be of at least 5% of the beam at the gunwale level of the section.
Mini 6.50 rule, J-9	Boats must be equipped with a walkway of at least 30 cm wide, measured between the plan determined between the lifelines and the coach roof.
Mini 6.50 rule, J-11 b	The cockpit floor must be a minimum of 15cm above the waterline.
OSR 3.09.2	The following minimum clear hatch openings if First Launch after 2013: any other shape with minimum dimension of 380 mm and minimum area of 0.18 m^2
OSR 3.09.7	The maximum combined volume below lowest coamings of all contained cockpits shall be: 9% (LWL x maximum beam x freeboard abreast the cockpit) (1.14m^3).

Throughout the design, emphasis has been put on creating a clean and functional deck layout. The weight of each item has been also carefully considered. Textile has been preferred to stainless steel fittings, where possible, to further reduce the weight. They also have the advantage to self-align with the loads. The principal features of this deck arrangement are summarised below:

- A circular mainsheet track to eliminate the need of a vang. Which will also give a better mainsail control than a straight rail. Each end of the rail will be supported in a recess of the deck, with two pillars breaking the span between the two side of the cockpit. The mainsail track also provide an effective way of closing the aft end of the cockpit.
- The aft part of the deck is removed after the mainsail track to lower the stacked equipment. The cockpit sole is used to create the top of the water ballast. A transparent

inspection hatch is installed to enable the level of water in the ballast to be checked and accessed if needed.

- A recess in the coach roof in way of the pit winch to lower its centre of gravity and enable the boom to be fitted lower on the mast. This will help maximise the P dimension of the main and will create a cleaner pit.
- The escape hatch tunnel is extended forward to stiffen the cockpit sole and create a foot step for the skipper when helming.
- A low friction ring is used as a 3D jib system with three different purchase used to create all the possible jib trim combinations. This set-up was preferred to a transverse rail because of the obvious gain in weight but also the improved trimming possibilities. InoBlock (IB 2.4) (Ino-Rope.com, 2017) are used for their weight/load characteristic and efficiency as jib block.
- All small to medium load deck fitting to be Ropeye Pro or Ropeye Twinline depending on the application.
- InoBlock (IB 2.4) are used for their weight/load characteristic and efficiency as spinnaker block. Spinnaker sheet are fitted with a tweaker to enable the gennaker to be run on the same sheet set. A reaching strut can be fitted on each side of the coachrof to open the sails even more.
- Karver KJP 10 jammer (Karver-Systems, 2017) are used in highly loaded applications such has bowsprit arm and backstay primary jammer. Constrictor ropes clutches are used in less loaded application such as halyards, tacklines as well has canting keel mechanism.
- NKE Multigraph display installed on companionway wall with full NKE auto pilot package as described in the following section.

14. Systems Arrangement

Refer to drawing: System Arrangement

14.1. Electrical System

Almost all the required electric power installed on the yacht has the primary function of feeding the auto pilot and its sensors. The chosen electronic package is provided by NKE and features the following items:

- A mast head unit measures the AWA and TWA. This information is fed to the system via a connecting box.
- Due to the high asymmetricity of the hull when heeled, two ultrasonic speed sensors have to be fitted. They are both connected to a dual log/sounder interface with the depth sounder. This is then connected to the system via the connecting box.
- A fluxgate compass, as well as a barometer are completing the measurement instruments. An AIS transmitter is also connected to the system and the VHF as required by the Mini 6.50 rule.
- The Gyropilot 2 calculator, analyse the data provided by the various sensors and translates it to the autopilot.

A Gyropilot graphic and a Multipgraph display and control the autopilot and sensors information.

With a total daily consumption of all the electrical system of 50 Amps, on average (See Appendix W for hotel load detail), and the mandatory batteries of a combined capacity of 200 A/h at 12V they may not need to be recharged every day. Three type of batteries are available for such an application: Deep cycle, AGM and Lithium Ion. The following table shows the different battery type with the weigh and price difference.

Table 16: Battery type comparison.

Type	Model	Weight (kg)	Price ($)
Deep Cycle	Minnkota Pro 100Ah	26.7	169
AGM	Universal 12v 100Ah Deep Cycle	29	339
Lithium Ion	$LifeMnPO^4$	12.8	615

Despite the important increase in price, the gain in weight being quite significant, and the batteries being more robust than standard deep cycle batteries. Lithium Ion batteries have been selected as house batteries for the yacht.

They are several ways of producing electricity on a small racing yacht like this, hydro generators, solar panels, standard generators and fuel cells being the most common. Not all these systems are best suited for a small and wet boat like this one. The following will compare the four options with an interest mostly on the power produced to weight ratio. Cost will also be considered but only marginally.

Table 17: Power generation comparison.

Power Plant	Weight kg	Production A/Day	Price £	Production/Weight A/Day/kg
Watt&Sea Hydro generator	7.5	240	3132	32
Efoy Comfort 80 Fuel Cell	7.1	80	2200	11.3
MaxPower Marine Fuel Cell 75	6.4	75	Unknown	11.7
Islanders Solar Panel HD (1155x560mm)	2.5	34	380	13.6
Honda EU1000i Fuel Generator	13	192	760	14.8

The most efficient power production device seems to be the hydro generator, it can produce almost 5 time the required daily consumption but requires a complicated installation if required to operate when heeled and on both tacks. It also creates drag when operating. The fuel cells are the less efficient but have the big advantage of being lighter than the hydro generator and fuel generator. They can be programmed to start when the battery reaches a pre-defined discharge level and will stop when this one is full, which means that they operate on their own and don't require the skipper to take care of them. The solar panel, if able to run for the predicted 6 hours fails to deliver the required power. It was therefore discarded. The standard generator, which produces more than enough power has the disadvantage of being the heaviest and the noisiest.

With its weight and ability to be programmed, despite its high price, the Efoy fuel cell was selected has the power generation unit for the yacht.

14.2. Water Ballast System

To increase the righting moment and trim the yacht on her stern, a water ballast system was fitted, as discussed in the previous section. To provide seawater to the system, a system of scoop are be installed. Usually this system features a connecting pipe between the water ballast and knife gate valves which is opened when the water has to be changed of side.

To fill and empty the tanks, small yachts like this usually rely on their speed and don't include a pump in the system. A first principle approach was used to calculate if a pump was required or not. Bernoulli's equation can be used to determine the speed required to push the water in the tank. To simulate for a worst-case scenario, the ambient pressure at the scoop inlet was assumed to be the atmospheric pressure and not the atmospheric pressure plus the water head. The results showed that above 5 knots of boat speed, the ballast (in the upright condition) can be filled without the use of a pump.

$$\frac{v^2}{2} + gz + \frac{p}{\rho} = constant$$

Equation 15: Bernoulli's principle.

The scoop provides the mean of filling, closing and emptying the ballast. To further reduce the weight, it was decided to fit only on scoop for the whole boat, this means that when the ballast have to be filled the first time, the boat may require to be kept flat for the duration of the filling procedure but this will not affect the overall performance. Once they have been filled, they can be stacked to the other side by simply using the knife gate valve which can be operated from the deck.

14.3. Canting Keel System

The canting keel being not only canting but also extending and yawing, a complex system had to be specified. The canting is actuated by purchase each side of the keel, which are redirected outside to the primary winches. They use built-in constrictor clutches attached to the companionway panel to lock the keel in the chosen position. The extension is controlled by the cant. The more the keel is canted, the more it extends. To be able to put the keel back in its centreline position, a purchase is also fitted above it, which enable the keel to be lifted and pulled back in its original position. The yaw is controlled on the aft bearing, which slide in a bearing made of Vesconite hi-lube thermopolymer, by a lead screw which can be operated from the cockpit. The lead crew offers the best option compared to a rope system which will give a bit when the keel will be under load.

15. Conclusion

Throughout the preliminary design of this Mini 6.50 area requiring future work and refinement have been highlighted. One of these area is the performance prediction of planing sailing yacht hull, apart from towing tank and computational fluid dynamic, no basic method can be used to efficiently estimate their performances. This leads to major differences between predictions and actual data. A regression method is available to assess the resistance and lift of such hull shape but because of the required number of boat which should be tested and the measurement capability of the towing tank, this option had to be disregarded.

The method presented at the onset of this project, to compare the hull shape in the towing tank, and which was discarded by one of the staff member because of being too time consuming should have been followed. Results considering the lift generated by the hull would have given a more valuable hull comparison.

Because of the preliminary nature of this work, some area had to be omitted or covered very briefly. Others, where investigates in more depth. At this preliminary stage, it should be remembered that the presented yacht still falls within the assumptions made:

- The hull comparison assumes that the different hull shape will be sailing at the same righting moment, this may not be true, as the yacht with less righting moment should heel more to compensate, which will reduce the sail side force and the heeling moment. The keel position was assumed to be fully canted in all the time, while being true for medium to strong wind conditions sailing, it may not be for light wind.
- The advanced VPP analysis didn't converged due to too many parameters being blocked to simplify and reduce the amount of data required, which led to the solver not finding any equilibrium. As stated previously, this could perhaps be resolved by adding the trim to the parameters of the yacht. Or by allowing the rake of the foil to be adjusted. If the use of the VPP had been defined earlier, it could also have been used to choose the different foil design by comparing them in real operating conditions.
- The choice of the foil geometry is based purely on a single flow analysis of the different candidate, thus not reflecting the actual operating conditions of the foil. This simplistic approach as the benefit of highly reducing the complexity of the simulation but is not very accurate.
- The structural calculations undertaken for the keel and foil is based on a first principle approach, where the actual loads acting on them are highly uncertain, this was dealt with a good factor of safety. More refined analysis of these structure could lead to an improvement, both in terms of load definition and scantlings.
- With the major requirements of the rules checked and passed during the design phase, it leaves an important number of small requirements to be checked if the design is carried on further.

To conclude, this preliminary design complies with most the objective set in the design brief except for the hull comparison, which turned out to be more challenging than expected. Performance, structural and stability aspect have been dealt with using various rules and regulations, as well as first principle approach. With the event of foils, more refined velocity prediction program accounting for more than three degrees of freedom and computational fluid dynamic analysis will certainly be a field of interest in the future.

16. References

A. Claughton, R. Pemberton, M. Prince, 2012. *Hull-Sailplan balance, "lead" of the 21th Century,* Southampton: Wolfson Unit M.T.I.A..

ANSYS, 2011. *ANSYS CFX-Solver Theory Guide*. Canonsbury: ANSYS, Inc.

Dr. J. Raymond, K. Cudby, 2012. *USING PARAMETRIC MODELLING, CFD, AND HISTORICAL DATA, TO ESTIMATE PLANING HULL PERFORMANCE ON A LAPTOP,* Auckland: 4th High Performance Yacht Design Conference.

Eng-tips, 2012. *Calculatinf Tension and Sag in a cable*. [Online] Available at: http://www.eng-tips.com/viewthread.cfm?qid=317545
[Accessed 25 February 2017].

ERS, 2017. *Equipment Rules of Sailing 2017-2020.* 2017 ed. Southampton: World Sailing.

Fossati, F., 2009. *Aero-hydrodynamics and the Performance of Sailing Yachts, the Science behind Sailing Yacht and their Design*. London: Adlard Coles Nautical.

Gurit, 2017. *Epoxy prepregs*. [Online] Available at: http://www.gurit.com/Our-Business/Composite-Materials/Prepregs/Epoxy-Prepregs/SE-70
[Accessed 2 March 2017].

H. Versteeg, W. Malalasrka, 2007. *An Introduction to Computational Fluid Dynamics: The Finite Volume Method, Second Version*. Harlow: Pearson Prentice Hall.

Hoerner, S. F., 1965. *Fluid-Dynamic Drag*. Bakersfield: Published by the Author.

Hydros-Innovation, 2017. *Hydros Innovation - Efficient Energy*. [Online] Available at: http://www.hydros.ch/en/hydros-innovation/expertise.html
[Accessed 24 April 2017].

I.B. Celik, U. G. P. R. C. F. H. C. P. R., 2008. *Procedure for Estimation and Reporting of Uncertainty Due to Discretization*. s.l.:Journal of Fluids Engineering.

Ino-Rope.com, 2017. *Ino-Rope*. [Online] Available at: http://www.inorope.com/shop/poulies-et-anneaux/poulie-textile-ino-block-2-4/
[Accessed 16 April 2017].

ISO, 2008. *Small craft-Hull construction and scantlings-Part5: Design pressures for monohulls, design stresses, scantlings determination*. Brussel: International Organization for Standardtization.

ISO, 2015. *Small craft-Stability and buoyancy assessment and categorization, Part 2: Sailing boats of hull length greater than or equal to 6 m*. Brussels: International Organization for Standartization.

J. A. Keuning, M. Katgert, K. J. Vemeulen, 2006. *Keel-Rudder Interaction on Sailing Yacht,* Amsterdam: HISWA.

J. A. Keuning, M. Katgert, 2008. *A Bare Hull Resistance Prediction Method Derived From The Results of the Delft Systematic Yacht Hull Series Extended to Higher Speeds*. Delft, RINA.

J. A: Keuning, U.B. Sonnenberg, n.d.. *Approximation of the Hydrodynamic Forces on a Sailing Yacht Based on the "Delft Systematic Yacht Hull Series"*. s.l., HISWA.

Karver-Systems, 2017. *Karver Systems*. [Online] Available at: http://www.karver-systems.com/fr/downloads/catalog
[Accessed 16 April 2017].

Kouyoumdjian, J., 2014. Effective design or fashion craze?. *Seahorse Magazine*, p. 34.

L. Larson, R. E. Eliasson, M. Orych, 2014. *Principles of Yacht Design*. 4th ed. London: Adlard Coles Nautical.

LEAP, 2017. *Wall Function and Y+ requirements*. [Online] Available at: https://www.computationalfluiddynamics.com.au/tips-tricks-turbulence-wall-functions-and-y-requirements/

M. Prince, A.R. Claughton, n.d. *Estimating a Yacht's Hull-Sailplan Balance and Sailing Performance using Experimental Results and VPP Methods*, Southampton: Wolfson Unit M.T.I.A..

Magicseaweed, 2016. *Mid Atlantic Charts*. [Online] Available at: http://magicseaweed.com/Mid-Atlantic-Surf-Chart/22/?chartType=WMAG&selectedStartTimestamp=1478822400&selectedEndTimestamp=1480204800

Mini, 2017. *Mini Rules 2016 Edition*. Lorient: Mini 6.50 Class.

NGA, 2016. *National Geospatial Intelligence Agency*. [Online] Available at: http://msi.nga.mil/NGAPortal/MSI.portal?_nfpb=true&_pageLabel=msi_portal_page_62&pubCode=0003
[Accessed 3 October 2016].

OSR, 2017. *Offshore Special Regulations 2017*. 2017 ed. Southampton: World Sailing.

Raymond, J., 2009. *Estimation Des Performances Des Voiliers au Planing et en Manoeuvre*, Nantes: Ecole Centrale de Nantes.

Ridley, J., 2017. *CFD run for 3D foil comparison*. Southampton: s.n.

RRS, 2017. *Racing Rules of Sailing 2017-2020*. 2017 ed. Southampton: World Sailing.

T. Whiden, M. Levitt, 2016. *The Art and Science of Sails, revised edition*. Brooklin: Seapoints Books and Media LLC.

Verdier, G., 2015. *Voile et Voiliers*. [Online] Available at: http://www.voilesetvoiliers.com/portraits/guillaume-verdier-2-la-confirmation-architecture-navale-safran/
[Accessed 23 November 2016].

Vesconite, 2017. *Vesconite Hilibe*. [Online] Available at: http://www.vesconite.com/vesconite-hilube/
[Accessed 20 March 2017].

17. Bibliography

Presles, D. Paulet, D. 1998. *Architecture Navale-Connaisance et pratique*. Revised Edition. Paris. Editions de la Villette.

Claughton, A. Wellicome, J. Shenoi, A. 2006. *Sailing Yacht Design: Theory*. Southampton. Henri Ling Ltd.

Claughton, A. Wellicome, J. Shenoi, A. 2006. *Sailing Yacht Design: Practice*. Southampton. Henri Ling Ltd.

18. Appendices

Appendix A: Parametric Study

Sail N°	Designer	Skipper	Year	L_{OA} (m)	B_{OA} (m)	L_{WL} (m)	B_{WL} (m)	T (m)	Air Draft (m)	Displ. (kg)	Ballast (kg)	Ballast Ratio	Sail Area (m^2) Upwind	Sail Area (m^2) Downwind	L_{WL}/B_{WL}	$L_{WL}/Vol.^{1/3}$	$S.A./Vol.^{2/3}$
747	D. Raison	D. Raison	2010	6.5	3	5.3	2.17	2	12	750	270	0.36	48	125	2.4	5.88	59
754	S.Manuard	B.Delnese	2009	6.5	3	6.5		2	11	710			54	120		7.35	69
787	S.Manuard	-	2010	6.5	3	6.5		2	11	700	240	0.34	42	140		7.38	54
800	M.Lombard	F.Denis	2011	6.5	3	6.5		2	12	750			48	130		7.21	59
850	M.Lombard	S.Malard	-	6.5	3	6.5		2	12	700	312	0.45				7.38	
865	D. Raison	I.Lipinski	2014	6.5	3	5.8		2	12								
888	Mer Forte	S.Koster	2015	6.5	3	5.8	2.56	2	12	750	300	0.40	49	110	2.3	6.44	60
894	E.Bertrand	-	2015	6.5	3	5.95		2	12	700			47	114		6.76	61
900	R.Neyhousser	-	2016	6.5	3	5.6		2	11.4	800			44	107		6.08	
v1.6	M.Lauber	-	2017	6.5	3	6.22	2.2	2	12	710	300	0.42	48	115	2.83	7.03	61
v2.6	M.Lauber	-	2017	6.5	3	5.64	2.34	2	12	710	300	0.42	48	115	2.41	6.37	61

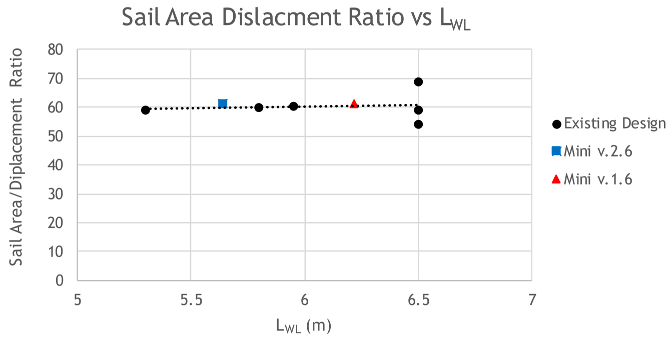

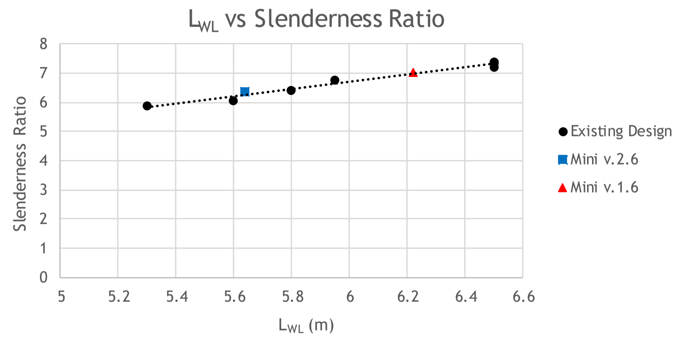

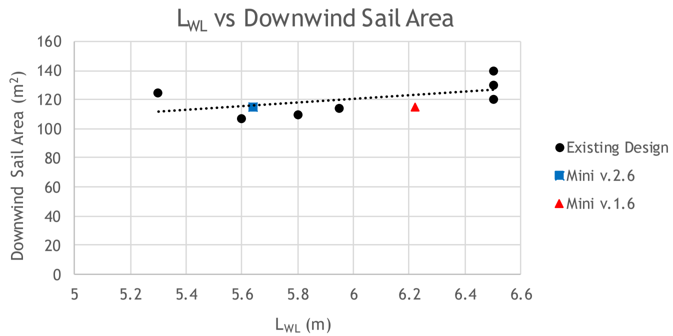

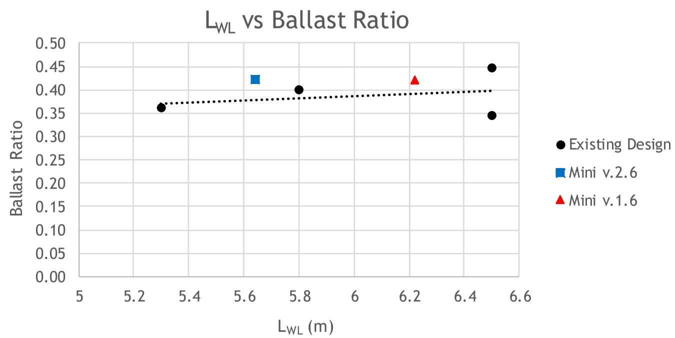

Appendix B: Preliminary Weight Estimate

Group 1- Hull, Deck & Appendages									
Item	Unit Weight (kg)	Quantity	Weight (kg)	LCG (m)	VCG (m)	TCG (m)	LM (kgm)	VM (kgm)	TM (kgm)
Hull Shell	67.3	1	67.3	0.3	0.2	0.0	18.4	10.2	0
Internal Structure	9.1	1	9.1	0.0	0.0	0.0	0.2	0.2	0
Deck & Coachroof	49.9	1	49.9	0.0	0.8	0.0	0.8	39.7	0
Bulkhead	22.4	1	22.4	0.2	0.5	0.0	5.1	10.3	0
Keel fin (Keel on CL)	9.0	1	9.0	0.3	-1.0	0.0	2.8	-8.6	0
Foils	10.2	2	20.5	0.7	-0.1	0.0	13.3	-1.7	0
Rudder	3.5	2	7.0	-2.9	-0.3	0.0	-20.4	-1.8	0
Ballast (1 full)	160.0	0	0.0	-2.5	0.2	-0.8	0.0	0.0	0
Bulb (Keel on CL)	300.0	1	300.0	0.3	-1.9	0.0	92.1	-567.0	0
Nominal Total			485.1				112.4	-518.6	0
Margin	10%		48.5				LCG (m)	VCG (m)	TCG (m)
Margin Total			533.7				0.21	-0.97	0

Group 2- Mast & Sails									
Item	Unit Weight (kg)	Quantity	Weight (kg)	LCG (m)	VCG (m)	TCG (m)	LM (kgm)	VM (kgm)	TM (kgm)
Mast Tube	15.0	1	15.0	0.32	6.56	0.00	4.86	98.45	0
Spreaders	2.0	1	2.0	0.45	5.14	0.00	0.90	10.28	0
Stays	2.0	1	2.0	-0.05	6.00	0.00	-0.10	12.00	0
Boom	3.5	1	3.5	-1.19	1.39	0.00	-4.17	4.85	0
Pole	3.5	1	3.5	1.87	1.00	0.00	6.53	3.50	0
Mainsail with 3 reefs (250 g/m^2+40% for reinforcement)	10.0	1	10.0	-1.07	6.23	0.00	-10.66	62.30	0
Jib with reef (4.6 Oz+75% for reincorcment)	6.3	1	6.3	1.37	4.41	0.00	8.65	27.78	0
Storm Jib (min. 340g/m^2)	2.7	1	2.7	0.50	0.20	0.00	1.36	0.54	0
A1.5/2 (.75 Oz)	5.8	1	5.8	0.50	0.20	0.00	2.88	1.15	0
A4 (.9 Oz)	5.8	1	5.8	0.50	0.20	0.00	2.88	1.15	0
Code 5 (1.5 Oz)	5.9	1	5.9	0.50	0.20	0.00	2.93	1.17	0
Gennaker (3 Oz)	5.4	1	5.4	0.50	0.20	0.00	2.70	1.08	0
Stanchions (Aluminium)	5.0	1	5.0	-0.25	0.96	0.00	-1.26	4.81	0
Lifelines, 35m 5mm Dyneema (15g/m)	0.5	1	0.5	-0.12	1.06	0.00	-0.06	0.56	0
Nominal Total			73.305				17.43	229.62	0
Margin	10%		7.3305				LCG (m)	VCG (m)	TCG (m)
Margin Total			80.6355				0.22	2.85	0

Group 3- Deck Hardware & Running Rigging									
Item	Unit Weight (kg)	Quantity	Weight (kg)	LCG (m)	VCG (m)	TCG (m)	LM (kgm)	VM (kgm)	TM (kgm)
20 Self-Tailing Performa™ Winch	2.400	2	4.8	-1.2	0.9	0.0	-5.6	4.2	0
20 Self-Tailing Performa™ Winch Pit	2.400	1	2.4	-0.6	1.2	0.0	-1.5	2.9	0
Winch Handle (SpeedGrip Lock-In)	0.600	2	1.2	-1.0	0.5	0.0	-1.2	0.6	0
Pit Which Handle (Harken Low Profile)	0.400	1	0.4	-1.0	0.5	0.0	-0.4	0.2	0
Harken Standard Cam-Matic Cleat with Fairlead	0.078	18	1.4	-1.0	0.8	0.0	-1.4	1.1	0
Backstay Jammer (Karver KJP10)	0.210	2	0.4	-1.6	0.5	0.0	-0.7	0.2	0
Clutches (Cousin Constrictor® for 6mm rope)	0.150	6	0.9	0.2	1.2	0.0	0.2	1.0	0
Pole Jammer (Karver KJP10)	0.210	2	0.4	-0.9	0.8	0.0	-0.4	0.3	0
Ropeye Pro 50/40-4	0.035	10	0.4	-0.4	0.9	0.0	-0.1	0.3	0
Ropeye SLR 10/7	0.005	10	0.1	-0.4	0.9	0.0	0.0	0.0	0
Ropeye Twinline 4	0.029	5	0.1	-0.4	0.9	0.0	-0.1	0.1	0
Harken 29mm T2 Block (Mast foot)	0.012	5	0.1	0.5	1.1	0.0	0.0	0.1	0
Halyards (Lancelin Helios 6 mm, 3kg/100m)	0.030	150	4.5	0.3	6.3	0.0	1.2	28.1	0
Sheet (Lancelin Helios 6 mm, 3kg/100m)	0.030	1	0.0	-2.2	0.9	0.0	-0.1	0.0	0
Control Ropes (5mm)	0.020	50	1.0	-0.4	0.9	0.0	-0.4	0.9	0
Spinnaker Blocks (IB 2.4)	0.043	4	0.2	-1.9	0.7	0.0	-0.3	0.1	0
Jib Blocks (IB 2.4)	0.043	2	0.1	-1.2	0.7	0.0	-0.1	0.1	0
Keel Cant Blocks (IB 2.4)	0.043	6	0.3	0.3	0.1	0.0	0.1	0.0	0
Keel Cant Blocks (IB 3.6)	0.048	2	0.1	0.3	0.1	0.0	0.0	0.0	0
Harken 22 mm End Control No. 2740	0.114	2	0.2	-2.0	0.8	0.0	-0.5	0.2	0
Harken 22m High Beam Slide Bolt Track No.2721 (710g/	0.710	3	2.1	-2.0	0.8	0.0	-4.3	1.6	0
Harken 29mm T2 Block (Mainsheet travler)	0.012	2	0.0	-2.0	0.8	0.0	0.0	0.0	0
Harken 29mm T2 Block (Mainsheet Car)	0.012	2	0.0	-2.0	0.8	0.0	0.0	0.0	0
Tiller System+Extension (Spinlock EA1200)	2.780	1	2.8	-2.3	0.5	0.0	-6.4	1.4	0
Mainsail Block	0.695	1	0.7	-2.1	1.0	0.0	-1.5	0.7	0
Sofo Scoop and Butterfly valve	1.230	2	2.5	-1.8	0.0	0.0	-4.428	0	0
Ballast Piping	2.200	1	2.2	-2.1	0.0	0.0	-4.62	0	0
Nominal Total			29.2				-32.5	44.3	0
Margin	20%		5.8				LCG (m)	VCG (m)	TCG (m)
Margin Total			35.1				-0.93	1.26	0

Group 5- Safety Equipment									
Item	Unit Weight (kg)	Quantity	Weight (kg)	LCG (m)	VCG (m)	TCG (m)	LM (kgm)	VM (kgm)	TM (kgm)
Liferaft ISO 9650-1 (4 person Viking RescYou™ in valise)	28	1	28	-2.2254	0.13	0	-62.31	3.64	0
Floating Knife near Liferaft	0.07	1	0.07	-2.2254	0.13	0	-0.16	0.01	0
Survival Container:									
Container	0.5	1	0.5	-1.9	0.19	0	-0.95	0.10	0
Knife	0.07	1	0.07	-1.9	0.19	0	-0.13	0.01	0
Survival Food (min 500g for each crew)	0.5	1	0.5	-1.9	0.19	0	-0.95	0.10	0
Signal Mirror	0.025	1	0.25	-1.9	0.19	0	-0.48	0.05	0
Waterproof Torch	0.075	1	0.075	-1.9	0.19	0	-0.14	0.01	0
Fishing Equipement	0.005	1	0.005	-1.9	0.19	0	-0.01	0.00	0
Automatic red hand Flare	0.05	4	0.2	-1.9	0.19	0	-0.38	0.04	0
Floating Smoke Signals	0.05	2	0.1	-1.9	0.19	0	-0.19	0.02	0
Handheld VHF (Standard Horizon HX870E VHF Radio DSC)	0.322	2	0.644	-1.9	0.19	0	-1.22	0.12	0
Survival Blanket	0.15	1	0.15	-1.9	0.19	0	-0.29	0.03	0
Lightstick	0.06	3	0.18	-1.9	0.19	0	-0.34	0.03	0
Seamark Dye Marker (min 40g)	0.04	1	0.04	-1.9	0.19	0	-0.08	0.01	0
Tube of Sunscreen	0.06	2	0.12	-1.9	0.19	0	-0.23	0.02	0
Survival Water Container (10 litres)	10	1	10	-1.9	0.19	0	-19.00	1.90	0
EPIRB (GlobalFix™ Pro) + Bracket for EPIRBs	0.725	1	0.725	-1.9	0.19	0	-1.38	0.14	0
Survival Suite ISO 15027-1, 0.75 clo (T.P.S. Manoeuvring	3.5	1	3.5	-1.9	0.19	0	-6.65	0.67	0
White Flare	0.01	2	0.02	-1.9	0.19	0	-0.04	0.00	0
Bildge Pump Outside (Plastimo 925, 0.9 l without By Pass	0.92	1	0.92	-1.9	0.19	0	-1.75	0.17	0
Bildge Pump inside	0.597	1	0.597	-1.9	0.19	0	-1.13	0.11	0
Radio									
Topmast VHF antenna with cable (min 4mm)	0.2	1	0.2	0.303	0.149	0	0.06	0.03	0
Emergency Entenna	0.2	1	0.2	0.303	0.149	0	0.06	0.03	0
12v Betteries of combined 200 A/h	12.7	2	25.4	0.303	0.149	0	7.70	3.78	0
Nautical Books	0.2	1	0.2	0.303	0.149	0	0.06	0.03	0
COLREGS	0.2	1	0.2	0.303	0.149	0	0.06	0.03	0
International Code Signals	0.01	1	0.01	0.303	0.149	0	0.00	0.00	0
Logbook	0.01	1	0.01	0.303	0.149	0	0.00	0.00	0
Tide Table	0.01	1	0.01	0.303	0.149	0	0.00	0.00	0
Sailing Directions	0.01	1	0.01	0.303	0.149	0	0.00	0.00	0
List of Lights	0.1	1	0.1	0.303	0.149	0	0.03	0.01	0
Charts	0.2	1	0.2	0.303	0.149	0	0.06	0.03	0
Anchore (Fortress FX7 1.8kg)	1.8	1	1.8	0.303	0.149	0	0.55	0.27	0
8m of 6mm chain (0.85 kg/m)	6.8	1	6.8	0.303	0.149	0	2.06	1.01	0
25m of 10mm rope	1.7	1	1.7	0.303	0.149	0	0.52	0.25	0
Radar Deflector	1	1	1	0.303	0.149	0	0.30	0.15	0
Mast Harness (Mast Prop Harness)	0.73	1	0.73	0.303	0.149	0	0.22	0.11	0
Safety Harness EN 1095 Standard (Lifejacket)	0	1	0	0.303	0.149	0	0.00	0.00	0
Lifejacket BSA 55kg ISO 12402-8 (Spinlock 5D Hammar 1	1.32	2	2.64	0.303	0.149	0	0.80	0.39	0
Spare gas bottle for lifejacket	0.033	1	0.033	0.303	0.149	0	0.01	0.00	0
ORC Tether	0.25	1	0.25	0.303	0.149	0	0.08	0.04	0
Fog horn	0.012	1	0.012	0.303	0.149	0	0.00	0.00	0
Dose of Seamerker (min 40g)	0.04	1	0.04	0.303	0.149	0	0.01	0.01	0
First Aid Kit	4.0215	1	4.0215	0.303	0.149	0	1.22	0.60	0
Lifebuoy such as defined in E-9-a	2.5	1	2.5	0.303	0.149	0	0.76	0.37	0
Floating line such as defined in E-9-b	3	1	3	0.303	0.149	0	0.91	0.45	0
Dan buoy such as defined in the OSR and a wistle connected to the lifefloat with a 3 metre floating line	3.3	1	3.3	0.303	0.149	0	1.00	0.49	0
Fire extinguisher type B34 or better, accessible from the outside, protected from tampering	4.1	1	4.1	0.303	0.149	0	1.24	0.61	0
Fire blanket		1	0.1	0.303	0.149	0	0.03	0.01	0
Rigid buckets (min. 9 l) with lines, including one adapted and dedicated to the use of toilets	0.5	2	1	0.303	0.149	0	0.30	0.15	0
Water bailer	0.15	1	0.15	0.303	0.149	0	0.05	0.02	0
Waterproof torches such as defined in article E-7	0.05	1	0.05	0.303	0.149	0	0.02	0.01	0
Steering compass	0.3	1	0.3	0.303	0.149	0	0.09	0.04	0
Hand bearing compass	0.3	1	0.3	0.303	0.149	0	0.09	0.04	0
Navigation ruler	0.015	1	0.015	0.303	0.149	0	0.00	0.00	0
Sextant (Davis Mark-15 Plastic Sextant)	0.45	1	0.45	0.303	0.149	0	0.14	0.07	0
Equipment and documents to complete celestial navigatio	0.2		0	0.303	0.149	0	0.00	0.00	0
Pair of binoculars (Fujinon 7X50 WPC-XL Mariner)	0.91	1	0.91	0.303	0.149	0	0.28	0.14	0
Boat hook	0.2	1	0.2	0.303	0.149	0	0.06	0.03	0
Tricolour light visible with sails hoisted(3)	0.005	1	0.005	0.303	0.149	0	0.00	0.00	0
Emergency lights visible with sails up	0.005	1	0.005	0.303	0.149	0	0.00	0.00	0
Tools	2.5	1	2.5	0.303	0.149	0	0.76	0.37	0
System to liberate the rigging	1.2	1	1.2	0.303	0.149	0	0.36	0.18	0
Oar with rowlock fixed to the transom	0.1	1	0.1	0.303	0.149	0	0.03	0.01	0
Set of Q, N, C, national and courtesy flags	0.1	1	0.1	0.303	0.149	0	0.03	0.01	0
Drogue anchore (0.5 X 1 m) with a swivel	0.54	1	0.54	0.303	0.149	0	0.16	0.08	0
Spare batteries	0.2	1	0.2	0.303	0.149	0	0.06	0.03	0
Spare bulbs	0.01	1	0.01	0.303	0.149	0	0.00	0.00	0
Spare fuses	0.005	1	0.005	0.303	0.149	0	0.00	0.00	0
Stacking Bag OUTILS OCEANS (60x28x28)	1.26	2	2.52	0.303	0.149	0	0.76	0.38	0
Tool bag OUTILS OCEANS CO3 (L35xH20xE10) ChargeMax	1.1	1	1.1	0.303	0.149	0	0.33	0.16	0
Nominal Total			116.89				-76.52	17.65	0
Margin	10%		11.69				LCG (m)	VCG (m)	TCG (m)
Margin Total			128.58				-0.60	0.14	0

Group 4- Navigation/Communication & Power									
Item	Unit Weight (kg)	Quantity	Weight (kg)	LCG (m)	VCG (m)	TCG (m)	LM (kgm)	VM (kgm)	TM (kgm)
Multigraphic	0.75	1	0.75	-0.6	1.1	0	-0.45	0.83	0
Gyropilot Graphic	0.74	1	0.74	-0.6	1.1	0	-0.44	0.81	0
NKE Mechanical Ram	3	1	3	-2.2	0.3	0	-6.60	0.90	0
Depth Sounder	0.7	1	0.7	1	-0.114	0	0.70	-0.08	0
Masthead Wind Sensor	0.52	1	0.52	0.05	12.2	0	0.03	6.34	0
Fluxgate Compas	0.27	2	0.54	-1	0.4	0	-0.54	0.22	0
Ultrasonic speed sensor	0.16	2	0.32	1	-0.114	0	0.32	-0.04	0
Dual Log/Sounder interface	0.16	1	0.16	1	-0.114	0	0.16	-0.02	0
Rudder angle sensor	0.45	1	0.45	-2.6	0.42	0	-1.17	0.19	0
Gyropilot Remote control	0.065	1	0.065	-1	0.4	0	-0.07	0.03	0
Universal radio reciever	0.26	1	0.26	-1	0.4	0	-0.26	0.10	0
AIS transponder	0.25	1	0.25	-1	0.4	0	-0.25	0.10	0
Gyropilot Processor - with embedded Gyrocompass	1	1	1	-1	0.4	0	-1.00	0.40	0
Baro HR 100	0.27	1	0.27	-1	0.4	0	-0.27	0.11	0
Icom-M423G 25 W	1.2	1	1.2	-1	0.4	0	-1.20	0.48	0
Nav Lights	0.03	1	0.03	0.032	12	0	0.00	0.36	0
BLU Sangean ATS 909-X (not on circuit)	0.735	1	0.735	-1	0.4	0	-0.74	0.29	0
Efoy Comfort 80 Fuel Cell	6	1	6	-1.5	0.1	0	-9.00	0.60	0
Efoy Methanol	15	1	15	-1.5	0.1	0	-22.50	1.50	0
Nominal Total			31.990				-9.84	9.89	0
Margin	10%		3.199				LCG (m)	VCG (m)	TCG (m)
Margin Total			35.189				-0.28	0.28	0

Group 6- Other & Consumables									
Item	Unit Weight (kg)	Quantity	Weight (kg)	LCG (m)	VCG (m)	TCG (m)	LM (kgm)	VM (kgm)	TM (kgm)
Skipper	75	1	75	-1.6	1	0	-120	75	0
Clothing	5	1	5	0.3	0.8	0	1.5	4	0
Water (3.5L/Person/Day)	60	1	60	-0.2	0.1	0	-12	6	0
Food	7	1	7	-0.2	0.1	0	-1.4	0.7	0
Other	2	1	2	-0.2	0.1	0	-0.4	0.2	0
Stacking Bag for Food OUTILS OCEANS (60x28x28, 45L)	1.26	1	1.26	-0.2	0.1	0	-0.252	0.126	0
Nominal Total			150.26				-132.55	86.03	-46.53
Margin	10%		15.026				LCG (m)	VCG (m)	TCG (m)
Margin Total			165.29				-0.80	0.52	-0.28

Total									
Item	Unit Weight (kg)	Quantity	Weight (kg)	LCG (m)	VCG (m)	TCG (m)	LM (kgm)	VM (kgm)	TM (kgm)
Group 1- Hull, Deck & Appendages	533.66	1	533.66	0.21	-0.97	0.00	112.41	-518.58	0
Group 2- Mast & Sails	80.64	1	80.64	0.22	2.85	0.00	17.43	229.62	0
Group 3- Deck Hardware & Running Rigging	35.08	1	35.08	-0.93	1.26	0.00	-32.55	44.29	0
Group 4- Navigation/Communication & Power	35.19	1	35.19	-0.28	0.28	0.00	-9.84	9.89	0
Group 5- Safety Equipment	128.58	1	128.58	-0.60	0.14	0.00	-76.52	17.65	0
Group 6- Other & Consumables	165.29	1	165.29	-0.80	0.52	-0.28	-132.55	86.03	-46.53
Total with Margin (Transat Start)			978.44				-121.6	-131.1	-46.5
Total with Margin (Transat Finish)			925.44				**LCG (m)**	**VCG (m)**	**TCG (m)**
Design Displacement (Average Transat)			**951.94**				**-0.12**	**-0.13**	**-0.05**

Appendix C: WinDesign VPP Results

Mini Transat- Course Deltas for range of true wind speeds														
Yacht/TWS	4	5	6	7	8	9	10	12	14	16	20	25	30	35
Mini v.1.4	0	0	0	0	0	0	0	0	0	0	0	0	0	0
Mini v.1.5	47.002	42.368	30.288	20.169	15.494	12.643	11.354	12.923	12.798	11.229	6.992	4.703	5.094	5.103
Mini v.1.6	109.426	86.739	46.469	7.472	-0.214	-0.747	0.21	13.143	16.91	17.807	13.596	12.363	19.607	22.516
Mini v.2.4	-38.594	-61.718	-83.878	-89.009	-94.766	-101.024	-102.601	-119.507	-110.008	-102.153	-83.766	-68.265	-59.312	-52.366
Mini v.2.5	-70.691	-103.271	-124.22	-123.469	-127.056	-132.904	-133.193	-155.48	-147.128	-136.437	-109.367	-88.355	-77.662	-69.119
Mini v.2.6	-45.39	-69.323	-87.426	-91.052	-94.849	-98.35	-98.708	-111.086	-101.116	-93.638	-73.475	-58.799	-52.468	-47.167

Course Deltas for range of true wind speeds														
Yacht/TWS	4	5	6	7	8	9	10	12	14	16	20	25	30	35
Mini v.1.4	0	0	0	0	0	0	0	0	0	0	0	0	0	0
Mini v.1.5	35.036	28.553	17.054	4.836	1.067	-0.41	-1.297	-2.295	-2.512	-2.616	-2.697	-2.666	-1.556	-0.406
Mini v.1.6	14.601	10.614	5.709	-1.305	-3.422	-4.043	-4.303	-4.402	-3.907	-3.584	-3.228	-2.942	-1.565	-0.142
Mini v.2.4	-13.524	-31.732	-49.244	-50.77	-48.754	-47.8	-47.007	-45.852	-45.698	-45.707	-45.516	-45.278	-40.166	-34.942
Mini v.2.5	-28.453	-50.223	-66.291	-62.389	-58.375	-57.151	-55.966	-54.732	-54.879	-55.028	-54.938	-55.054	-50.543	-45.923
Mini v.2.6	-16.345	-32.379	-43.816	-40.401	-37.632	-35.639	-34.786	-33.864	-33.738	-33.573	-33.16	-32.772	-27.515	-22.145

Best Boatspeeds (kt)		Values greater than 1 means an advantage for the scow												
TWA/TWS	2	4	5	6	7	8	9	10	12	14	16	20	25	30	35
32	1.050	0.996	0.971	0.966	0.959	0.961	0.963	0.961	0.961	0.962	0.961	0.959	0.961	0.963	0.966
36	1.073	0.993	0.971	0.960	0.956	0.961	0.959	0.960	0.960	0.958	0.958	0.957	0.956	0.959	0.960
40	1.072	0.988	0.964	0.955	0.955	0.958	0.959	0.957	0.958	0.957	0.957	0.955	0.954	0.946	0.941
45	1.101	0.981	0.963	0.949	0.956	0.955	0.957	0.957	0.955	0.955	0.952	0.948	0.946	0.946	0.946
52	1.036	0.973	0.954	0.949	0.948	0.951	0.956	0.955	0.951	0.947	0.944	0.940	0.938	0.936	0.935
60	1.011	0.972	0.949	0.944	0.942	0.944	0.953	0.953	0.944	0.941	0.937	0.932	0.932	0.933	0.934
70	1.016	0.969	0.945	0.939	0.938	0.934	0.934	0.947	0.938	0.933	0.933	0.931	0.929	0.927	0.926
75	1.089	0.955	0.937	0.917	0.930	0.932	0.923	0.935	0.927	0.932	0.931	0.929	0.927	0.926	0.926
80	0.991	0.912	0.897	0.889	0.910	0.931	0.917	0.919	0.934	0.932	0.931	0.927	0.925	0.924	0.923
90	0.791	0.842	0.873	0.887	0.922	0.918	0.907	0.902	0.918	0.933	0.929	0.925	0.924	0.924	0.924
100	0.819	0.861	0.891	0.899	0.914	0.908	0.898	0.888	0.889	0.907	0.938	0.925	0.923	0.921	0.920
110	0.840	0.880	0.905	0.909	0.904	0.896	0.890	0.882	0.873	0.867	0.882	0.922	0.921	0.919	0.917
120	0.931	0.916	0.916	0.914	0.913	0.895	0.881	0.882	0.877	0.871	0.867	0.876	0.920	0.917	0.914
135	0.954	0.947	0.935	0.935	0.930	0.929	0.921	0.913	0.900	0.888	0.886	0.887	0.887	0.874	0.863
140	1.005	0.958	0.953	0.946	0.943	0.939	0.940	0.928	0.916	0.909	0.901	0.897	0.885	0.893	0.900
150	1.022	0.994	0.985	0.981	0.969	0.960	0.954	0.947	0.935	0.925	0.922	0.916	0.915	0.908	0.902
160	1.050	1.000	0.991	0.987	0.982	0.977	0.967	0.960	0.952	0.945	0.941	0.934	0.930	0.924	0.920
165	1.048	1.004	0.997	0.992	0.988	0.986	0.976	0.968	0.959	0.951	0.947	0.943	0.940	0.936	0.933
170	1.034	1.004	1.000	0.994	0.990	0.987	0.981	0.972	0.963	0.956	0.952	0.947	0.945	0.942	0.940
180	1.026	1.004	1.000	0.994	0.993	0.989	0.985	0.974	0.964	0.957	0.953	0.950	0.947	0.945	0.944
Up.Vs		0.965	0.953	0.948	0.959	0.952	0.958	0.956	0.952	0.951	0.953	0.952	0.946	0.898	
Up.Bt		0.980	0.984	0.995	1.005	0.984	0.997	0.989	0.983	0.983	0.989	0.989	0.979	0.896	
Up.Vmg	1.089	0.977	0.963	0.951	0.956	0.958	0.960	0.961	0.961	0.958	0.957	0.956	0.957	0.962	0.967
Dn.Vs		0.908	0.857	0.915	0.926	0.920	0.932	0.933	0.875	0.865	0.876	0.909	0.916	0.888	
Dn.Bt		1.027	1.050	1.019	1.021	1.024	1.013	1.009	1.030	1.032	1.021	1.003	0.998	1.006	
Dn.Vmg	0.987	0.959	0.950	0.951	0.960	0.956	0.950	0.949	0.925	0.918	0.911	0.913	0.913	0.896	0.883

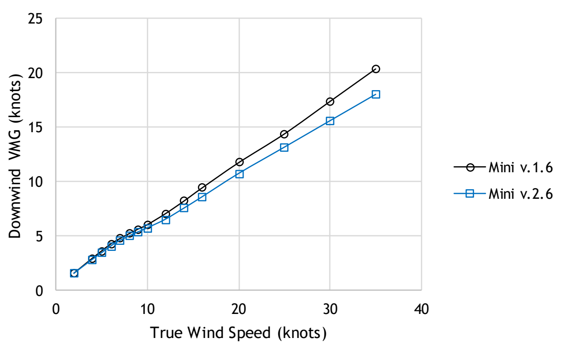

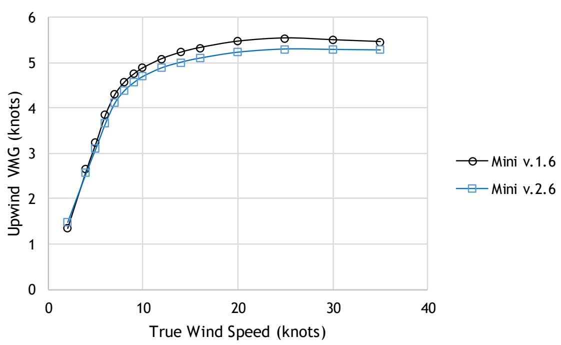

Appendix D: Tank Testing Matrix Extrapolated

Typical Run Layout for each diplacement. (Total 150 Runs)

	Run ID	Keel Cant (°)	Fn	Heel (°)	Leeway (°)	Req. Speed (m/s)
	M_100_1	40	0.175	0	0	0.58
	M_100_1	40	0.200	0	0	0.67
UPRIGHT PROHASKA	M_100_1	40	0.225	0	0	0.75
	M_100_1	40	0.250	0	0	0.83
	M_100_1	40	0.275	0	0	0.91
	M_100_1	40	0.300	0	0	1.00
	M_100_1	40	0.400	0	0	1.33

	Run ID	Keel Cant (°)	Fn	Heel (°)	Leeway (°)	Req. Speed (m/s)
	M_100_1	40	0.5	0	0	1.66
	M_100_1	40	0.6	0	0	2.00
UPRIGHT	M_100_1	40	0.7	0	0	2.33
	M_100_1	40	0.8	0	0	2.66
	M_100_1	40	0.9	0	0	2.99
	M_100_1	40	1	0	0	3.33

	Run ID	Keel Cant (°)	Fn	Heel (°)	Leeway (°)	Req. Speed (m/s)
	M_100_2	40	0.55	5	1	1.83
	M_100_2	40	0.75	5	1	2.49
	M_100_2	40	1	5	1	3.33
1 degree leeway	M_100_3	40	0.55	10	1	1.83
	M_100_3	40	0.75	10	1	2.49
	M_100_3	40	1	10	1	3.33
	M_100_4	40	0.55	15	1	1.83
	M_100_4	40	0.75	15	1	2.49
	M_100_4	40	1	15	1	3.33

	Run ID	Keel Cant (°)	Fn	Heel (°)	Leeway (°)	Req. Speed (m/s)
	M_100_2	40	0.55	5	2	1.83
	M_100_2	40	0.75	5	2	2.49
	M_100_2	40	1	5	2	3.33
2 degree leeway	M_100_3	40	0.55	10	2	1.83
	M_100_3	40	0.75	10	2	2.49
	M_100_3	40	1	10	2	3.33
	M_100_4	40	0.55	15	2	1.83
	M_100_4	40	0.75	15	2	2.49
	M_100_4	40	1	15	2	3.33

	Run ID	Keel Cant (°)	Fn	Heel (°)	Leeway (°)	Req. Speed (m/s)
	M_100_2	40	0.55	5	3	1.83
	M_100_2	40	0.75	5	3	2.49
	M_100_2	40	1	5	3	3.33
3 degree leeway	M_100_3	40	0.55	10	3	1.83
	M_100_3	40	0.75	10	3	2.49
	M_100_3	40	1	10	3	3.33
	M_100_4	40	0.55	15	3	1.83
	M_100_4	40	0.75	15	3	2.49
	M_100_4	40	1	15	3	3.33

	Run ID	Keel Cant (°)	Fn	Heel (°)	Leeway (°)	Req. Speed (m/s)
	M_100_2	40	0.55	5	4	1.83
	M_100_2	40	0.75	5	4	2.49
	M_100_2	40	1	5	4	3.33
4 degree leeway	M_100_3	40	0.55	10	4	1.83
	M_100_3	40	0.75	10	4	2.49
	M_100_3	40	1	10	4	3.33
	M_100_4	40	0.55	15	4	1.83
	M_100_4	40	0.75	15	4	2.49
	M_100_4	40	1	15	4	3.33

Appendix E: Testing Scaled Results

100% Displacement

Fn	Speed (m/s)	Heel (°)	Leeway (°)	C_W	R_W (N)	Re	$C_{F\ Hull}$	$R_{V\ Hull}$ (N)	$R_{T\ Hull}$ (N)	SF (N)	$C_{F\ Keel}$	$R_{V\ Keel}$ (N)	$C_{F\ Bulb}$	$R_{V\ Bulb}$ (N)	R_T (N)
0.17	1.27	0	0	0.000	1.18888	6.2E+6	0.003	37.84	39.03	1.28	0.0066	5.44	0.0043	2.897	47.37
0.20	1.51	0	0	0.000	4.38836	7.3E+6	0.003	51.48	55.87	1.28	0.0063	7.31	0.0041	3.924	67.10
0.23	1.68	0	0	0.000	3.6058	8.2E+6	0.003	62.68	66.28	0.00	0.0061	8.84	0.0041	4.764	79.88
0.25	1.85	0	0	0.000	9.01905	9.0E+6	0.003	74.38	83.40	6.41	0.0060	10.42	0.0040	5.641	99.46
0.27	2.04	0	0	0.001	17.3032	9.9E+6	0.003	89.30	106.60	7.69	0.0058	12.42	0.0039	6.756	125.78
0.30	2.21	0	0	0.001	35.376	10.8E+6	0.003	103.54	138.91	7.30	0.0057	14.32	0.0038	7.817	161.05
0.35	2.61	0	0	0.002	79.4777	12.7E+6	0.003	139.43	218.91	72.01	0.0055	19.08	0.0037	10.487	248.47
0.37	2.73	0	0	0.003	104.801	13.3E+6	0.003	151.71	256.51	67.65	0.0054	20.70	0.0037	11.398	288.61
0.40	2.99	0	0	0.004	183.632	14.5E+6	0.003	179.41	363.04	66.24	0.0053	24.33	0.0036	13.451	400.82

Fn	Speed (m/s)	Heel (°)	Leeway (°)	C_W	R_W (N)	Re	$C_{F\ Hull}$	$R_{V\ Hull}$ (N)	$R_{T\ Hull}$ (N)	SF (N)	$C_{F\ Keel}$	$R_{V\ Keel}$ (N)	$C_{F\ Bulb}$	$R_{V\ Bulb}$ (N)	R_T (N)
0.50	3.69	0	0	0.006	450.662	17.9E+6	0.003	263.82	714.48	-61.63	0.0051	35.32	0.0035	19.688	769.49
0.61	4.51	0	0	0.006	614.378	21.9E+6	0.003	381.81	996.19	-563.75	0.0049	50.50	0.0034	28.370	1075.06
0.70	5.24	0	0	0.005	696.973	25.5E+6	0.003	503.21	1200.18	-1182.59	0.0047	65.98	0.0033	37.273	1303.44
0.81	6.01	0	0	0.004	741.348	29.2E+6	0.003	646.03	1387.38	-2219.13	0.0046	84.07	0.0032	47.720	1519.17
0.91	6.74	0	0	0.003	672.903	32.7E+6	0.002	798.75	1471.65	-3260.40	0.0045	103.29	0.0031	58.866	1633.81
1.00	7.41	0	0	0.002	622.831	36.0E+6	0.002	951.93	1574.76	-3750.99	0.0044	122.47	0.0031	70.025	1767.25

Fn	Speed (m/s)	Heel (°)	Leeway (°)	C_W	R_W (N)	Re	$C_{F\ Hull}$	$R_{V\ Hull}$ (N)	$R_{T\ Hull}$ (N)	SF (N)	$C_{F\ Keel}$	$R_{V\ Keel}$ (N)	$C_{F\ Bulb}$	$R_{V\ Bulb}$ (N)	R_T (N)
0.54	4.05	5	1	0.007	585.033	19.7E+6	0.003	302.72	887.76	-735.44	0.0050	41.63	0.0034	23.292	952.68
0.75	5.58	5	1	0.005	746.379	27.2E+6	0.003	545.63	1292.01	-2418.87	0.0046	73.66	0.0032	41.701	1407.37
1.00	7.40	5	1	0.002	653.44	36.1E+6	0.002	919.39	1572.83	-3874.24	0.0044	122.20	0.0031	69.872	1764.90
0.55	4.05	10	1	0.007	574.579	19.8E+6	0.003	279.32	853.89	-645.75	0.0050	41.74	0.0034	23.356	918.99
0.75	5.59	10	1	0.004	674.203	27.3E+6	0.003	503.82	1178.02	-2270.71	0.0046	73.91	0.0032	41.846	1293.78
1.00	7.41	10	1	0.005	1264.78	36.2E+6	0.002	847.38	2112.16	-1910.34	0.0044	122.40	0.0031	69.987	2304.55
0.55	4.05	15	1	0.008	608.511	19.8E+6	0.003	252.20	860.71	-503.28	0.0050	41.74	0.0034	23.356	925.81
0.75	5.59	15	1	0.005	673.817	27.3E+6	0.003	454.90	1128.72	-1951.86	0.0046	73.91	0.0032	41.846	1244.47
1.00	7.41	15	1	0.006	1408.37	36.3E+6	0.002	765.11	2173.48	-1703.93	0.0044	122.40	0.0031	69.987	2365.87

Fn	Speed (m/s)	Heel (°)	Leeway (°)	C_W	R_W (N)	Re	$C_{F\ Hull}$	$R_{V\ Hull}$ (N)	$R_{T\ Hull}$ (N)	SF (N)	$C_{F\ Keel}$	$R_{V\ Keel}$ (N)	$C_{F\ Bulb}$	$R_{V\ Bulb}$ (N)	R_T (N)
0.54	4.05	5	2	0.008	645.199	19.7E+6	0.003	302.72	947.92	-816.16	0.0050	41.63	0.0034	23.292	1012.85
0.75	5.58	5	2	0.005	821.107	27.2E+6	0.003	545.63	1366.74	-2529.83	0.0046	73.66	0.0032	41.701	1482.10
1.00	7.40	5	2	0.001	298.322	36.1E+6	0.002	919.39	1217.71	-3749.71	0.0044	122.20	0.0031	69.872	1409.79
0.55	4.05	10	2	0.006	455.295	19.8E+6	0.003	279.32	734.61	-769.01	0.0050	41.74	0.0034	23.356	799.71
0.75	5.59	10	2	0.004	539.8	27.3E+6	0.003	503.82	1043.62	-2393.38	0.0046	73.91	0.0032	41.846	1159.37
1.00	7.41	10	2	0.005	1247.96	36.2E+6	0.002	847.38	2095.34	-1816.30	0.0044	122.40	0.0031	69.987	2287.73
0.55	4.05	15	2	0.008	606.333	19.8E+6	0.003	252.20	858.53	-585.53	0.0050	41.74	0.0034	23.356	923.63
0.75	5.59	15	2	0.005	700.723	27.3E+6	0.003	454.90	1155.63	-2052.56	0.0046	73.91	0.0032	41.846	1271.38
1.00	7.41	15	2	0.006	1455.65	36.3E+6	0.002	765.11	2220.76	-1551.21	0.0044	122.40	0.0031	69.987	2413.15

Fn	Speed (m/s)	Heel (°)	Leeway (°)	C_W	R_W (N)	Re	$C_{F\ Hull}$	$R_{V\ Hull}$ (N)	$R_{T\ Hull}$ (N)	SF (N)	$C_{F\ Keel}$	$R_{V\ Keel}$ (N)	$C_{F\ Bulb}$	$R_{V\ Bulb}$ (N)	R_T (N)
0.54	4.05	5	3	0.008	652.352	19.7E+6	0.003	302.72	955.08	-1023.72	0.0050	41.63	0.0034	23.292	1020.00
0.75	5.58	5	3	0.005	821.107	27.2E+6	0.003	545.63	1366.74	-2766.22	0.0046	73.66	0.0032	41.701	1482.10
1.00	7.40	5	3	0.003	755.887	36.1E+6	0.002	919.39	1675.28	-3818.00	0.0044	122.20	0.0031	69.872	1867.35
0.55	4.05	10	3	0.006	501.291	19.8E+6	0.003	279.32	780.61	-938.00	0.0050	41.74	0.0034	23.356	845.71
0.75	5.59	10	3	0.004	616.803	27.3E+6	0.003	503.82	1120.62	-2559.94	0.0046	73.91	0.0032	41.846	1236.38
1.00	7.41	10	3	0.004	1130.98	36.2E+6	0.002	847.38	1978.36	-2366.60	0.0044	122.40	0.0031	69.987	2170.75
0.55	4.05	15	3	0.007	513.442	19.8E+6	0.003	252.20	765.64	-702.13	0.0050	41.74	0.0034	23.356	830.74
0.75	5.59	15	3	0.004	612.957	27.3E+6	0.003	454.90	1067.86	-2194.40	0.0046	73.91	0.0032	41.846	1183.61
1.00	7.41	15	3	0.007	1732.66	36.3E+6	0.002	765.11	2497.77	-1736.86	0.0044	122.40	0.0031	69.987	2690.16

Fn	Speed (m/s)	Heel (°)	Leeway (°)	C_W	R_W (N)	Re	$C_{F\ Hull}$	$R_{V\ Hull}$ (N)	$R_{T\ Hull}$ (N)	SF (N)	$C_{F\ Keel}$	$R_{V\ Keel}$ (N)	$C_{F\ Bulb}$	$R_{V\ Bulb}$ (N)	R_T (N)
0.54	4.05	5	4	0.007	620.289	19.7E+6	0.003	302.72	923.01	-1350.31	0.0050	41.63	0.0034	23.292	987.94
0.75	5.58	5	4	0.004	705.119	27.2E+6	0.003	545.63	1250.75	-3156.28	0.0046	73.66	0.0032	41.701	1366.11
1.00	7.40	5	4	0.002	697.254	36.1E+6	0.002	919.39	1616.64	-4207.88	0.0044	122.20	0.0031	69.872	1808.72
0.55	4.05	10	4	0.008	609.941	19.8E+6	0.003	279.32	889.26	-1192.98	0.0050	41.74	0.0034	23.356	954.36
0.75	5.59	10	4	0.005	688.169	27.3E+6	0.003	503.82	1191.99	-2790.31	0.0046	73.91	0.0032	41.846	1307.74
1.00	7.41	10	4	0.006	1498.57	36.2E+6	0.002	847.38	2345.95	-2139.56	0.0044	122.40	0.0031	69.987	2538.34
0.55	4.05	15	4	0.009	619.145	19.8E+6	0.003	252.20	871.34	-921.22	0.0050	41.74	0.0034	23.356	936.44
0.75	5.59	15	4	0.004	612.317	27.3E+6	0.003	454.90	1067.22	-2481.14	0.0046	73.91	0.0032	41.846	1182.97
1.00	7.41	15	4	0.009	2107.79	36.3E+6	0.002	765.11	2872.91	-2022.97	0.0044	122.40	0.0031	69.987	3065.29

80% Displacement

Fn	Speed (m/s)	Heel (°)	Leeway (°)	C_W	R_W (N)	Re	$C_{F\,Hull}$	$R_{V\,Hull}$ (N)	$R_{T\,Hull}$ (N)	SF (N)	$C_{F\,Keel}$	$R_{V\,Keel}$ (N)	$C_{F\,Bulb}$	$R_{V\,Bulb}$ (N)	R_T (N)
0.17	1.27	0	0	0.001	6.13662	6.2E+6	0.003	36.43	42.57	32.8	0.0066	5.4720	0.0043	2.897	50.93
0.20	1.51	0	0	0.001	7.56174	7.3E+6	0.003	49.56	57.12	43.4344	0.0063	7.3511	0.0041	3.924	68.39
0.23	1.68	0	0	0.001	11.6509	8.2E+6	0.003	60.34	71.99	63.2297	0.0061	8.8811	0.0041	4.764	85.63
0.25	1.85	0	0	0.001	14.4027	9.0E+6	0.003	71.60	86.01	79.95	0.0060	10.4699	0.0040	5.641	102.12
0.27	2.04	0	0	0.001	21.9998	9.9E+6	0.003	85.97	107.97	100.271	0.0058	12.4834	0.0039	6.756	127.20
0.30	2.21	0	0	0.001	34.603	10.8E+6	0.003	99.67	134.27	112.75	0.0057	14.3942	0.0038	7.817	156.48
0.35	2.61	0	0	0.002	80.2211	12.7E+6	0.003	134.22	214.44	138.375	0.0055	19.1771	0.0037	10.487	244.11
0.37	2.73	0	0	0.003	95.089	13.3E+6	0.003	146.05	241.13	141.578	0.0054	20.8043	0.0037	11.398	273.34
0.40	2.99	0	0	0.003	157.922	14.5E+6	0.003	172.71	330.63	153.75	0.0053	24.4592	0.0036	13.451	368.54

Fn	Speed (m/s)	Heel (°)	Leeway (°)	C_W	R_W (N)	Re	$C_{F\,Hull}$	$R_{V\,Hull}$ (N)	$R_{T\,Hull}$ (N)	SF (N)	$C_{F\,Keel}$	$R_{V\,Keel}$ (N)	$C_{F\,Bulb}$	$R_{V\,Bulb}$ (N)	R_T (N)
0.50	3.69	0	0	0.006	378.672	17.9E+6	0.003	253.97	632.64	51.7625	0.0051	35.5026	0.0035	19.688	687.83
0.61	4.51	0	0	0.005	498.704	21.9E+6	0.003	367.55	866.25	-434.73	0.0049	50.7693	0.0034	28.370	945.39
0.70	5.24	0	0	0.004	563.387	25.5E+6	0.003	484.42	1047.80	-1142.9	0.0047	66.3369	0.0033	37.273	1151.41
0.81	6.01	0	0	0.003	571.647	29.2E+6	0.003	621.90	1193.55	-2255.4	0.0046	84.5205	0.0032	47.720	1325.79
0.91	6.74	0	0	0.002	461.061	32.7E+6	0.002	768.92	1229.98	-2987.6	0.0044	103.8454	0.0031	58.866	1392.69
1.00	7.41	0	0	0.001	413.689	36.0E+6	0.002	916.38	1330.07	-3362.8	0.0044	123.1309	0.0031	70.025	1523.22

Fn	Speed (m/s)	Heel (°)	Leeway (°)	C_W	R_W (N)	Re	$C_{F\,Hull}$	$R_{V\,Hull}$ (N)	$R_{T\,Hull}$ (N)	SF (N)	$C_{F\,Keel}$	$R_{V\,Keel}$ (N)	$C_{F\,Bulb}$	$R_{V\,Bulb}$ (N)	R_T (N)
0.55	4.08	5	1	0.006	471.886	19.6E+6	0.003	296.00	767.89	-640.75	0.0050	42.4134	0.0034	23.611	833.91
0.76	5.62	5	1	0.003	531.473	27.0E+6	0.003	533.50	1064.97	-2319.8	0.0046	75.0481	0.0032	42.273	1182.30
1.00	7.46	5	1	0.001	296.102	35.8E+6	0.002	898.93	1195.03	-3360.2	0.0044	124.5226	0.0031	70.832	1390.38
0.55	4.05	10	1	0.006	477.669	19.6E+6	0.003	269.93	747.60	-577.2	0.0050	41.9655	0.0034	23.356	812.93
0.75	5.59	10	1	0.003	464.385	26.9E+6	0.003	486.51	950.90	-2079	0.0046	74.2523	0.0032	41.815	1066.96
1.00	7.41	10	1	0.004	1079.3	35.8E+6	0.002	819.75	1899.04	-1306	0.0044	123.1974	0.0031	70.064	2092.30
0.55	4.05	15	1	0.007	492.771	19.6E+6	0.003	242.59	735.36	-410.58	0.0050	41.9655	0.0034	23.356	800.69
0.75	5.59	15	1	0.004	456.276	27.0E+6	0.003	437.23	893.51	-1688.2	0.0046	74.2523	0.0032	41.815	1009.58
1.00	7.41	15	1	0.005	1173.29	35.8E+6	0.002	736.72	1910.00	-1302.1	0.0044	123.1974	0.0031	70.064	2103.27

Fn	Speed (m/s)	Heel (°)	Leeway (°)	C_W	R_W (N)	Re	$C_{F\,Hull}$	$R_{V\,Hull}$ (N)	$R_{T\,Hull}$ (N)	SF (N)	$C_{F\,Keel}$	$R_{V\,Keel}$ (N)	$C_{F\,Bulb}$	$R_{V\,Bulb}$ (N)	R_T (N)
0.55	4.08	5	2	0.006	460.734	19.6E+6	0.003	296.00	756.74	-869.97	0.0050	42.4134	0.0034	23.611	822.76
0.76	5.62	5	2	0.004	573.355	27.0E+6	0.003	533.50	1106.86	-2510	0.0046	75.0481	0.0032	42.273	1224.18
1.00	7.46	5	2	0.001	319.701	35.8E+6	0.002	898.93	1218.63	-3359.2	0.0044	124.5226	0.0031	70.832	1413.98
0.55	4.05	10	2	0.007	495.863	19.6E+6	0.003	269.93	765.80	-816.54	0.0050	41.9655	0.0034	23.356	831.12
0.75	5.59	10	2	0.003	487.832	26.9E+6	0.003	486.51	974.34	-2215.4	0.0046	74.2523	0.0032	41.815	1090.41
1.00	7.41	10	2	0.004	916.193	35.8E+6	0.002	819.75	1735.94	-1753.4	0.0044	123.1974	0.0031	70.064	1929.20
0.55	4.05	15	2	0.007	486.737	19.6E+6	0.003	242.59	729.33	-598.34	0.0050	41.9655	0.0034	23.356	794.65
0.75	5.59	15	2	0.004	466.014	27.0E+6	0.003	437.23	903.25	-1839	0.0046	74.2523	0.0032	41.815	1019.32
1.00	7.41	15	2	0.006	1390.84	35.8E+6	0.002	736.72	2127.56	-1249.2	0.0044	123.1974	0.0031	70.064	2320.82

Fn	Speed (m/s)	Heel (°)	Leeway (°)	C_W	R_W (N)	Re	$C_{F\,Hull}$	$R_{V\,Hull}$ (N)	$R_{T\,Hull}$ (N)	SF (N)	$C_{F\,Keel}$	$R_{V\,Keel}$ (N)	$C_{F\,Bulb}$	$R_{V\,Bulb}$ (N)	R_T (N)
0.55	4.08	5	3	0.006	462.29	19.6E+6	0.003	296.00	758.29	-1048.1	0.0050	42.4134	0.0034	23.611	824.32
0.76	5.62	5	3	0.004	556.369	27.0E+6	0.003	533.50	1089.87	-2737.8	0.0046	75.0481	0.0032	42.273	1207.19
1.00	7.46	5	3	0.001	350.431	35.8E+6	0.002	898.93	1249.36	-3707.6	0.0044	124.5226	0.0031	70.832	1444.71
0.55	4.05	10	3	0.007	487.023	19.6E+6	0.003	269.93	756.96	-999.63	0.0050	41.9655	0.0034	23.356	822.28
0.75	5.59	10	3	0.003	479.914	26.9E+6	0.003	486.51	966.43	-2407.9	0.0046	74.2523	0.0032	41.815	1082.49
1.00	7.41	10	3	0.005	1283.66	35.8E+6	0.002	819.75	2103.40	-1383.1	0.0044	123.1974	0.0031	70.064	2296.66
0.55	4.05	15	3	0.008	502.496	19.6E+6	0.003	242.59	745.09	-760.93	0.0050	41.9655	0.0034	23.356	810.41
0.75	5.59	15	3	0.004	497.533	27.0E+6	0.003	437.23	934.77	-1954.8	0.0046	74.2523	0.0032	41.815	1050.83
1.00	7.41	15	3	0.006	1391.23	35.8E+6	0.002	736.72	2127.95	-1379.9	0.0044	123.1974	0.0031	70.064	2321.21

Fn	Speed (m/s)	Heel (°)	Leeway (°)	C_W	R_W (N)	Re	$C_{F\,Hull}$	$R_{V\,Hull}$ (N)	$R_{T\,Hull}$ (N)	SF (N)	$C_{F\,Keel}$	$R_{V\,Keel}$ (N)	$C_{F\,Bulb}$	$R_{V\,Bulb}$ (N)	R_T (N)
0.55	4.08	5	4	0.004	351.945	19.6E+6	0.003	296.00	647.95	-1285.1	0.0050	42.4134	0.0034	23.611	713.97
0.76	5.62	5	4	0.003	453.804	27.0E+6	0.003	533.50	987.31	-2902.5	0.0046	75.0481	0.0032	42.273	1104.63
1.00	7.46	5	4	0.001	298.825	35.8E+6	0.002	898.93	1197.75	-3760.2	0.0044	124.5226	0.0031	70.832	1393.10
0.55	4.05	10	4	0.005	392.466	19.6E+6	0.003	269.93	662.40	-1157.7	0.0050	41.9655	0.0034	23.356	727.72
0.75	5.59	10	4	0.003	451.572	26.9E+6	0.003	486.51	938.08	-2566.7	0.0046	74.2523	0.0032	41.815	1054.15
1.00	7.41	10	4	0.005	1343.36	35.8E+6	0.002	819.75	2163.11	-1560.3	0.0044	123.1974	0.0031	70.064	2356.37
0.55	4.05	15	4	0.007	450.349	19.6E+6	0.003	242.59	692.94	-892.9	0.0050	41.9655	0.0034	23.356	758.26
0.75	5.59	15	4	0.005	572.486	27.0E+6	0.003	437.23	1009.72	-2074.5	0.0046	74.2523	0.0032	41.815	1125.79
1.00	7.41	15	4	0.007	1484.63	35.8E+6	0.002	736.72	2221.35	-1580.3	0.0044	123.1974	0.0031	70.064	2414.61

50% Displacement

Fn	Speed (m/s)	Heel (°)	Leeway (°)	C_W	R_W (N)	Re	$C_{F\ Hull}$	$R_{V\ Hull}$ (N)	$R_{T\ Hull}$ (N)	SF (N)	$C_{F\ Keel}$	$R_{V\ Keel}$ (N)	$C_{F\ Bulb}$	$R_{V\ Bulb}$ (N)	R_T (N)
0.17	1.27	0	0	0.001	7.43979	6.2E+6	0.003	30.79	38.23	32.4156	0.0066	5.4442	0.0043	2.897	46.57
0.20	1.51	0	0	0.000	1.36791	7.3E+6	0.003	41.89	43.26	53.6588	0.0063	7.3135	0.0041	3.924	54.49
0.23	1.68	0	0	0.000	3.18494	8.2E+6	0.003	51.00	54.19	71.75	0.0061	8.8355	0.0041	4.764	67.79
0.25	1.85	0	0	0.001	9.44718	9.0E+6	0.003	60.52	69.97	97.375	0.0060	10.4160	0.0040	5.641	86.03
0.27	2.04	0	0	0.001	10.5316	9.9E+6	0.003	72.66	83.19	97.375	0.0058	12.4188	0.0039	6.756	102.37
0.30	2.21	0	0	0.001	17.86	10.8E+6	0.003	84.25	102.11	115.441	0.0057	14.3195	0.0038	7.817	124.24
0.40	2.99	0	0	0.002	81.0334	14.5E+6	0.003	145.98	227.02	164	0.0053	24.3310	0.0036	13.451	264.80

Fn	Speed (m/s)	Heel (°)	Leeway (°)	C_W	R_W (N)	Re	$C_{F\ Hull}$	$R_{V\ Hull}$ (N)	$R_{T\ Hull}$ (N)	SF (N)	$C_{F\ Keel}$	$R_{V\ Keel}$ (N)	$C_{F\ Bulb}$	$R_{V\ Bulb}$ (N)	R_T (N)
0.50	3.69	0	0	0.003	173.34	17.9E+6	0.003	214.67	388.01	43.9469	0.0051	35.3151	0.0035	19.688	443.01
0.61	4.51	0	0	0.002	187.899	21.9E+6	0.003	310.68	498.58	-389.5	0.0049	50.4994	0.0034	28.370	577.44
0.70	5.24	0	0	0.003	379.621	25.5E+6	0.003	409.46	789.08	-1214.6	0.0047	65.9826	0.0033	37.273	892.33
0.81	6.01	0	0	0.001	139.571	29.2E+6	0.003	525.67	665.24	-2207.6	0.0046	84.0674	0.0032	47.720	797.03
0.91	6.74	0	0	0.000	35.4129	32.7E+6	0.002	649.94	685.35	-2652.2	0.0045	103.2868	0.0031	58.866	847.50
1.00	7.41	0	0	-0.001	-173.39	36.0E+6	0.002	774.58	601.19	-3200.6	0.0044	122.4667	0.0031	70.025	793.68

Fn	Speed (m/s)	Heel (°)	Leeway (°)	C_W	R_W (N)	Re	$C_{F\ Hull}$	$R_{V\ Hull}$ (N)	$R_{T\ Hull}$ (N)	SF (N)	$C_{F\ Keel}$	$R_{V\ Keel}$ (N)	$C_{F\ Bulb}$	$R_{V\ Bulb}$ (N)	R_T (N)
0.58	4.31	5	1	0.004	273.265	18.5E+6	0.003	279.00	552.27	-535.56	0.0049	46.5162	0.0034	26.087	624.87
0.80	5.94	5	1	0.001	200.954	25.5E+6	0.003	502.74	703.70	-2124.3	0.0046	82.3383	0.0032	46.720	832.76
1.06	7.88	5	1	-0.0012	-290.42	33.9E+6	0.002	846.93	556.52	-3097.7	0.0043	136.6605	0.0030	78.302	771.48
0.55	4.05	10	1	0.005	255.365	18.0E+6	0.003	208.28	463.65	-453.56	0.0050	41.7432	0.0034	23.356	528.75
0.75	5.59	10	1	0.002	199.095	24.8E+6	0.003	375.26	574.36	-1773.3	0.0046	73.8550	0.0032	41.815	690.03
1.00	7.41	10	1	0.002	318.279	32.9E+6	0.002	632.11	950.39	-1829.6	0.0044	122.5329	0.0031	70.064	1142.99
0.55	4.05	15	1	0.004	223.71	18.4E+6	0.003	207.43	431.14	-257.4	0.0050	41.7432	0.0034	23.356	496.24
0.75	5.59	15	1	0.003	262.168	25.4E+6	0.003	373.76	635.93	-1182.6	0.0046	73.8550	0.0032	41.815	751.60
1.00	7.41	15	1	0.002	392.094	33.7E+6	0.002	629.64	1021.73	-1651.5	0.0044	122.5329	0.0031	70.064	1214.33

Fn	Speed (m/s)	Heel (°)	Leeway (°)	C_W	R_W (N)	Re	$C_{F\ Hull}$	$R_{V\ Hull}$ (N)	$R_{T\ Hull}$ (N)	SF (N)	$C_{F\ Keel}$	$R_{V\ Keel}$ (N)	$C_{F\ Bulb}$	$R_{V\ Bulb}$ (N)	R_T (N)
0.58	4.31	5	2	0.003	221.308	18.5E+6	0.003	279.00	500.31	-824.48	0.0049	46.5162	0.0034	26.087	572.92
0.80	5.94	5	2	0.002	273.318	25.5E+6	0.003	502.74	776.06	-2302.4	0.0046	82.3383	0.0032	46.720	905.12
1.06	7.88	5	2	-0.001	-252.79	33.9E+6	0.002	846.93	594.14	-3201.8	0.0043	136.6605	0.0030	78.302	809.11
0.55	4.05	10	2	0.004	194.121	18.0E+6	0.003	208.28	402.41	-690.34	0.0050	41.7432	0.0034	23.356	467.50
0.75	5.59	10	2	0.002	245.22	24.8E+6	0.003	375.26	620.48	-1767.7	0.0046	73.8550	0.0032	41.815	736.15
1.00	7.41	10	2	-0.001	-245.47	32.9E+6	0.002	632.11	386.64	-2649.6	0.0044	122.5329	0.0031	70.064	579.24
0.55	4.05	15	2	0.004	227.554	18.4E+6	0.003	207.43	434.98	-430.5	0.0050	41.7432	0.0034	23.356	500.08
0.75	5.59	15	2	0.003	283.949	25.4E+6	0.003	373.76	657.71	-1328.5	0.0046	73.8550	0.0032	41.815	773.38
1.00	7.41	15	2	0.003	572.751	33.7E+6	0.002	629.64	1202.39	-1552.9	0.0044	122.5329	0.0031	70.064	1394.98

Fn	Speed (m/s)	Heel (°)	Leeway (°)	C_W	R_W (N)	Re	$C_{F\ Hull}$	$R_{V\ Hull}$ (N)	$R_{T\ Hull}$ (N)	SF (N)	$C_{F\ Keel}$	$R_{V\ Keel}$ (N)	$C_{F\ Bulb}$	$R_{V\ Bulb}$ (N)	R_T (N)
0.58	4.31	5	3	0.005	324.065	18.5E+6	0.003	279.00	603.07	-986.56	0.0049	46.5162	0.0034	26.087	675.67
0.80	5.94	5	3	0.002	322.236	25.5E+6	0.003	502.74	824.98	-2403	0.0046	82.3383	0.0032	46.720	954.04
1.06	7.88	5	3	-0.001	-274.5	33.9E+6	0.002	846.93	572.44	-3287.4	0.0043	136.6605	0.0030	78.302	787.40
0.55	4.05	10	3	0.006	295.596	18.0E+6	0.003	208.28	503.88	-854.59	0.0050	41.7432	0.0034	23.356	568.98
0.75	5.59	10	3	0.003	305.439	24.8E+6	0.003	375.26	680.70	-1830.9	0.0046	73.8550	0.0032	41.815	796.37
1.00	7.41	10	3	-0.001	-144.25	32.9E+6	0.002	632.11	487.86	-2693.2	0.0044	122.5329	0.0031	70.064	680.46
0.55	4.05	15	3	0.004	222.429	18.4E+6	0.003	207.43	429.86	-530.44	0.0050	41.7432	0.0034	23.356	494.96
0.75	5.59	15	3	0.003	275.493	25.4E+6	0.003	373.76	649.26	-1422.8	0.0046	73.8550	0.0032	41.815	764.93
1.00	7.41	15	3	0.004	745.719	33.7E+6	0.002	629.64	1375.36	-1226.2	0.0044	122.5329	0.0031	70.064	1567.95

Fn	Speed (m/s)	Heel (°)	Leeway (°)	C_W	R_W (N)	Re	$C_{F\ Hull}$	$R_{V\ Hull}$ (N)	$R_{T\ Hull}$ (N)	SF (N)	$C_{F\ Keel}$	$R_{V\ Keel}$ (N)	$C_{F\ Bulb}$	$R_{V\ Bulb}$ (N)	R_T (N)
0.58	4.31	5	4	0.002	140.261	18.5E+6	0.003	279.00	419.26	-1248.3	0.0049	46.5162	0.0034	26.087	491.87
0.80	5.94	5	4	0.002	221.216	25.5E+6	0.003	502.74	723.96	-2531.8	0.0046	82.3383	0.0032	46.720	853.02
1.06	7.88	5	4	-0.001	-249.9	33.9E+6	0.002	846.93	597.04	-3354.3	0.0043	136.6605	0.0030	78.302	812.00
0.55	4.05	10	4	0.004	229.612	18.0E+6	0.003	208.28	437.90	-1072.4	0.0050	41.7432	0.0034	23.356	503.00
0.75	5.59	10	4	0.003	266.489	24.8E+6	0.003	375.26	641.75	-1914.2	0.0046	73.8550	0.0032	41.815	757.42
1.00	7.41	10	4	0.004	760.311	32.9E+6	0.002	632.11	1392.42	-1476	0.0044	122.5329	0.0031	70.064	1585.02
0.55	4.05	15	4	0.004	191.679	18.4E+6	0.003	207.43	399.11	-718.78	0.0050	41.7432	0.0034	23.356	464.21
0.75	5.59	15	4	0.002	183.243	25.4E+6	0.003	373.76	557.01	-1585.8	0.0046	73.8550	0.0032	41.815	672.68
1.00	7.41	15	4	-0.001	-162.69	33.7E+6	0.002	629.64	466.95	-2266.5	0.0044	122.5329	0.0031	70.064	659.55

Appendix F: Delft Series Results

100% Displacement

	GZ(m)	0.326				0.588				0.76			
	Heel	5.571				11.829				18.711			
	Leeway	1	2	3	4	1	2	3	4	1	2	3	4
Fn	v (knots)	R_T (N)	R_T (N)	R_T (N)	R_T (N)	R_T (N)	R_T (N)	R_T (N)	R_T (N)	R_T (N)	R_T (N)	R_T (N)	R_T (N)
0.15	2.28	33.8	34.0	34.4	35.0	34.0	34.2	34.6	35.2	34.3	34.6	35.0	35.5
0.2	3.04	61.6	62.0	62.7	63.7	62.0	62.4	63.1	64.1	62.6	63.1	63.8	64.7
0.25	3.80	104.8	105.4	106.5	108.0	105.4	106.0	107.1	108.6	106.3	107.0	108.1	109.6
0.3	4.56	156.3	157.3	158.8	161.0	159.3	160.2	161.8	164.0	164.0	165.0	166.6	168.8
0.35	5.31	241.2	242.5	244.6	247.6	248.2	249.5	251.6	254.6	259.6	260.8	263.0	266.0
0.4	6.07	409.9	411.5	414.3	418.2	420.1	421.8	424.6	428.5	436.9	438.6	441.4	445.3
0.45	6.83	624.2	626.4	629.9	634.8	642.0	644.1	647.6	652.5	670.9	673.0	676.5	681.5
0.5	7.59	888.8	891.4	895.8	901.9	960.7	963.4	967.7	973.8	1078.4	1081.0	1085.4	1091.5
0.55	8.35	1080.9	1084.1	1089.4	1096.7	1173.8	1177.0	1182.3	1189.6	1325.7	1328.8	1334.1	1341.5
0.6	9.11	1220.1	1223.9	1230.2	1239.0	1373.9	1377.6	1383.9	1392.7	1625.2	1629.0	1635.3	1644.0
0.65	9.87	1328.4	1332.8	1340.2	1350.5	1588.3	1592.8	1600.1	1610.4	2013.3	2017.7	2025.1	2035.4
0.7	10.63	1591.8	1597.0	1605.5	1617.4	2020.6	2025.7	2034.3	2046.2	2721.6	2726.8	2735.3	2747.3
0.75	11.39	1648.7	1654.5	1664.3	1678.1	2358.2	2364.1	2373.9	2387.6	3518.4	3524.3	3534.1	3547.8

80% Displacement

	GZ (m)	0.335				0.603				0.781			
	Heel	5.397				11.75				18.888			
	Leeway	1	2	3	4	1	2	3	4	1	2	3	4
Fn	v (knots)	R_T (N)	R_T (N)	R_T (N)	R_T (N)	R_T (N)	R_T (N)	R_T (N)	R_T (N)	R_T (N)	R_T (N)	R_T (N)	R_T (N)
0.15	2.28	33.9	34.1	34.5	35.0	34.4	34.6	35.0	35.5	35.2	35.4	35.8	36.4
0.2	3.04	62.2	62.6	63.3	64.3	63.2	63.6	64.3	65.2	64.8	65.2	65.9	66.9
0.25	3.80	103.0	103.7	104.8	106.3	104.5	105.2	106.2	107.8	107.0	107.7	108.8	110.3
0.3	4.56	148.0	148.9	150.5	152.7	154.0	155.0	156.5	158.7	164.2	165.2	166.7	168.9
0.35	5.31	220.9	222.1	224.3	227.3	237.8	239.1	241.2	244.2	266.4	267.7	269.8	272.8
0.4	6.07	368.7	370.3	373.1	377.0	394.3	396.0	398.8	402.7	437.7	439.4	442.2	446.1
0.45	6.83	557.0	559.1	562.7	567.6	600.1	602.2	605.7	610.7	673.0	675.1	678.6	683.5
0.5	7.59	855.8	858.4	862.8	868.9	1032.3	1034.9	1039.3	1045.4	1330.9	1333.5	1337.9	1344.0
0.55	8.35	1097.7	1100.8	1106.1	1113.5	1310.5	1313.7	1318.9	1326.3	1670.5	1673.7	1679.0	1686.4
0.6	9.11	1296.2	1300.0	1306.2	1315.0	1653.1	1656.9	1663.2	1672.0	2257.0	2260.8	2267.1	2275.8
0.65	9.87	1517.2	1521.6	1529.0	1539.3	2122.9	2127.3	2134.7	2145.0	3147.6	3152.0	3159.4	3169.7
0.7	10.63	1813.0	1818.2	1826.7	1838.6	2810.5	2815.7	2824.2	2836.2	4498.1	4503.3	4511.8	4523.8
0.75	11.39	2086.3	2092.2	2102.0	2115.7	3737.2	3743.1	3752.9	3766.6	6530.2	6536.1	6545.9	6559.6

50% Displacement

	GZ (m)	0.355				0.63				0.819			
	Heel	5.135				11.489				19.323			
	Leeway	1	2	3	4	1	2	3	4	1	2	3	4
Fn	v (knots)	R_T (N)	R_T (N)	R_T (N)	R_T (N)	R_T (N)	R_T (N)	R_T (N)	R_T (N)	R_T (N)	R_T (N)	R_T (N)	R_T (N)
0.15	2.28	28.2	28.4	28.8	29.3	28.3	28.6	29.0	29.5	28.7	28.9	29.3	29.9
0.2	3.04	50.6	51.0	51.7	52.6	50.9	51.3	52.0	53.0	51.6	52.0	52.7	53.7
0.25	3.80	80.9	81.6	82.7	84.2	81.5	82.1	83.2	84.7	82.5	83.1	84.2	85.8
0.3	4.56	118.7	119.7	121.2	123.4	121.0	122.0	123.5	125.7	125.4	126.4	127.9	130.1
0.35	5.31	170.6	171.8	174.0	177.0	176.7	178.0	180.1	183.1	188.4	189.7	191.8	194.8
0.4	6.07	249.9	251.6	254.4	258.3	259.6	261.2	264.0	267.9	277.9	279.6	282.3	286.2
0.45	6.83	362.1	364.2	367.7	372.6	378.5	380.6	384.2	389.1	409.9	412.0	415.5	420.5
0.5	7.59	506.1	508.7	513.1	519.2	571.3	574.0	578.3	584.4	695.6	698.2	702.6	708.7
0.55	8.35	627.0	630.2	635.5	642.9	707.4	710.6	715.9	723.2	860.5	863.7	869.0	876.4
0.6	9.11	748.9	752.7	758.9	767.7	883.3	887.1	893.4	902.2	1139.4	1143.1	1149.4	1158.2
0.65	9.87	861.8	866.2	873.6	883.9	1089.6	1094.0	1101.4	1111.7	1523.5	1527.9	1535.2	1545.6
0.7	10.63	1000.1	1005.3	1013.8	1025.8	1375.5	1380.6	1389.1	1401.1	2090.3	2095.4	2104.0	2115.9
0.75	11.39	1115.9	1121.8	1131.6	1145.3	1737.1	1742.9	1752.7	1766.5	2920.2	2926.0	2935.8	2949.6

Comparison 100% Displacement

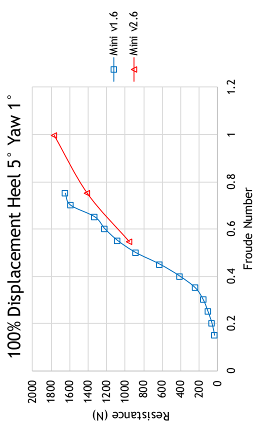

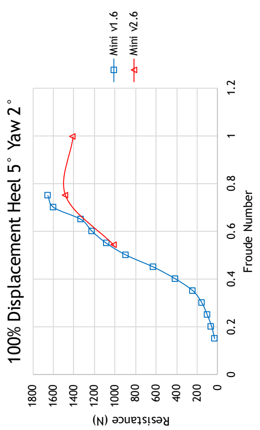

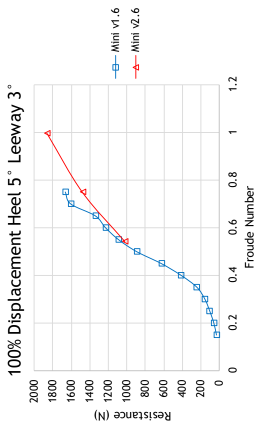

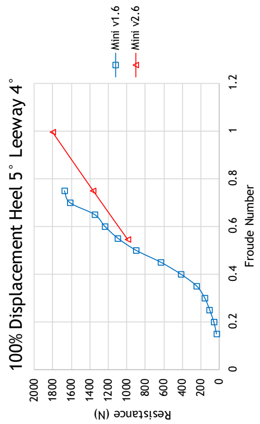

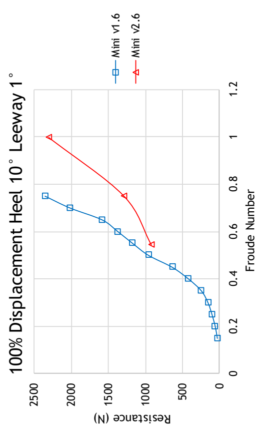

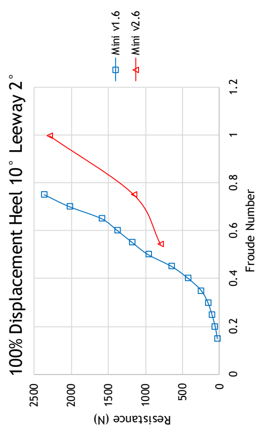

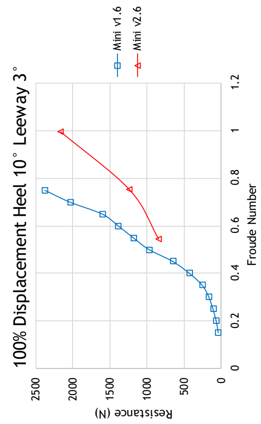

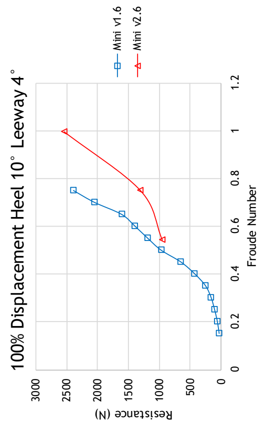

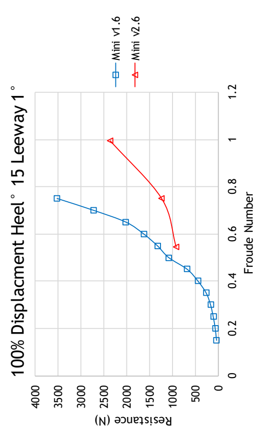

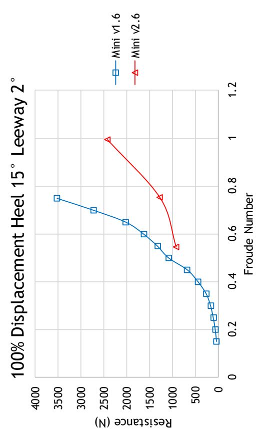

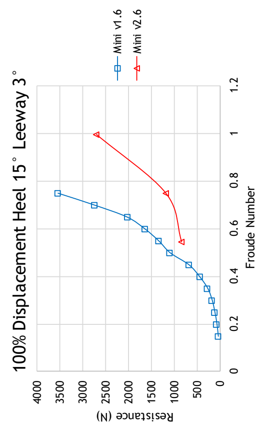

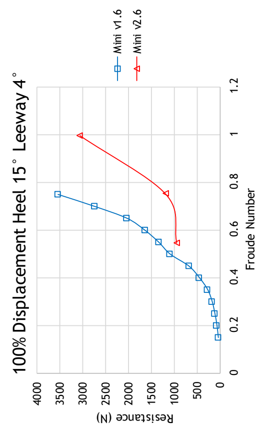

Comparison 80% Displacement

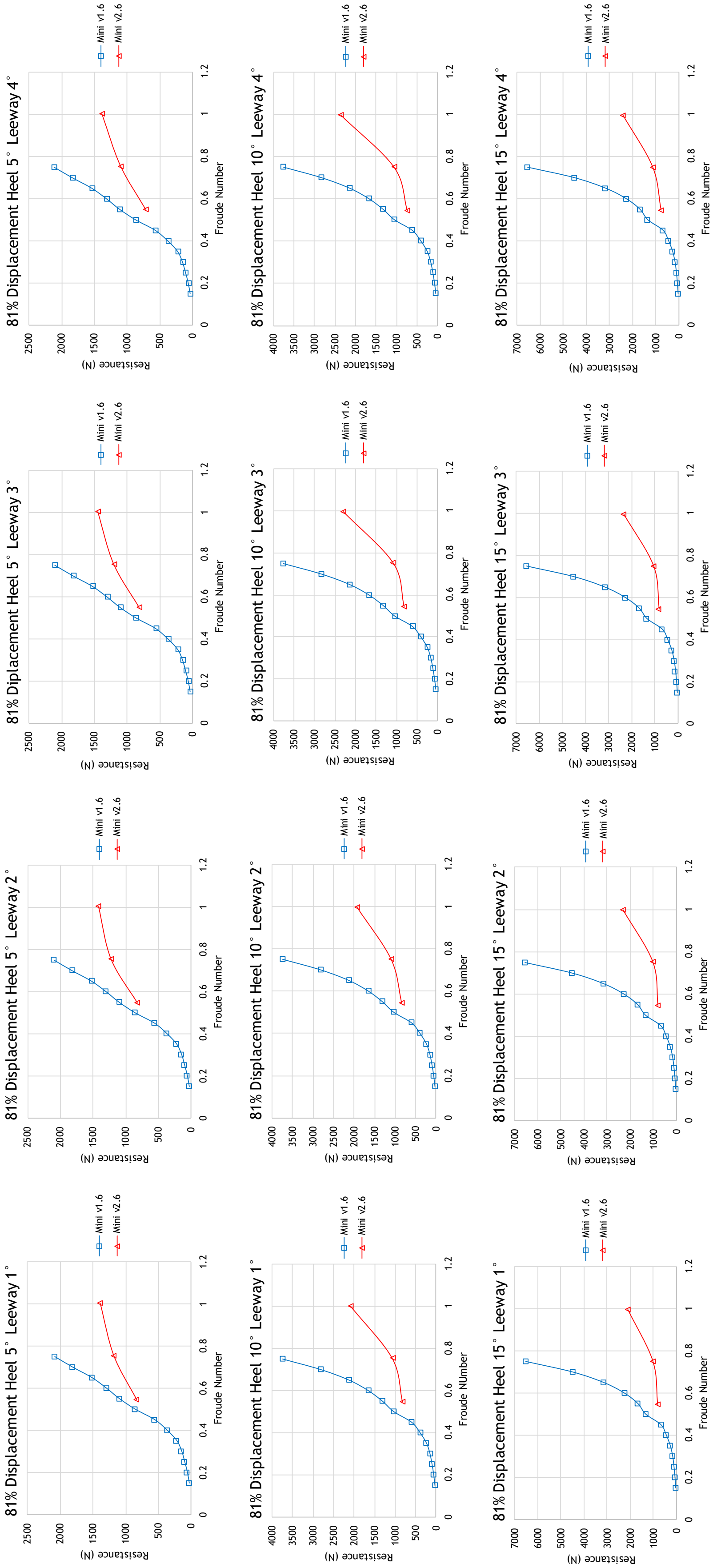

Comparison 50% Displacement

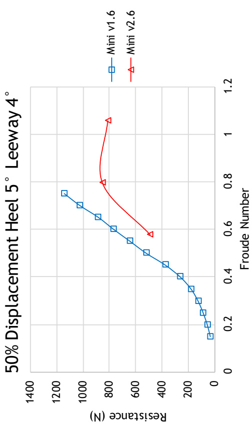

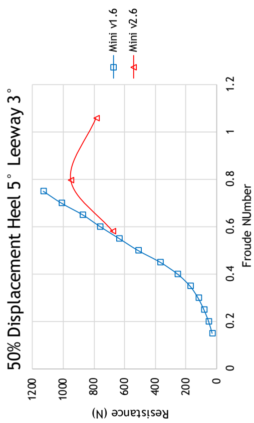

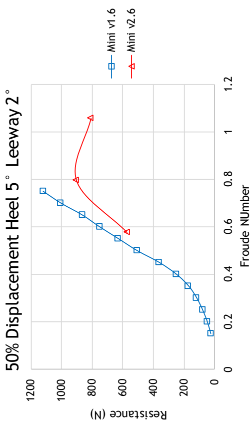

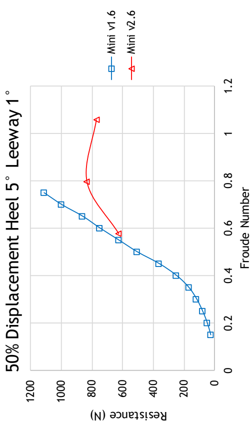

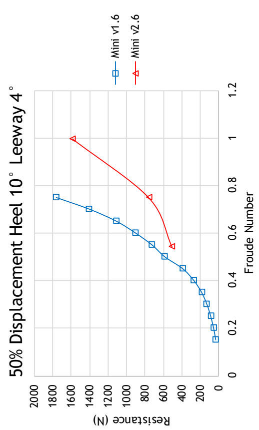

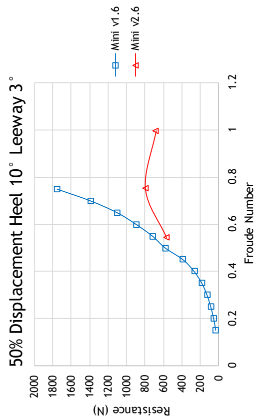

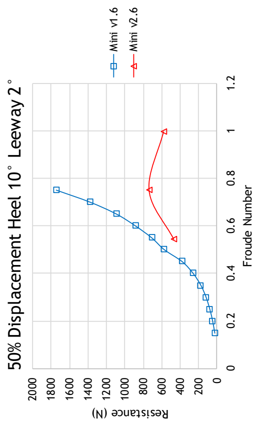

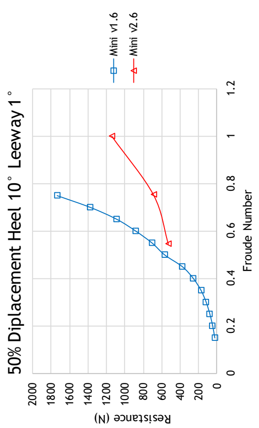

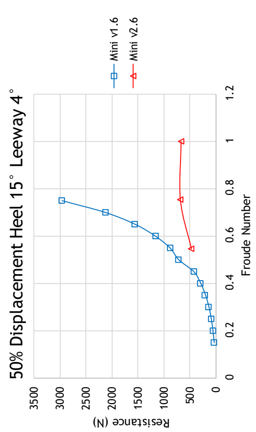

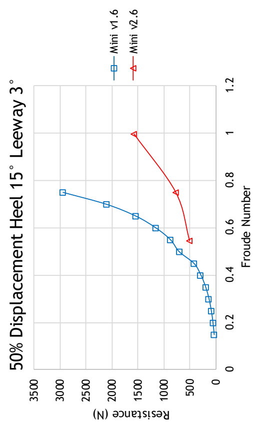

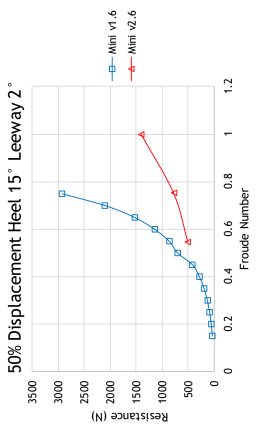

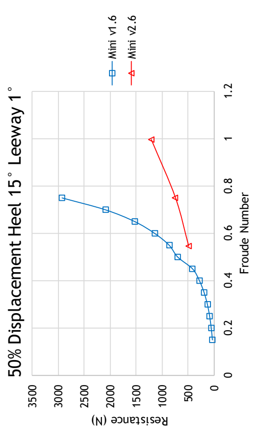

Appendix G: Advanced VPP Report

Using the Hydros VPP set up for the mini 6.50 scow, we saw that the Optimizer could not find any equilibrium going downwind. We observed that the VPP was always trying to reduce as much as possible the leeway, and at the minimum leeway it was already providing too much side force on the foil. From this simple observation, we would suggest to further investigate if

- there is an error in the set-up of the VPP.

- the sails model provides not enough side force, hence there is a mistake in the measures of the sail plan.

- the strut of the foil is producing too much side force with respect to leeway.

- the tip camber is underestimated and hence the lift is insufficient. Here the leeway is required to produce lift, but then the side force is too large.

We also believe that this analysis is missing the trim parameter, which would help to estimate if the leeway could be augmented by having more lift on the foil, or compensate the side force with rake.

The lack of time lets us only suggest the above hints, but a stronger relation with the designer could help us first find out if the set-up is correct, for later try to refine the foil analysis. Nevertheless, we believe that the analysis is biased without the trim of the boat varying.

Hydros Innovation SA

Appendix H: Wing Mast Framework Analysis

Sail Dimension		
I	10.64	m
J	3.16	m
P	10.54	m
E	3.33	m
LP % J	1.089	-
Roach allowance	1.6	-
LP	3.44	m
Genoa Area	19.30	m^2
Main Area	28.70	m^2
Wind Pressure	74.0	N/m^2
Total Load in Genoa	1427.47	N
Genoa Load at Mast Head	611.77	N
Total Load in Main	2122.72	N
Mainsail distributed load	201.40	N/m

Rig Dimension		
Total Mast Length	10.85	m
V_1 Base Width	1.5	m
V_1 Attachment height	9.8	m
S_1 (Diamond Length)	0.5	m
P_1	4.892	m
P_2	4.892	m
P_3	1.067	m
λ_1 (V_1 Angle)	8.7	°
λ_2 (D_2 Angle)	5.8	°
λ_3 (D_3 Angle)	5.8	°

Masthead		
V_1 Tension	18073.4	N
Compression From V_1	17865.3	N
V_1 Vert	17865	N

Diamond Resolution		
BM_1	602.35	Nm
BM_2	602.35	Nm
A_1	1964.25	m^2
A_2	1964.25	m^2
x_{A1}	2.45	m
x_{A2}	2.45	m
BM_B	602.35	Nm
R_A	369.42	N
R_B	1231.41	N
R_C	369.42	N
D_2 Tension	6054.8	N
D_3 Tension	6054.84	N
Compression	12047	N
Total Rig Compression	29912.2	N

Yacht Particular		
Hull RM_{MAX} @30°	17865	Nm
RM_{MAX} @30° Foils	26798	Nm
Heeling Moment	26798	Nm
FoS Mast Buckling	2	-
FoS Rigging	1.9	-

Euler Buckling Required Section EI_{XX}		
Panel	**EI_{XX} (Nm^2)**	**EI_{XX} (Ncm^2)**
P_1	145.0E+3	145.0E+9
P_2	145.0E+3	145.0E+9
Required EI_{XX}	145	$GNmm^2$

Rigging Loads		
V_1 Tension	34E+3	N
D_2 Tension	12E+3	N
D_3 Tension	12E+3	N

Rigging Diameter		
V_1	7.0	mm
D_2	4.0	mm
D_3	4.0	mm

Longitudinal Strength		
Forestay Length	10.675	m
Forestay to Mast	3.07	m
Backstay to Mast	3.35	m
Forestay Angle	16.0	°
Allowed Sag	2.0%	-
Jib Area	19.7	m^2
TWS	14	Knots
TWA	28	°
C_L	1.2	-
Lift	754.02	N
Forestay Tension	4712.60	N
Horizontal Component	1302.49	N
Vertical Component	4436.77	N
Backstay Angle	17.4	°
Backtasy Tension	4350.06	N
Backstay Compression	4150.48	N
Total Mast Compression	8587.26	N
Mast Length	10.85	m
Factor of safety	2.2	-
EI_{YY}	225	$GNmm^2$

Appendix I: Standard Rig Framework Analysis

Sail Dimension		
I	*10.64*	m
J	*3.16*	m
P	*10.54*	m
E	*3.33*	m
LP % J	*1.089*	-
Roach allowance	*1.6*	-
LP	*3.44*	m
Genoa Area	19.30	m^2
Main Area	28.70	m^2
Wind Pressure	*109.0*	N/m^2
Total Load in Genoa	2104.54	N
Genoa Load at Mast Head	901.95	N
Total Load in Main	3129.55	N
Mainsail distributed load	296.92	N/m

Rig Dimension		
Total Mast Length	10.85	m
V1 Base Width	*1.5*	m
D1 Base Width	*1*	m
Spreader Width	*1.4*	m
P_1	*4.374*	m
P_2	5.409	m
P_3	*1.067*	m
V_1 Angle	1.3	°
D_1 Angle	12.9	°
D_2 Angle	14.5	°

Forestay Attachement		
Load from Main	1120	N
Load from Jib	902	N
Total Load	2022	N
D_2 Tension	8069	N
C_2 Compression	7811	N

Spreader Outboard		
D_2 Tension	8069	N
D_2 Vertical	7811	N
D_2 Spreader Compression	2022	N
V_1 Vertical	7811	N
V_1 Tension	7813	N
V_1 Spreader Compression	-179	N
Total Spreader Comp.	1843	N

Spreader Inboard		
Load from Main	1452	N
Load from Jib	0	N
Total Load	3296	N
D_1 Tension	14787	N
C_1 Compression	22226	N
V_1 Tension	7813	N
D_1 Vert	15168	N
V_1 Vert	7811	N

Yacht Particular		
Hull RM_{MAX} @30°	17865	Nm
RM_{MAX} @30° Foils	26798	Nm
Heeling Moment	26885	Nm
FoS Mast Buckling	*2*	-
FoS Rigging	*1.9*	-

Euler Buckling Required Section EI_{XX}		
Panel	**EI_{XX} (Nm^2)**	**EI_{XX} (Nmm^2)**
P_2	46.3E+3	46.3E+9
P_1	86.2E+3	86.2E+9
Required EI_{XX}	86	$GNmm^2$

Rigging Loads		
V_1 Tension	15E+3	N
D_1 Tension	28E+3	N
D_2 Tension	15E+3	N

Rigging Diameter UHMWPE DM20		
V_1	5.0	mm
D_1	6.0	mm
D_2	5.0	mm
D_3	5.0	mm
D_4	5.0	mm

Longitudinal Strength		
Forestay Length	10.675	m
Forestay to Mast	3.07	m
Backstay to Mast	3.35	m
Forestay Angle	16.0	°
Allowed Sag	2.0%	-
Jib Area	19.7	m^2
TWS	14	Knots
TWA	28	°
C_L	1.2	-
Lift	754.02	N
Forestay Tension	4712.60	N
Horizontal Component	1302.49	N
Vertical Component	4436.77	N
Backstay Angle	17.4	°
Backtasy Tension	4350.06	N
Backstay Compression	4150.48	N
Total Mast Compression	8587.26	N
Mast Length	10.85	m
Factor of safety	2.2	-
EI_{YY}	225	$GNmm^2$

Appendix J: Rig Laminate

Wing Mast

Gurit SE 70 Pre-Preg		
ρ_F	1.8	g/cm^3
ρ_R	1.28	g/cm^3
ψ	63.0%	W_F
φ	54.8%	V_F
w	200	g/m^2

Laminate Properties		
E_X	106.2E+3	N/mm^2
E_Y	23.5E+3	N/mm^2
G_{XY}	5.0E+3	N/mm^2
v_{xy}	0.3	-
Thickness	1.97	mm

Rig Properties		
I_{XX}	1.4E+6	mm^4
I_{YY}	10.6E+6	mm^4
EI_{XX}	145.4	GNmm^2
EI_{YY}	1126.9	GNmm^2
Area	1278	mm^2

Requirements		
EI_{XX}	145.0	GNmm^2
EI_{YY}	225.3	GNmm^2

Tube Mass		
Mass	2.00	kg/m

Ply	φ	1-φ	E_F (Pa)	E_R (Pa)	v_F	v_R	G_F (Pa)	G_R (Pa)	E_1 (Pa)	E_2 (Pa)	G_{12} (Pa)	v_{12}	v_{21}	θ (Degs)	θ (Rad)	sin(θ)	cos(θ)	E_X (Pa)	E_Y (Pa)	G_{XY} (Pa)	v_{xy}	t (mm)	ρ (g/cm^3)
1	0.55	0.452	235.0E+9	3.5E+9	0.3	0.3	52.0E+9	2.3E+9	130E+9	8E+9	5E+9	0.3	0.02	45	0.8	0.7071	0.7071	12E+9	12E+9	7E+9	0.23	0.197	1.56
2	0.55	0.452	235.0E+9	3.5E+9	0.3	0.3	52.0E+9	2.3E+9	130E+9	8E+9	5E+9	0.3	0.02	90	1.6	1.0	0.0	8E+9	130E+9	5E+9	0.02	0.197	1.56
3	0.55	0.452	235.0E+9	3.5E+9	0.3	0.3	52.0E+9	2.3E+9	130E+9	8E+9	5E+9	0.3	0.02	0	0.0	0.0	1.0	130E+9	8E+9	5E+9	0.30	0.197	1.56
4	0.55	0.452	235.0E+9	3.5E+9	0.3	0.3	52.0E+9	2.3E+9	130E+9	8E+9	5E+9	0.3	0.02	0	0.0	0.0	1.0	130E+9	8E+9	5E+9	0.30	0.197	1.56
5	0.55	0.452	235.0E+9	3.5E+9	0.3	0.3	52.0E+9	2.3E+9	130E+9	8E+9	5E+9	0.3	0.02	0	0.0	0.0	1.0	130E+9	8E+9	5E+9	0.30	0.197	1.56
6	0.55	0.452	235.0E+9	3.5E+9	0.3	0.3	52.0E+9	2.3E+9	130E+9	8E+9	5E+9	0.3	0.02	0	0.0	0.0	1.0	130E+9	8E+9	5E+9	0.30	0.197	1.56
7	0.55	0.452	235.0E+9	3.5E+9	0.3	0.3	52.0E+9	2.3E+9	130E+9	8E+9	5E+9	0.3	0.02	0	0.0	0.0	1.0	130E+9	8E+9	5E+9	0.30	0.197	1.56
8	0.55	0.452	235.0E+9	3.5E+9	0.3	0.3	52.0E+9	2.3E+9	130E+9	8E+9	5E+9	0.3	0.02	0	0.0	0.0	1.0	130E+9	8E+9	5E+9	0.30	0.197	1.56
9	0.55	0.452	235.0E+9	3.5E+9	0.3	0.3	52.0E+9	2.3E+9	130E+9	8E+9	5E+9	0.3	0.02	0	0.0	0.0	1.0	130E+9	8E+9	5E+9	0.30	0.197	1.56
10	0.55	0.452	235.0E+9	3.5E+9	0.3	0.3	52.0E+9	2.3E+9	130E+9	8E+9	5E+9	0.3	0.02	0	0.0	0.0	1.0	130E+9	8E+9	5E+9	0.30	0.197	1.56

Standard Mast

Gurit SE 70 Pre-Preg		
ρ_F	1.8	g/cm^3
ρ_R	1.28	g/cm^3
ψ	63.0%	W_F
φ	54.8%	V_F
w	200	g/m^2

Laminate Properties		
E_X	100.1E+3	N/mm^2
E_Y	23.5E+3	N/mm^2
G_{XY}	5.0E+3	N/mm^2
v_{xy}	0.3	-
Thickness	1.58	mm

Rig Properties		
I_{XX}	897.9E+3	mm^4
I_{YY}	2.5E+6	mm^4
EI_{XX}	89.9	GNmm^2
EI_{YY}	250.3	GNmm^2
Area	707.37	mm^2

Requirements		
EI_{XX}	86.2	GNmm^2
EI_{YY}	225.3	GNmm^2

Tube Mass		
Mass	1.11	kg/m

Ply	φ	1-φ	E_F (Pa)	E_R (Pa)	v_F	v_R	G_F (Pa)	G_R (Pa)	E_1 (Pa)	E_2 (Pa)	G_{12} (Pa)	v_{12}	v_{21}	θ (Degs)	θ (Rad)	sin(θ)	cos(θ)	E_X (Pa)	E_Y (Pa)	G_{XY} (Pa)	v_{xy}	t (mm)	ρ (g/cm^3)
1	0.55	0.452	235.0E+9	3.5E+9	0.3	0.3	52.0E+9	2.3E+9	130E+9	8E+9	5E+9	0.3	0.02	45	0.8	0.71	0.7071	12E+9	12E+9	7E+9	0.23	0.197	1.56
2	0.55	0.452	235.0E+9	3.5E+9	0.3	0.3	52.0E+9	2.3E+9	130E+9	8E+9	5E+9	0.3	0.02	90	1.6	1.0	0.0	8E+9	130E+9	5E+9	0.02	0.197	1.56
3	0.55	0.452	235.0E+9	3.5E+9	0.3	0.3	52.0E+9	2.3E+9	130E+9	8E+9	5E+9	0.3	0.02	0	0.0	0.0	1.0	130E+9	8E+9	5E+9	0.30	0.197	1.56
4	0.55	0.452	235.0E+9	3.5E+9	0.3	0.3	52.0E+9	2.3E+9	130E+9	8E+9	5E+9	0.3	0.02	0	0.0	0.0	1.0	130E+9	8E+9	5E+9	0.30	0.197	1.56
5	0.55	0.452	235.0E+9	3.5E+9	0.3	0.3	52.0E+9	2.3E+9	130E+9	8E+9	5E+9	0.3	0.02	0	0.0	0.0	1.0	130E+9	8E+9	5E+9	0.30	0.197	1.56
6	0.55	0.452	235.0E+9	3.5E+9	0.3	0.3	52.0E+9	2.3E+9	130E+9	8E+9	5E+9	0.3	0.02	0	0.0	0.0	1.0	130E+9	8E+9	5E+9	0.30	0.197	1.56
7	0.55	0.452	235.0E+9	3.5E+9	0.3	0.3	52.0E+9	2.3E+9	130E+9	8E+9	5E+9	0.3	0.02	0	0.0	0.0	1.0	130E+9	8E+9	5E+9	0.30	0.197	1.56
8	0.55	0.452	235.0E+9	3.5E+9	0.3	0.3	52.0E+9	2.3E+9	130E+9	8E+9	5E+9	0.3	0.02	0	0.0	0.0	1.0	130E+9	8E+9	5E+9	0.30	0.197	1.56

Appendix K: Stability Report

ISO 12217-2 Cat. C

Large Angle Stability				Departure			50% Load			Arrival		
Code	Criteria	Value	Units	Actual	Status	Margin %	Actual	Status	Margin %	Actual	Status	Margin %
ISO 12217-2:2002(E)	6.2.3 Downflooding angle	40	deg	146.8	Pass	237	147	Pass	267.5	147.4	Pass	268.5
ISO 12217-2:2002(E)	6.3 Angle of vanishing stability	90	deg	130.9	Pass	45.44	129.5	Pass	45.44	129.9	Pass	44.33
ISO 12217-2:2002(E)	6.4 STIX	14	See ISO 12217-2	23.1	Pass	65.19	22.6	Pass	61.14	22.4	Pass	60.13
ISO 12217-2:2002(E)	6.6.2 Dynamic stability factor	(2.594)	See ISO 12217-2	1.5	Pass	-	1.5	Pass	-	1.5	Pass	-
ISO 12217-2:2002(E)	6.6.3 Inversion recovery factor	(1.044)	See ISO 12217-2	1.037	Pass	-	1.044	Pass	-	1.044	Pass	-
ISO 12217-2:2002(E)	6.6.4 Knockdown recovery test	(0.935)	See ISO 12217-2	0.937	Pass	-	0.935	Pass	-	0.926	Pass	-
ISO 12217-2:2002(E)	6.6.5 Displacement-length factor	(0.9)	See ISO 12217-2	0.903	Pass	-	0.9	Pass	-	0.898	Pass	-
ISO 12217-2:2002(E)	6.6.6 Beam-displacement factor	(0.554)	See ISO 12217-2	0.75	Pass	-	0.75	Pass	-	0.75	Pass	-
ISO 12217-2:2002(E)	6.6.7 Wind moment factor	(1)	See ISO 12217-2	1	Pass	-	1	Pass	-	1	Pass	-
ISO 12217-2:2002(E)	6.6.8 Downflooding factor	(1.633)	See ISO 12217-2	1.25	Pass	-	1.25	Pass	-	1.25	Pass	-
ISO 12217-2:2002(E)	6.5 Knockdown-recovery test	90	deg	130.9	Pass	45.44	129.5	Pass	43.89	129.9	Pass	44.33
ISO 12217-2:2002(E)	6.6.6 Wind stiffness test*	45	deg	74.7	Fail	-65.89	75.2	Fail	-67.11	75.4	Fail	-67.54

*Complies if the angle of heel is less than the downflooding angle or 45°

Mini 6.50 Stability Test

Test				Stability configuration		
Code	Criteria	Value	Units	Actual	Status	Margin %
Large angle stability	J-21-a (minimum RM at masthead)	45	kg	48.5	Pass	7.8
Small angle stability	J-21-b (Angle of list)	10	deg	8.7	Pass	14.9

Appendix L: Rudder and keel Section

NACA 63-010								NACA 0010							
α	C_L	C_D	C_{Dp}	C_{DTotal}	C_L/C_D	x	y	α	C_L	C_D	C_{Dp}	C_{DTotal}	C_L/C_D	x	y
-10	-0.9757	0.02605	0.02206	0.04811	-20	0	0	-10	-1.0535	0.01841	0.01325	0.03166	-33	0	0
-9	-0.9132	0.02159	0.01704	0.03863	-24	0.005	0.00816	-9	-0.976	0.01421	0.00858	0.02279	-43	0.0125	0.01578
-8	-0.847	0.01655	0.01145	0.028	-30	0.0075	0.00983	-8	-0.8783	0.013	0.00728	0.02028	-43	0.025	0.02178
-7	-0.7697	0.01418	0.00888	0.02306	-33	0.0125	0.0125	-7	-0.788	0.01116	0.00528	0.01644	-48	0.05	0.02962
-6	-0.6782	0.01226	0.00677	0.01903	-36	0.025	0.01737	-6	-0.6955	0.01	0.00409	0.01409	-49	0.075	0.035
-5	-0.5476	0.00957	0.00379	0.01336	-41	0.05	0.02412	-5	-0.5974	0.00891	0.00314	0.01205	-50	0.1	0.03902
-4	-0.4148	0.00812	0.00244	0.01056	-39	0.075	0.02917	-4	-0.4588	0.00761	0.00233	0.00994	-46	0.15	0.04455
-3	-0.3101	0.00575	0.00136	0.00711	-44	0.1	0.03324	-3	-0.3234	0.00632	0.00171	0.00803	-40	0.2	0.04782
-2	-0.2112	0.00507	0.00103	0.0061	-35	0.15	0.0395	-2	-0.209	0.00539	0.00132	0.00671	-31	0.25	0.04952
-1	-0.1073	0.00489	0.00093	0.00582	-18	0.2	0.044	-1	-0.1045	0.00483	0.00107	0.0059	-18	0.3	0.05002
0	0	0.00485	0.0009	0.00575	0	0.25	0.04714	0	0	0.00464	0.00099	0.00563	0	0.4	0.04837
1	0.1073	0.00489	0.00093	0.00582	18	0.3	0.04913	1	0.1045	0.00483	0.00107	0.0059	18	0.5	0.04412
2	0.2112	0.00507	0.00103	0.0061	35	0.35	0.04995	2	0.209	0.00539	0.00132	0.00671	31	0.6	0.03803
3	0.3101	0.00575	0.00136	0.00711	44	0.4	0.04968	3	0.3233	0.00632	0.00171	0.00803	40	0.7	0.03053
4	0.4149	0.00812	0.00244	0.01056	39	0.45	0.04837	4	0.4588	0.00761	0.00233	0.00994	46	0.8	0.02187
5	0.5476	0.00957	0.00379	0.01336	41	0.5	0.04613	5	0.5974	0.00891	0.00314	0.01205	50	0.9	0.01207
6	0.6783	0.01226	0.00677	0.01903	36	0.55	0.04311	6	0.6954	0.01	0.00409	0.01409	49	0.95	0.00672
7	0.7696	0.01418	0.00888	0.02306	33	0.6	0.03943	7	0.7879	0.01116	0.00528	0.01644	48	1	0.00105
8	0.847	0.01655	0.01144	0.02799	30	0.65	0.03517	8	0.8782	0.013	0.00728	0.02028	43		
9	0.9132	0.02159	0.01704	0.03863	24	0.7	0.03044	9	0.9761	0.01421	0.00858	0.02279	43		
10	0.9757	0.02605	0.02206	0.04811	20	0.75	0.02545	10	1.0537	0.01841	0.01325	0.03166	33		
						0.8	0.0204								
						0.85	0.01535								
						0.9	0.0103								
						0.95	0.00525								
						1	0.00021								

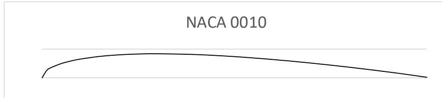

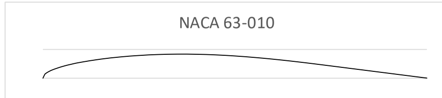

NACA 63-010					
α	C_L	C_D	C_{Dp}	C_{DTotal}	C_L/C_D
-10	-0.9757	0.02605	0.02206	0.04811	-20
-9	-0.9132	0.02159	0.01704	0.03863	-24
-8	-0.847	0.01655	0.01145	0.028	-30
-7	-0.7697	0.01418	0.00888	0.02306	-33
-6	-0.6782	0.01226	0.00677	0.01903	-36
-5	-0.5476	0.00957	0.00379	0.01336	-41
-4	-0.4148	0.00812	0.00244	0.01056	-39
-3	-0.3101	0.00575	0.00136	0.00711	-44
-2	-0.2112	0.00507	0.00103	0.0061	-35
-1	-0.1073	0.00489	0.00093	0.00582	-18
0	0	0.00485	0.0009	0.00575	0
1	0.1073	0.00489	0.00093	0.00582	18
2	0.2112	0.00507	0.00103	0.0061	35
3	0.3101	0.00575	0.00136	0.00711	44
4	0.4149	0.00812	0.00244	0.01056	39
5	0.5476	0.00957	0.00379	0.01336	41
6	0.6783	0.01226	0.00677	0.01903	36
7	0.7696	0.01418	0.00888	0.02306	33
8	0.847	0.01655	0.01144	0.02799	30
9	0.9132	0.02159	0.01704	0.03863	24
10	0.9757	0.02605	0.02206	0.04811	20

NACA 64-010					
α	C_L	C_D	C_{Dp}	C_{DTotal}	C_L/C_D
-10	-1.023	0.02286	0.01854	0.0414	-25
-9	-0.9335	0.02052	0.01594	0.03646	-26
-8	-0.8436	0.01645	0.01142	0.02787	-30
-7	-0.7423	0.01458	0.00935	0.02393	-31
-6	-0.6333	0.01165	0.00614	0.01779	-36
-5	-0.5366	0.01009	0.00424	0.01433	-37
-4	-0.4326	0.00885	0.00274	0.01159	-37
-3	-0.3299	0.00688	0.00159	0.00847	-39
-2	-0.2252	0.00528	0.00103	0.00631	-36
-1	-0.1136	0.00507	0.00096	0.00603	-19
0	0	0.00504	0.0009	0.00594	0
1	0.1136	0.00507	0.00095	0.00602	19
2	0.2252	0.00528	0.00103	0.00631	36
3	0.3299	0.00688	0.00159	0.00847	39
4	0.4326	0.00885	0.00274	0.01159	37
5	0.5366	0.01009	0.00424	0.01433	37
6	0.6333	0.01165	0.00614	0.01779	36
7	0.7424	0.01458	0.00935	0.02393	31
8	0.8436	0.01645	0.01142	0.02787	30
9	0.9335	0.02052	0.01594	0.03646	26
10	1.023	0.02286	0.01854	0.0414	25

NACA 66-010					
α	C_L	C_D	C_{Dp}	C_{DTotal}	C_L/C_D
-7	-0.7098	0.01971	0.01462	0.03433	-21
-6	-0.6144	0.01465	0.00894	0.02359	-26
-5	-0.5152	0.01202	0.00603	0.01805	-29
-4	-0.4177	0.0098	0.00356	0.01336	-31
-3	-0.3117	0.00871	0.00235	0.01106	-28
-2	-0.2241	0.0052	0.00116	0.00636	-35
-1	-0.1139	0.00519	0.00131	0.0065	-18
0	0	0.00526	0.00137	0.00663	0
1	0.1139	0.00519	0.00131	0.0065	18
2	0.2241	0.0052	0.00116	0.00636	35
3	0.3117	0.00871	0.00235	0.01106	28
4	0.4177	0.0098	0.00356	0.01336	31
5	0.5152	0.01202	0.00603	0.01805	29
6	0.6144	0.01465	0.00894	0.02359	26
7.5	0.7457	0.02615	0.02191	0.04806	16

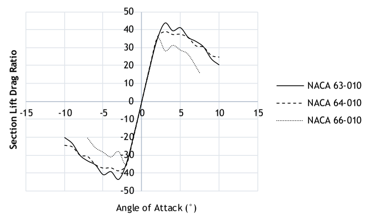

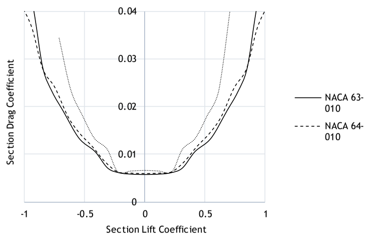

NACA 63-010

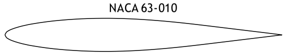

NACA 64-010

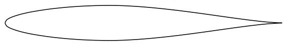

NACA 66-010

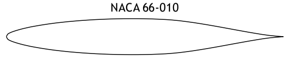

Appendix M: Bulb Calculations

	Mass	300 kg	Density	1025	kg/m^3	Viscosity	0.00119	N s/m^2								
	Bulb N°	Chord (m)	T (m)	Height (m)	T average (m)	T/C	WSA (m^2)	SA (m^2)	Fn	v (m/s)	Re	C_F	(1+K)	R_F (N)	R_V (N)	% Difference
NACA XX	1	1.797	0.213	0.146	0.180	10%	0.7521	0.031	0.35	2.8	4.33E+06	0.0035	1.15	10.51	12.08	101.43%
	2	1.464	0.237	0.163	0.200	14%	0.6838	0.033	0.35	2.8	3.52E+06	0.0036	1.20	9.93	11.96	100.45%
	3	1.375	0.244	0.167	0.206	15%	0.662	0.037	0.35	2.8	3.31E+06	0.0037	1.22	9.73	11.91	100.00%
	4	1.25	0.256	0.176	0.216	17%	0.6334	0.041	0.35	2.8	3.01E+06	0.0037	1.26	9.48	11.94	100.24%
	5	1.134	0.269	0.185	0.227	20%	0.6056	0.027	0.35	2.8	2.73E+06	0.0038	1.30	9.24	12.01	100.87%

	Mass	300 kg	Density	1025	kg/m^3	Viscosity	0.00119	N s/m^2								
	Bulb N°	Chord (m)	T (m)	Height (m)	T average (m)	T/C	WSA (m^2)	SA (m^2)	Fn	v (m/s)	Re	C_F	(1+K)	R_F (N)	R_V (N)	% Difference
NACA 66	1	1.835	0.183	0.183	0.183	10%	0.7121	0.027	0.35	2.8	4.42E+06	0.0035	1.15	9.91	11.39	95.64%
	2	1.581	0.198	0.198	0.198	13%	0.6624	0.041	0.35	2.8	3.81E+06	0.0036	1.19	9.48	11.26	94.54%
	3	1.401	0.21	0.21	0.210	15%	0.626	0.037	0.35	2.8	3.37E+06	0.0037	1.22	9.17	11.23	94.27%
	4	1.266	0.222	0.222	0.222	18%	0.5987	0.033	0.35	2.8	3.05E+06	0.0037	1.26	8.94	11.29	94.81%
	5	1.157	0.231	0.231	0.231	20%	0.5733	0.031	0.35	2.8	2.79E+06	0.0038	1.30	8.71	11.32	95.06%

	Mass	300 kg	Density	1025	kg/m^3	Viscosity	0.00119	N s/m^2								
	Bulb N°	Chord (m)	T (m)	Height (m)	T average (m)	T/C	WSA (m^2)	SA (m^2)	Fn	v (m/s)	Re	C_F	(1+K)	R_F (N)	R_V (N)	% Difference
NACA 63	1	1.901	0.19	0.19	0.190	10%	0.7098	0.027	0.35	2.8	4.58E+06	0.0035	1.15	9.81	11.28	94.73%
	2	1.637	0.205	0.205	0.205	13%	0.6601	0.041	0.35	2.8	3.94E+06	0.0036	1.19	9.38	11.15	93.59%
	3	1.45	0.218	0.218	0.218	15%	0.6232	0.037	0.35	2.8	3.49E+06	0.0036	1.23	9.07	11.11	93.29%
	4	1.308	0.229	0.229	0.229	18%	0.5936	0.033	0.35	2.8	3.15E+06	0.0037	1.26	8.81	11.12	93.38%
	5	1.223	0.237	0.237	0.237	19%	0.5761	0.031	0.35	2.8	2.94E+06	0.0038	1.29	8.66	11.18	93.85%

Appendix N: 2D case Grid Dependency Study

Case Setup Coars Mesh			
AoA	4	deg	
U	1.14	m/s	
Re	1.00E+06	-	
Forces Summary			
Lift	62.551	N	
Drag	1.04598	N	
C_L	0.96262	-	
C_D	0.01610	-	
C_L/C_D	59.8013	-	
Mesh Summary			
Total Number of Nodes			36552
Total Number of Elements			18093
Prisms			73
Hexahedrons			18017
Total Number of Faces			-

Case Setup Medium Mesh			
AoA	4	deg	
U	1.14	m/s	
Re	1.00E+06	-	
Forces Summary			
Lift	62.9733	N	
Drag	0.968067	N	
C_L	0.96912	-	
C_D	0.01490	-	
C_L/C_D	65.0506	-	
Mesh Summary			
Total Number of Nodes			89654
Total Number of Elements			44571
Prisms			499
Hexahedrons			44672
Total Number of Faces			-

Case Setup Fine Mesh			
AoA	4	deg	
U	1.14	m/s	
Re	1.00E+06	-	
Forces Summary			
Lift	63.0005	N	
Drag	0.96144	N	
C_L	0.96954	-	
C_D	0.01480	-	
C_L/C_D	65.5272	-	
Mesh Summary			
Total Number of Nodes			164160
Total Number of Elements			81941
Prisms			427
Hexahedrons			81514
Total Number of Faces			-

Total Number of Elements		L	D
N_1	164.2E+3	63.0005	0.9614
N_2	89.7E+3	62.9733	0.9681
N_3	36.6E+3	62.5510	1.0460

h_1	0.0025	Φ_1	63.0005
h_2	0.0033	Φ_2	62.9733
h_3	0.0052	Φ_3	62.5510

h_1	0.013	Φ_1	0.96144
h_2	0.018	Φ_2	0.96807
h_3	0.028	Φ_3	1.04598

r_{21}	1.35	ε_{21}	-0.0272
r_{32}	1.57	ε_{32}	-0.4223

r_{21}	1.35	ε_{21}	0.00663
r_{32}	1.57	ε_{32}	0.07791

p	1.106	
$q(p)$	-0.48	apparent order
s	1	
Φ_{ext}^{21}	63.07	extrapolated values
Φ_{ext}^{32}	63.63	extrapolated values
e^{21}_{a}	0.04%	approximate relative error
e^{21}_{ext}	0.11%	extrapolated relative error
e^{32}_{a}	0.67%	approximate relative error
e^{32}_{ext}	1.03%	extrapolated relative error
GCI^{21}_{fine}	**0.14%**	fine-grid convergence index

p	1.1060	
$q(p)$	-0.48	apparent order
s	1	
Φ_{ext}^{21}	0.94	extrapolated values
Φ_{ext}^{32}	0.85	extrapolated values
e^{21}_{a}	0.69%	approximate relative error
e^{21}_{ext}	2%	extrapolated relative error
e^{32}_{a}	8.05%	approximate relative error
e^{32}_{ext}	14.32%	extrapolated relative error
GCI^{21}_{fine}	**2.2%**	fine-grid convergence index

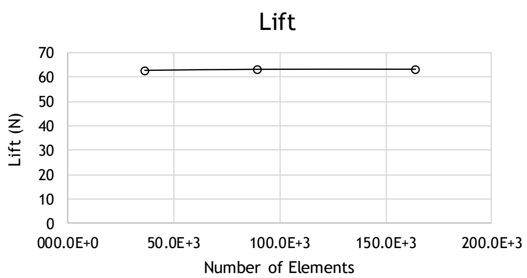

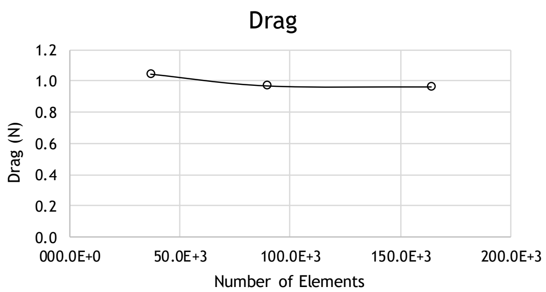

Appendix O: 2D Section results

Eppler 214, Re 1e6			
AoA (°)	C_L	C_D	L/D
-2	0.3269	0.0119	27.4
0	0.5456	0.0121	45.1
2	0.7611	0.0131	57.9
4	0.9695	0.0148	65.6
6	1.1640	0.0177	65.6
8	1.3377	0.0177	75.4

NACA 63-412, Re 1e6			
AoA (°)	C_L	C_D	L/D
-2	-0.0876	0.0111	-7.9
0	0.1258	0.0109	11.6
2	0.3361	0.0113	29.8
4	0.5438	0.0129	42.2
6	0.7376	0.0162	45.5
8	0.9093	0.0227	40.0

Eppler 817, Re 1e6			
AoA (°)	C_L	C_D	L/D
-2	0.1263	0.0115	11.0
0	0.3432	0.0116	29.5
2	0.5525	0.0127	43.6
4	0.7496	0.0155	48.5
6	0.9201	0.0207	44.4
8	1.0266	0.0329	31.2

Eppler 387, Re 1e6			
AoA (°)	C_L	C_D	L/D
-2	0.1399	0.0122	11.4
0	0.3542	0.0114	30.9
2	0.5674	0.0119	47.8
4	0.7758	0.0134	58.0
6	0.9769	0.0163	60.1
8	1.1533	0.0210	54.9

Section Lift Coefficent for Different Angle of Attack

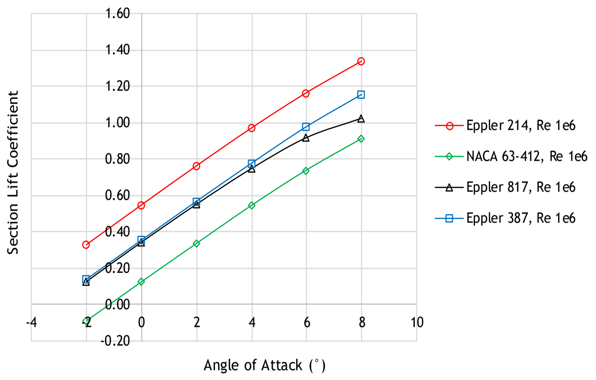

Section Lift/Drag Ratio for Different Angle of Attack

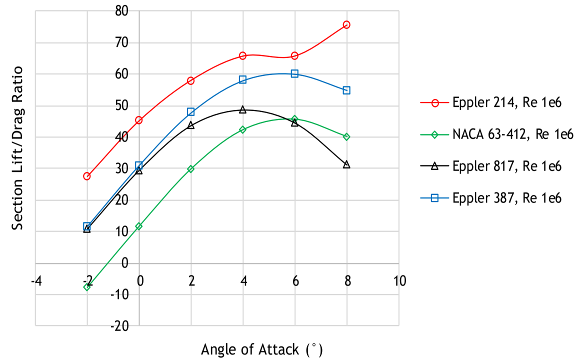

Section Drag Coefficent for Different Angle of Attack

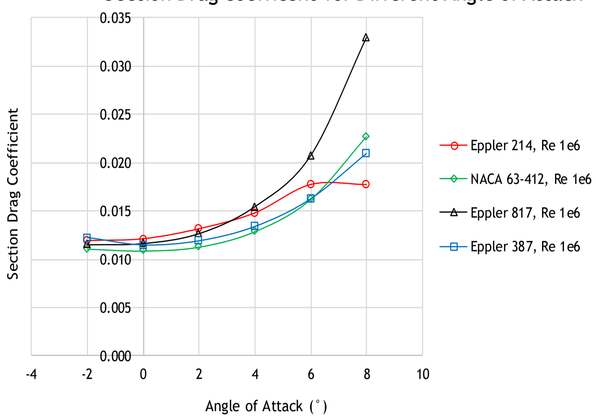

Section Lift Coefficient for Different Section Drag Coefficient

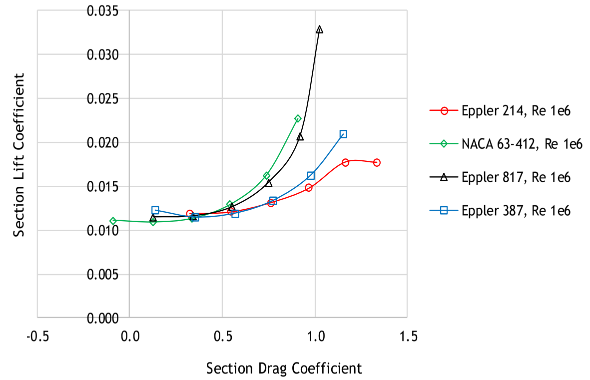

Appendix P: 3D Case Grid Dependency Study

Case Setup Coars Mesh		
AoA	2	deg
U	4.00	m/s
Re	1.0E+06	-
Forces Summary		
Drag	133.271	N
Lift	1773.73	N
Sideforce	1195.68	-
Mesh Summary		
Total Number of Nodes		1.16E+06
Total Number of Elements		4.77E+06
Tetrahedra		3.78E+06
Wedges		9.89E+05
Total Number of Faces		-

Case Setup Medium Mesh		
AoA	2	deg
U	4.00	m/s
Re	1.0E+06	-
Forces Summary		
Drag	133.279	N
Lift	1773.96	N
Sideforce	1196.16	-
Mesh Summary		
Total Number of Nodes		1.45E+06
Total Number of Elements		6.52E+06
Tetrahedra		5.53E+06
Wedges		9.89E+05
Total Number of Faces		-

Case Setup Fine Mesh		
AoA	2	deg
U	4.00	m/s
Re	1.0E+06	-
Forces Summary		
Drag	132.453	N
Lift	1779.36	N
Sideforce	1198.12	N
Mesh Summary		
Total Number of Nodes		2.57E+06
Total Number of Element		1.31E+07
Tetrahedra		1.21E+07
Wedges		9.89E+05
Total Number of Faces		-

Total Number of Elements		Drag	Sideforce
N_1	2.6E+6	132.45	1198.12
N_2	1.5E+6	133.28	1196.16
N_3	1.2E+6	133.27	1195.68

h_1	0.0006	Φ_1	132.4530
h_2	0.0008	Φ_2	133.2790
h_3	0.0009	Φ_3	133.2710

h_1	0.003	Φ_1	1198.12000
h_2	0.004	Φ_2	1196.16000
h_3	0.005	Φ_3	1195.68000

r_{21}	1.33	ε_{21}	0.8260
r_{32}	1.12	ε_{32}	-0.0080

r_{21}	1.33	ε_{21}	-1.96000
r_{32}	1.12	ε_{32}	-0.48000

p	3.978	
$q(p)$	1.30	apparent order
s	-1	
Φ_{ext}^{21}	132.06	extrapolated values
Φ_{ext}^{32}	133.29	extrapolated values
e^{21}_{a}	0.62%	approximate relative error
e^{21}_{ext}	0.30%	extrapolated relative error
e^{32}_{a}	0.01%	approximate relative error
e^{32}_{ext}	0.01%	extrapolated relative error
GCI^{21}_{fine}	**0.37%**	fine-grid convergence index

p	3.9783	
$q(p)$	1.30	apparent order
s	1	
Φ_{ext}^{21}	1199.06	extrapolated values
Φ_{ext}^{32}	1197.00	extrapolated values
e^{21}_{a}	0.16%	approximate relative error
e^{21}_{ext}	0%	extrapolated relative error
e^{32}_{a}	0.04%	approximate relative error
e^{32}_{ext}	0.07%	extrapolated relative error
GCI^{21}_{fine}	**0.10%**	fine-grid convergence index

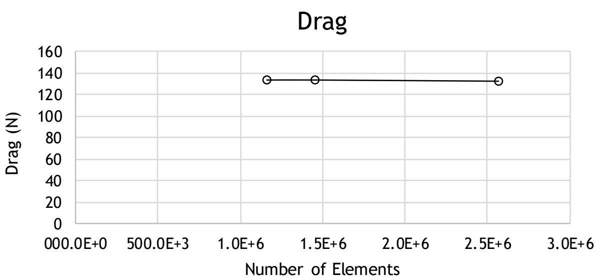

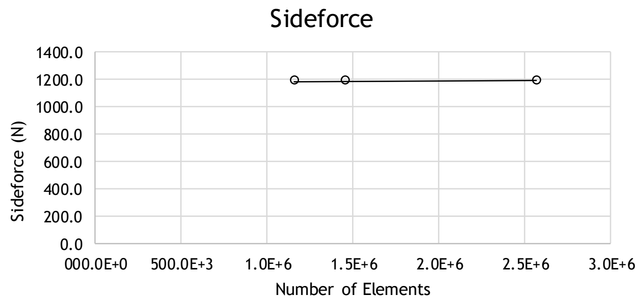

Appendix Q: 3D Foil CFX Results and Plots

Mk_ii_AoA_0_Re_1e6		
U	4	m/s
Re	1E+06	-
Fx	117.698	N
Fy	1728.29	N
Fz	-881.65	N

Mk_ii_AoA_2_Re_1e6		
U	4	m/s
Re	1E+06	-
Fx	132.453	N
Fy	1779.36	N
Fz	-1198.1	N

Mk_ii_AoA_4_Re_1e6		
U	4	m/s
Re	1E+06	-
Fx	157.51	N
Fy	1823.61	N
Fz	-1503.9	N

Mk_ii_AoA_6_Re_1e6		
U	4	m/s
Re	1E+06	-
Fx	191.893	N
Fy	1867.5	N
Fz	-1801.3	N

Mk ii						
AoA (°)	Lift (N)	Drag (N)	Sideforce (N)	L/D	L/SF	SF/D
0	1728.29	117.698	881.65	14.68	1.96	7.49
2	1779.36	132.453	1198.12	13.43	1.49	9.05
4	1823.61	157.51	1503.91	11.58	1.21	9.55
6	1867.5	191.893	1801.26	9.73	1.04	9.39

Medium Mesh

Mk_ii_AoA_2_Re_1e6		
U	4	m/s
Re	1E+06	-
Fx	133.279	N
Fy	1773.96	N
Fz	-1196.2	N

Coarse Mesh

Mk_ii_AoA_2_Re_1e6		
U	4	m/s
Re	1E+06	-
Fx	133.271	N
Fy	1773.73	N
Fz	-1195.7	N

Mk_iii_AoA_0_Re_1e6		
U	4	m/s
Re	1E+06	-
Fx	113.245	N
Fy	1687.37	N
Fz	-781.3	N

Mk_iii_AoA_2_Re_1e6		
U	4	m/s
Re	1E+06	-
Fx	126.404	N
Fy	1711.64	N
Fz	-1070.4	N

Mk_iii_AoA_4_Re_1e6		
U	4	m/s
Re	1E+06	-
Fx	147.577	N
Fy	1746.85	N
Fz	-1354.1	N

Mk_iii_AoA_6_Re_1e6		
U	4	m/s
Re	1E+06	-
Fx	176.56	N
Fy	1790.91	N
Fz	-1631.6	N

Mk iii						
AoA (°)	Lift (N)	Drag (N)	Sideforce (N)	L/D	L/SF	SF/D
0	1687.37	113.245	781.298	14.90	2.16	6.90
2	1711.64	126.404	1070.4	13.54	1.60	8.47
4	1746.85	147.577	1354.07	11.84	1.29	9.18
6	1790.91	176.56	1631.62	10.14	1.10	9.24

Mk_iv_AoA_0_Re_1e6		
U	4	m/s
Re	1E+06	-
Fx	127.884	N
Fy	1693.64	N
Fz	-0.417	N

Mk_iv_AoA_2_Re_1e6		
U	4	m/s
Re	1E+06	-
Fx	122.565	N
Fy	1580.87	N
Fz	-378.18	N

Mk_iv_AoA_4_Re_1e6		
U	4	m/s
Re	1E+06	-
Fx	140.235	N
Fy	1446.7	N
Fz	-752.23	N

Mk_iv_AoA_6_Re_1e6		
U	4	m/s
Re	1E+06	-
Fx	55.439	N
Fy	0.311	N
Fz	2.421	N

Mk iv						
AoA (°)	Lift (N)	Drag (N)	Sideforce (N)	L/D	L/SF	SF/D
0	1693.64	127.884	0.417	13.24	4061.49	0.00
2	1580.87	122.565	378.177	12.90	4.18	3.09
4	1446.7	140.235	752.227	10.32	1.92	5.36
6	0.311	55.439	-2.421	0.01	-0.13	-0.04

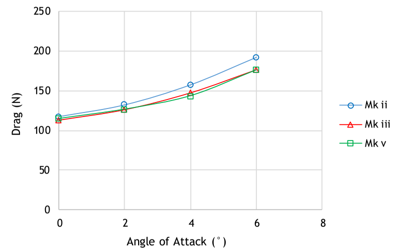

Mk_v_AoA_0_Re_1e6		
U	4	m/s
Re	1E+06	-
Fx	114.757	N
Fy	1701.45	N
Fz	-772.22	N

Mk_v_AoA_2_Re_1e6		
U	4	m/s
Re	1E+06	-
Fx	126.59	N
Fy	1728.81	N
Fz	-1062.3	N

Mk_v_AoA_4_Re_1e6		
U	4	m/s
Re	1E+06	-
Fx	143.583	N
Fy	1738.87	N
Fz	-1351.4	N

Mk_v_AoA_6_Re_1e6		
U	4	m/s
Re	1E+06	-
Fx	176.271	N
Fy	1784.11	N
Fz	-1618.5	N

Mk v						
AoA (°)	Lift (N)	Drag (N)	Sideforce (N)	L/D	L/SF	SF/D
0	1701.45	114.757	772.224	14.83	2.20	6.73
2	1728.81	126.59	1062.26	13.66	1.63	8.39
4	1738.87	143.583	1351.4	12.11	1.29	9.41
6	1784.11	176.271	1618.45	10.12	1.10	9.18

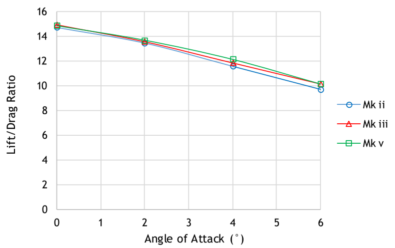

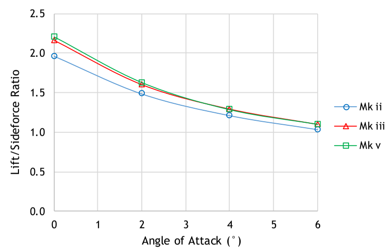

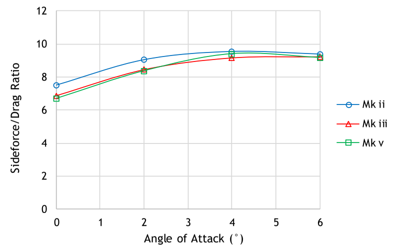

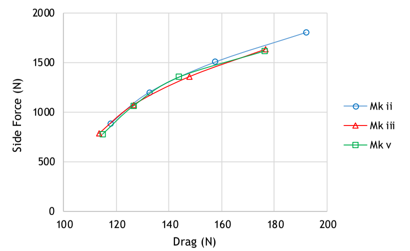

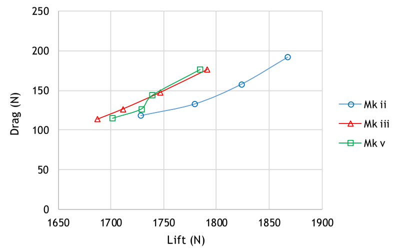

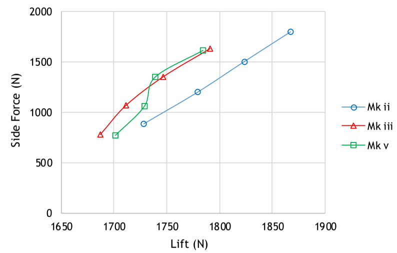

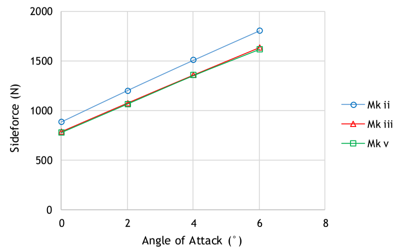

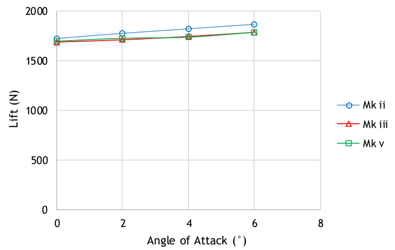

Appendix R: ISO 12215-5 Panel Requirements

	ID	1	2	3	4	5	6	7	8	9	10	11	12	13	14
Dimensions and Location	Label	Bottom	Bottom	Bottom	Bottom	Bottom	Bottom	Bottom	Bottom	Bottom Light	Bottom Light	Bottom Light	Bottom Light	Bottom Light	Bottom Light
	Length (mm)	1002	914	1121	1121	1124	1124	930	930	930	930	930	930	600	1189
	Width (mm)	746	358	465	791	572	865	627	886	627	907	626	893	600	600
	Aspect Ratio	1.343	2.553	2.411	1.418	1.965	1.299	1.484	1.05	1.484	1.026	1.486	1.041	1	1.982
	x (m)	6	6	5.1	5.1	4	4	2.92	2.92	2	2	1.07	1.07	0.3	0.3
	Location	Side	Side	B & S	B & S	Bottom	B & S	Bottom	B & S	Bottom	B & S	Bottom	B & S	Bottom	B & S
	z	0.85	0.85	--	--	--	--	--	--	--	--	--	--	--	--
Calculations to ISO Standard	k_L	1	1	1	1	1	1	0.932	0.932	0.796	0.796	0.659	0.659	0.545	0.545
	k_{AR}	0.4	0.549	0.463	0.4	0.425	0.4	0.432	0.4	0.432	0.4	0.432	0.4	0.502	0.409
	k_2	0.5	0.5	0.5	0.5	0.5	0.5	0.5	0.472	0.5	0.467	0.5	0.47	0.462	0.5
	k_3	0.028	0.028	0.028	0.028	0.028	0.028	0.028	0.026	0.028	0.025	0.028	0.026	0.025	0.028
	k_z	0.765	0.635	1.072	0.831	--	0.949	--	0.987	--	1	--	1	--	0.938
	Design Pressure (kN/m$^{2)}$	7.8	9.8	10.4	8.3	9.5	8.7	9	8.3	8.1	7.6	8.1	6.9	8.1	6
Requirements	M_{db} (Nmm/mm)	361.4	104.9	187.2	430	259.1	542.4	294.6	512.5	265.3	489.4	264.9	432.2	224.8	180.8
	M_{dl} (Nmm/mm)	94.9	25.9	46.4	112.4	65.6	142.9	76.6	145.8	69	140.8	68.9	123.4	65.6	45.7
	Eib (Nm^2/mm)	0.444	0.062	0.143	0.56	0.244	0.773	0.304	0.728	0.274	0.708	0.273	0.618	0.214	0.179
	w_{os} (kg/m^2)	0.243	0.243	0.27	0.27	0.27	0.27	0.27	0.27	0.27	0.27	0.27	0.27	0.27	0.27
	w_{is} (kg/m^2)	0.17	0.17	0.189	0.189	0.189	0.189	0.189	0.189	0.189	0.189	0.189	0.189	0.189	0.189
	Shear Force (N/mm)	2.3	1.7	2.3	2.7	2.5	3	2.4	2.6	2.1	2.4	2.1	2.1	1.7	1.7
Offered	M_{db} (Nmm/mm)	839.6	839.6	839.6	839.6	839.6	839.6	839.6	839.6	581.6	581.6	581.6	581.6	581.6	581.6
	M_{dl} (Nmm/mm)	147.5	147.5	147.5	147.5	147.5	147.5	147.5	147.5	147.5	147.5	147.5	147.5	147.5	147.5
	Eib (Nm^2/mm)	2.943	2.943	2.943	2.943	2.943	2.943	2.943	2.943	2.943	2.943	2.943	2.943	2.943	2.943
	w_{os} (kg/m^2)	0.4	0.4	0.4	0.4	0.4	0.4	0.4	0.4	0.4	0.4	0.4	0.4	0.4	0.4
	w_{is} (kg/m^2)	0.4	0.4	0.4	0.4	0.4	0.4	0.4	0.4	0.4	0.4	0.4	0.4	0.4	0.4
	Shear Force (N/mm)	7	7	7	7	7	7	7	7	4.1	4.1	4.1	4.1	4.1	4.1
Results	b Min Ply No. and Stress Ratio	5, 2.323	5, 8.005	5, 4.484	5, 1.952	5, 3.240	5, 1.548	5, 2.850	5, 1.638	5, 2.192	5, 1.188	5, 2.195	5, 1.346	5, 2.587	5, 3.217
	l Min Ply No. and Stress Ratio	2, 1.554	2, 5.704	2, 3.177	2, 1.312	2, 2.249	2, 1.032	2, 1.924	2, 1.012	2, 2.136	2, 1.047	2, 2.140	2, 1.195	2, 2.250	2, 3.226
	El_b Ratio	6.628	47.586	20.524	5.256	12.055	3.808	9.681	4.045	10.749	4.156	10.774	4.763	13.743	16.47
	w_{os} Ratio	1.647	1.647	1.482	1.482	1.482	1.482	1.482	1.482	1.482	1.482	1.482	1.482	1.482	1.482
	w_{is} Ratio	2.352	2.352	2.117	2.117	2.117	2.117	2.117	2.117	2.117	2.117	2.117	2.117	2.117	2.117
	Shear Force Ratio	2.978	4.099	3.01	2.582	2.771	2.34	2.924	2.704	1.929	1.731	1.93	1.925	2.505	2.472
	Plating Comply	yes	yes	yes	yes	yes	yes	yes	yes	yes	yes	yes	yes	yes	yes
	Core Comply	yes	yes	yes	yes	yes	yes	yes	yes	yes	yes	yes	yes	yes	yes

Notes:
-Panels are assumed to have no curvature
- B & S stands for Bottom and side

	ID	15	16	17	18	19	20	21	22	23	24	25	26	27	28	29	30	31	-	-	-	-
Dimensions and Location	Label	Topside	Topside	Topside	Topside	Topside	Topside	Topside	Topside	Topside	Topside	Topside	Topside	Topside	Topside	Topside	Topside	Topside	WTBHD	WTBHD	WTBHD	Topside
	Length (mm)	1328	1160	1135	930	930	930	600	836	1100	1124	930	930	930	1200	1124	930	648	2020	1180	600	1100
	Width (mm)	372	460	555	560	574	527	483	505	610	571	443	501	630	496	459	500	509	664	277	350	300
	Aspect Ratio	3.57	2.52	2.05	1.66	1.62	1.77	1.24	1.66	1.80	1.97	2.10	1.86	1.48	2.42	2.45	1.86	1.27	3.04	4.27	1.72	3.67
	x (m)	6.16	5.06	4	2.9	2	1.1	0.3	6	5.1	4	3	2	1	1.5	4	3	2	0	0	0	0
	Location	Side	Side	Side	Side	Side	Side	Side	Deck	Deck	Deck	Deck	Deck	Deck	Deck	SS	SS	SS	WTBHD	WTBHD	WTBHD	Side
	z	0.85	0.83	0.79	0.76	0.7	0.7	0.65	--	--	--	--	--	--	--	--	--	--	--	--	--	0.75
Calculations to ISO Standard	k_L	1	1	1	0.929	0.796	0.663	0.545	1	1	1	0.943	0.796	0.648	0.722	--	--	--	--	--	--	0.501
	k_{AR}	0.535	0.462	0.429	0.454	0.449	0.466	0.55	0.489	0.416	0.425	0.5	0.475	0.431	0.442	0.465	0.476	0.526	0.354	0.652	0.624	0.618
	k_2	0.5	0.5	0.5	0.489	0.486	0.495	0.43	0.489	0.497	0.5	0.5	0.5	0.472	0.5	0.5	0.5	0.436	0.5	0.5	0.48	0.5
	k_3	0.028	0.028	0.028	0.027	0.027	0.028	0.022	0.027	0.028	0.028	0.028	0.028	0.026	0.028	0.028	0.028	0.023	0.028	0.028	0.026	0.028
	k_z	0.206	0.259	0.323	0.329	0.343	0.371	0.331	--	--	--	--	--	--	--	--	--	--	--	--	--	0.733
	Design Pressure (kN/m$^{2)}$	6.7	6.1	6	6	5.1	5	5	5	5	5	5	5	5	5	5	5	5	4.6	1.9	1.9	5.9
Requirements	M_{db} (Nmm/mm)	77.8	108.1	154.8	152.3	136.4	114.5	83.5	103.9	154.1	135.9	81.6	104.6	155.8	102.3	87.8	104.2	94.1	169.7	12	18.5	44.3
	M_{dl} (Nmm/mm)	38.1	54.7	80	82	74	60.5	52.2	56	81.1	70.5	42.1	54.6	87.9	52	44.8	54.6	58.2	--	7.1	12.4	21.6
	Eib (Nm^2/mm)	0.048	0.082	0.142	0.139	0.127	0.099	0.062	0.086	0.155	0.128	0.059	0.086	0.157	0.083	0.066	0.086	0.074	0.186	0.005	0.01	0.022
	w_{os} (kg/m^2)	0.243	0.243	0.243	0.243	0.243	0.243	0.243	0.189	0.189	0.189	0.189	0.189	0.189	0.189	0.189	0.189	0.189	--	--	--	0.243
	w_{is} (kg/m^2)	0.17	0.17	0.17	0.17	0.17	0.17	0.17	0.132	0.132	0.132	0.132	0.132	0.132	0.132	0.132	0.132	0.132	--	--	--	0.17
	Shear Force (N/mm)	1.3	1.4	1.6	1.5	1.3	1.2	0.9	1.1	1.4	1.3	1	1.1	1.3	1.2	1.1	1.1	1	1.5	0.3	0.3	0.9
Offered	M_{db} (Nmm/mm)	157.6	157.6	157.6	157.6	157.6	157.6	157.6	157.6	157.6	157.6	157.6	157.6	157.6	157.6	105.6	105.6	105.6	238.8	156.2	156.2	157.6
	M_{dl} (Nmm/mm)	146.2	146.2	146.2	146.2	146.2	146.2	146.2	146.2	146.2	146.2	146.2	146.2	146.2	146.2	99.3	99.3	99.3	--	156.2	156.2	146.2
	Eib (Nm^2/mm)	0.597	0.597	0.597	0.597	0.597	0.597	0.597	0.597	0.597	0.597	0.597	0.597	0.597	0.597	0.271	0.271	0.271	0.517	0.332	0.332	0.597
	w_{os} (kg/m^2)	0.4	0.4	0.4	0.4	0.4	0.4	0.4	0.4	0.4	0.4	0.4	0.4	0.4	0.4	0.4	0.4	0.4	--	--	--	0.4
	w_{is} (kg/m^2)	0.2	0.2	0.2	0.2	0.2	0.2	0.2	0.2	0.2	0.2	0.2	0.2	0.2	0.2	0.2	0.2	0.2	--	--	--	0.2
	Shear Force (N/mm)	4.1	4.1	4.1	4.1	4.1	4.1	4.1	4.1	4.1	4.1	4.1	4.1	4.1	4.1	2.8	2.8	2.8	4.1	4.1	4.1	4.1
Results	b Min Ply No. and Stress Ratio	4, 2.025	4, 1.458	4, 1.018	4, 1.035	4, 1.156	4, 1.377	4, 1.887	4, 1.517	4, 1.023	4, 1.160	4, 1.932	4, 1.507	4, 1.012	4, 1.541	4, 1.203	4, 1.014	4, 1.122	3, 1.407	3, 12.974	3, 8.451	4, 3.555
	l Min Ply No. and Stress Ratio	2, 3.843	2, 2.672	2, 1.828	2, 1.783	2, 1.976	2, 2.416	2, 2.802	2, 2.610	2, 1.803	2, 2.075	2, 3.477	2, 2.680	2, 1.664	2, 2.812	2, 2.218	2, 1.819	2, 1.706	--	3, 21.930	3, 12.563	2, 6.763
	El_b Ratio	12.528	7.295	4.221	4.286	4.691	6.015	9.652	6.968	3.845	4.676	10.046	6.922	3.8	7.155	4.077	3.154	3.654	2.782	60.511	31.749	27.269
	w_{os} Ratio	1.647	1.647	1.647	1.647	1.647	1.647	1.647	2.117	2.117	2.117	2.117	2.117	2.117	2.117	2.117	2.117	2.117	--	--	--	1.647
	w_{is} Ratio	1.176	1.176	1.176	1.176	1.176	1.176	1.176	1.512	1.512	1.512	1.512	1.512	1.512	1.512	1.512	1.512	1.512	--	--	--	1.176
	Shear Force Ratio	3.267	3.019	2.634	2.788	3.199	3.461	4.405	3.687	2.97	3.11	3.966	3.588	3.098	3.458	2.516	2.426	2.784	2.711	15.575	13.809	4.625
	Plating Comply	yes	yes	yes	yes	yes	yes	yes	yes	yes	yes	yes	yes	yes	yes	yes	yes	yes	yes	yes	yes	yes
	Core Comply	yes	yes	yes	yes	yes	yes	yes	yes	yes	yes	yes	yes	yes	yes	yes	yes	yes	yes	yes	yes	yes

Notes:
-Panels are assumed to have no curvature
- SS stands for Superstructure
- WTBHD stands for Waterthight Bulkhead

Appendix S: ISO 12215-5 Stiffeners Requirements

	ID	A	B	C	D	E	G	H	I	J	K	L	M	N	O	P	Q	R	S	T	U
Label	Label	Bow Ringframe	Mast Ringframe	Keel Ringframe	Aft Ringframe	Side Ringframe	Bow Stiffener	Bow Stiffener	Bow Stiffener	Side Stiffener	Side Stiffener	Side Stiffener	Side Stiffener	Aft Stiffener	Aft Stiffener	Aft Stiffener	Aft Stiffener	Aft Stiffener	Deck Stiffener	Deck Stiffener	Deck Stiffener
	l_u *(mm)*	2580	2864	2678	2728	539	914	1125	1130	1125	1130	930	930	930	930	930	930	600	863	1124	1124
	s (mm)	1124	799	694	930	1124	552	464	627	572	719	627	906	627	907	626	893	901	505	565	459
	x (m)	4.5	3.38	2.45	1.53	4.5	6	5.1	5.1	4	4	2.92	2.92	1.995	1.995	1.097	1.067	0.3	6	5.1	3.9
	Location	Side		320	300	Deck	Side	Bottom	Bottom	Bottom	Bottom	Bottom	Bottom	Bottom	Bottom	Bottom	Bottom	Bottom	Deck	Deck	Deck
Calculations to ISO Standard	k_L	1	0.999	0.862	0.727	1	1	1	1	1	1	0.932	0.932	0.795	0.795	0.663	0.658	0.545	1	1	1
	k_{AR}	0.25	0.25	0.25	0.25	0.29	0.281	0.264	0.25	0.25	0.25	0.268	0.25	0.268	0.25	0.268	0.25	0.296	0.297	0.25	0.265
	z	0.8	0.725	0.69	0.69	--	0.85	--	--	--	--	--	--	--	--	--	--	--	--	--	--
	k_z	0.75	0.724	0.71	0.71	--	0.765	--	--	--	--	--	--	--	--	--	--	--	--	--	--
	P (kN/m^2)	5	7.2	7.2	7.2	5	5.5	8.1	8.1	8.1	8.1	8.1	8.1	8.1	8.1	8.1	8.1	8.1	5	5	5
Required	Bending Moment (Nm)	1718.4	2691.6	2088	3063.2	136	210.3	396.4	541	489.2	620	366.5	529.5	366.2	529.9	365.9	521.9	219.2	156.6	297	241.5
	Shear Force (N)	7249.8	8208.3	6665.9	9185	1514.6	1381.3	2115	2873.8	2610.1	3293.2	2365.1	3417.6	2363.3	3419.8	2361.4	3368.5	2192.7	1089.5	1586.2	1289.8
	EI (Nm^2)	2055.2	3989.3	2924.9	4468.6	45.8	120	278.4	381.6	343.6	437.3	212.7	307.4	212.6	307.6	212.4	303	82.1	84.4	208.4	169.5
	t_w (mm)	7.5	9.3	7.9	8.7	2.7	2.8	3.5	4.1	4.5	5	4.3	5.1	3.7	4.4	3.4	4.4	3.6	1.8	2.1	1.9
Offered	Bending Moment (Nm)	1799.1	5847.3	2316.7	3875	339.4	633.2	633.2	633.2	876.9	876.9	876.9	876.9	648.5	648.5	431	648.5	648.5	309.1	309.1	309.1
	Shear Force (N)	17023.7	23407.6	20854	18300.5	10639.8	12767.8	12767.8	12767.8	17023.7	17023.7	17023.7	17023.7	12767.8	12767.8	11065.4	12767.8	12767.8	6383.9	6383.9	6383.9
	EI (Nm^2)	79670.1	361428.9	123943.6	186610.8	11262.6	19750.5	19750.5	19750.5	35690.5	35690.5	35690.5	35690.5	21934.3	21934.3	13918.7	21934.3	21934.3	5171.8	5171.8	5171.8
	t_w (mm)	15.8	15.8	15.8	15.8	15.8	15.8	15.8	15.8	15.8	15.8	15.8	15.8	15.8	15.8	15.8	15.8	15.8	15.8	15.8	15.8
Results	Bending Moment Ratio	1.047	2.172	1.109	1.265	2.495	3.011	1.597	1.17	1.793	1.414	2.393	1.656	1.771	1.224	1.178	1.242	2.959	1.973	1.041	1.28
	Shear Force Ratio	2.348	2.852	3.128	1.992	7.025	9.244	6.037	4.443	6.522	5.169	7.198	4.981	5.403	3.734	4.686	3.79	5.823	5.859	4.025	4.95
	EI Ratio	38.764	90.6	42.376	41.761	246.112	164.581	70.947	51.753	103.886	81.611	167.763	116.101	103.184	71.306	65.529	72.391	267.181	61.283	24.814	30.518
	t_w Ratio	2.122	1.701	2	1.819	5.873	5.614	4.537	3.892	3.537	3.149	3.716	3.091	4.292	3.568	4.612	3.595	4.456	8.94	7.409	8.216
	Comply	yes	yes	yes	yes	yes	yes	yes	yes	yes	yes	yes	yes	yes	yes	yes	yes	yes	yes	yes	yes

Notes:
-Stiffeners are assumed to have no curvature

Appendix T: ISO 12215-9 Keel Loads

Boat Partiulars		
m_{keel}	300	kg
L_{WL}	5.64	m
h_k	1.84	m
L_F	1.9	m
a	1.67	m
c	0.125	m
m_{LDC}	960	kg
θ (Cant)	40	
bi	0.228	m
$B_i=b_i/L_F$	0.12	-

Loadcase 1		
F_1	2943	N
$M_{1.1}$	4915	Nm
$M_{1.2}$	8822	Nm

Loadcase 2		
F_2	4120	N
$M_{2.1}$	6466	Nm
$M_{2.2}$	6723	Nm

Loadcase 3		
F_3	6474.6	N

Loadcase 4		
F_4	7770	N
h_{F4}	1.128	m
$M_{4.1}$	8764	Nm
$M_{4.2}$	9735	Nm

Floor 1		
L_{F1}	1.614	m
b_i	0.194	m
EI	361.4E+9	Nmm^2
k_{EF}	4	-
K_{FLOOR1}	3.44E+11	-
K_B	1	-
F_{FLOOR1}	3.44E+11	-
M_i (LC 1)	8365.3	Nm
M_i (LC 2)	6375.2	Nm
F_{vi} (LC 3)	6139	N
x_i	0.473	m
x_r	0.449	m
F_{VF4i}	-20582	N
F_{CVF4i} (LC 4)	318.7	N
LOADCASE 1 Fully Fixed		
$f_{A/D}$	7774.5	N
$f_{B/C}$	7774.5	N
$m_{A/D}$	2091.3	Nm
$m_{B/C}$	4182.7	Nm
LOADCASE 2 Fully Fixed		
$f_{A/D}$	5924.9	N
$f_{B/C}$	5924.9	N
$m_{A/D}$	1593.8	Nm
$m_{B/C}$	3187.6	Nm
LOADCASE 3 Fully Fixed		
$f_{A/D}$	3069.7	N
$f_{B/C}$	3069.7	N
$m_{A/D}$	1238.6	Nm
$m_{B/C}$	1238.6	Nm
LOADCASE 4 Fully Fixed		
$f_{A/D}$	159.3	N
$f_{B/C}$	159.3	N
$m_{A/D}$	64.3	Nm
$m_{B/C}$	64.3	Nm

Floor 2		
L_{F2}	1.876	m
b_i	0.225	m
EI	123.9E+9	Nmm^2
k_{EF}	1	-
K_{FLOOR2}	1.88E+10	-
K_B	1	-
F_{FLOOR1}	1.88E+10	-
M_i (LC 1)	456.7	Nm
M_i (LC 2)	348.1	Nm
F_{vi} (LC 3)	165	N
x_i	0	m
x_r	0.449	m
F_{VF4i}	20582	N
F_{CVF4i} (LC 4)	-318.70	N
LOADCASE 1 Fully Fixed		
$f_{A/D}$	365.2	N
$f_{B/C}$	365.2	N
$m_{A/D}$	0	Nm
$m_{B/C}$	228.4	Nm
LOADCASE 2 Fully Fixed		
$f_{A/D}$	185.5	N
$f_{B/C}$	185.5	N
$m_{A/D}$	0	Nm
$m_{B/C}$	174.0	Nm
LOADCASE 3 Fully Fixed		
$f_{A/D}$	82.5	N
$f_{B/C}$	82.5	N
$m_{A/D}$	0	Nm
$m_{B/C}$	77.4	Nm
LOADCASE 4 Fully Fixed		
$f_{A/D}$	-159.3	N
$f_{B/C}$	-159.3	N
$m_{A/D}$	0	Nm
$m_{B/C}$	-149.5	Nm

Girder 1		
L_{G1}	2.3	m
EI	29.4E+9	Nmm^2
k_{EF}	4	-
K_{FLOOR1}	9.6E+9	-
K_{GFSR}	0.05	-
x	-1.27	-
P_G	1.02	-
F_{CVG41}	10450.3	N

Floor 1 Max Load		
Offered		
EI	361.4E+9	Nmm^2
BM	5.8E+3	Nm
SF	23407.56	N
Required		
f_{MAX}	7774.5	N
m_{MAX}	4182.7	Nm
Passing Ratio		
BM	1.40	-
SF	3.01	-

Girder 2		
L_{G1}	2.3	m
EI	29.4E+9	Nmm^2
k_{EF}	4	-
K_{FLOOR1}	9.6E+9	-
K_{GFSR}	0.05	-
x	-1.27	-
PG	1.02	-
F_{CVG42}	10450.3	N

Floor 2 Max Loads		
Offered		
EI	123.9E+9	Nmm^2
BM	3179.94	Nm
SF	23407.56	N
Required		
f_{MAX}	365.2	N
m_{MAX}	228.4	Nm
Passing Ratio		
BM	13.92	-
SF	64.10	-

Appendix U: Keel Laminate

Gurit SE 70 Pre-Preg		
ρ_F	1.8	g/cm^3
ρ_R	1.28	g/cm^3
ψ	63.0%	W_F
φ	54.8%	V_F
w	200	g/m^2
σ_{UT}	2524	N/mm^2

Shell Laminate Properties		
E_X	92.4E+3	N/mm^2
E_Y	6.6E+3	N/mm^2
G_{XY}	3.8E+3	N/mm^2
v_{xy}	0.3	-
Thickness	1.58	mm

Shell Properties		
I_{XX}	97.6E+3	mm^4
I_{YY}	4.4E+6	mm^4
EI_{XX}	9.0	GNmm^2
EI_{YY}	409.5	GNmm^2
Area	814.42	mm^2

Keel Deflection		
δ_{max}	0.08	m
δ_{max}	77.5	mm

Keel Fin Mass		
m_{Fin}	2.50	kg/m

Stress Analysis		
L_{keel}	1.984	m
m_{keel}	300	kg
BM_{max}	5839	Nm
Fos	5	-
σ_{MAX}	2470	N/mm^2
Passing Ratio	1.022	-

Ply	φ	1-φ	E_F (Pa)	E_R (Pa)	v_F	v_R	G_F (Pa)	G_R (Pa)	E_1 (Pa)	E_2 (Pa)	G_{12} (Pa)	v_{12}	v_{21}	θ (Degs)	θ (Rad)	sin(θ)	cos(θ)	E_X (Pa)	E_Y (Pa)	G_{XY} (Pa)	v_{xy}	t (mm)	ρ (g/cm^3)
1	0.55	0.452	235.0E+9	3.5E+9	0.3	0.3	52.0E+9	2.3E+9	130E+9	8E+9	5E+9	0.3	0.02	45	0.8	0.71	0.7	12E+9	12E+9	7E+9	0.23	0.197	1.56
2	0.55	0.452	235.0E+9	3.5E+9	0.3	0.3	52.0E+9	2.3E+9	130E+9	8E+9	5E+9	0.3	0.02	0	0.0	0.0	1.0	130E+9	8E+9	5E+9	0.30	0.197	1.56
3	0.55	0.452	235.0E+9	3.5E+9	0.3	0.3	52.0E+9	2.3E+9	130E+9	8E+9	5E+9	0.3	0.02	0	0.0	0.0	1.0	130E+9	8E+9	5E+9	0.30	0.197	1.56
4	0.55	0.452	235.0E+9	3.5E+9	0.3	0.3	52.0E+9	2.3E+9	130E+9	8E+9	5E+9	0.3	0.02	0	0.0	0.0	1.0	130E+9	8E+9	5E+9	0.30	0.197	1.56
7	0.55	0.452	235.0E+9	3.5E+9	0.3	0.3	52.0E+9	2.3E+9	130E+9	8E+9	5E+9	0.3	0.02	0	0.0	0.0	1.0	130E+9	8E+9	5E+9	0.30	0.197	1.56
8	0.55	0.452	235.0E+9	3.5E+9	0.3	0.3	52.0E+9	2.3E+9	130E+9	8E+9	5E+9	0.3	0.02	0	0.0	0.0	1.0	130E+9	8E+9	5E+9	0.30	0.197	1.56
9	0.55	0.452	235.0E+9	3.5E+9	0.3	0.3	52.0E+9	2.3E+9	130E+9	8E+9	5E+9	0.3	0.02	0	0.0	0.0	1.0	130E+9	8E+9	5E+9	0.30	0.197	1.56
10	0.55	0.452	235.0E+9	3.5E+9	0.3	0.3	52.0E+9	2.3E+9	130E+9	8E+9	5E+9	0.3	0.02	0	0.0	0.0	1.0	130E+9	8E+9	5E+9	0.30	0.197	1.56

Gurit SE 70 Pre-Preg		
ρ_F	1.8	g/cm^3
ρ_R	1.28	g/cm^3
ψ	63.0%	W_F
φ	54.8%	V_F
w	200	g/m^2
σ_{UT}	2524	N/mm^2

Shear Box Laminate Properties		
E_X	11.7E+3	N/mm^2
E_Y	11.7E+3	N/mm^2
G_{XY}	7.1E+3	N/mm^2
v_{xy}	0.2	-
Thickness	2.76	mm

Shear Box		
I_{XX}	90975.055	mm^4
I_{YY}	702.9E+3	mm^4
EI_{XX}	1.1	GNmm^2
EI_{YY}	8.2	GNmm^2
Area	783.1224	mm^2

Stress Analysis		
Shear Force	2943	N
τ_U	205.6	N/mm^2
Shear Area	71.57	mm^2
Passing Ratio	10.9	-

Ply	φ	1-φ	E_F (Pa)	E_R (Pa)	v_F	v_R	G_F (Pa)	G_R (Pa)	E_1 (Pa)	E_2 (Pa)	G_{12} (Pa)	v_{12}	v_{21}	θ (Degs)	θ (Rad)	sin(θ)	cos(θ)	E_X (Pa)	E_Y (Pa)	G_{XY} (Pa)	v_{xy}	t (mm)	ρ (g/cm^3)
1	0.55	0.452	235.0E+9	3.5E+9	0.3	0.3	52.0E+9	2.3E+9	130E+9	8E+9	5E+9	0.3	0.02	45	0.8	0.71	0.7	12E+9	12E+9	7E+9	0.23	0.197	1.56
2	0.55	0.452	235.0E+9	3.5E+9	0.3	0.3	52.0E+9	2.3E+9	130E+9	8E+9	5E+9	0.3	0.02	45	0.8	0.7	0.7	12E+9	12E+9	7E+9	0.23	0.197	1.56
3	0.55	0.452	235.0E+9	3.5E+9	0.3	0.3	52.0E+9	2.3E+9	130E+9	8E+9	5E+9	0.3	0.02	45	0.8	0.7	0.7	12E+9	12E+9	7E+9	0.23	0.197	1.56
4	0.55	0.452	235.0E+9	3.5E+9	0.3	0.3	52.0E+9	2.3E+9	130E+9	8E+9	5E+9	0.3	0.02	45	0.8	0.7	0.7	12E+9	12E+9	7E+9	0.23	0.197	1.56
5	0.55	0.452	235.0E+9	3.5E+9	0.3	0.3	52.0E+9	2.3E+9	130E+9	8E+9	5E+9	0.3	0.02	45	0.8	0.7	0.7	12E+9	12E+9	7E+9	0.23	0.197	1.56
6	0.55	0.452	235.0E+9	3.5E+9	0.3	0.3	52.0E+9	2.3E+9	130E+9	8E+9	5E+9	0.3	0.02	45	0.8	0.7	0.7	12E+9	12E+9	7E+9	0.23	0.197	1.56
7	0.55	0.452	235.0E+9	3.5E+9	0.3	0.3	52.0E+9	2.3E+9	130E+9	8E+9	5E+9	0.3	0.02	45	0.8	0.7	0.7	12E+9	12E+9	7E+9	0.23	0.197	1.56
8	0.55	0.452	235.0E+9	3.5E+9	0.3	0.3	52.0E+9	2.3E+9	130E+9	8E+9	5E+9	0.3	0.02	45	0.8	0.7	0.7	12E+9	12E+9	7E+9	0.23	0.197	1.56
9	0.55	0.452	235.0E+9	3.5E+9	0.3	0.3	52.0E+9	2.3E+9	130E+9	8E+9	5E+9	0.3	0.02	45	0.8	0.7	0.7	12E+9	12E+9	7E+9	0.23	0.197	1.56
10	0.55	0.452	235.0E+9	3.5E+9	0.3	0.3	52.0E+9	2.3E+9	130E+9	8E+9	5E+9	0.3	0.02	45	0.8	0.7	0.7	12E+9	12E+9	7E+9	0.23	0.197	1.56
11	0.55	0.452	235.0E+9	3.5E+9	0.3	0.3	52.0E+9	2.3E+9	130E+9	8E+9	5E+9	0.3	0.02	45	0.8	0.7	0.7	12E+9	12E+9	7E+9	0.23	0.197	1.56
12	0.55	0.452	235.0E+9	3.5E+9	0.3	0.3	52.0E+9	2.3E+9	130E+9	8E+9	5E+9	0.3	0.02	45	0.8	0.7	0.7	12E+9	12E+9	7E+9	0.23	0.197	1.56
13	0.55	0.452	235.0E+9	3.5E+9	0.3	0.3	52.0E+9	2.3E+9	130E+9	8E+9	5E+9	0.3	0.02	45	0.8	0.7	0.7	12E+9	12E+9	7E+9	0.23	0.197	1.56
14	0.55	0.452	235.0E+9	3.5E+9	0.3	0.3	52.0E+9	2.3E+9	130E+9	8E+9	5E+9	0.3	0.02	45	0.8	0.7	0.7	12E+9	12E+9	7E+9	0.23	0.197	1.56

Appendix V: Foil Structure

CFX Results		
F_X	191.9E+0	N
F_Y	1.9E+3	N
F_Z	1.8E+3	N
M_X	2.1E+3	Nm
M_Y	185.9E+0	Nm
M_Z	402.5E+0	Nm
Fos	5	-

Foil Support		
Length in Box	270	mm
Length outside Box	1500	mm
$Lift_{CFX}$	1.9E+3	N
BM_{CFX}	2.1E+3	Nm
Lift Centroid	1.10	m
Outside Reaction	61.2E+3	N
Inside Reaction	51.9E+3	N

UD Tapes in BHD		
Tension	51.9E+3	N
Width	100	mm
σ_{UT}	940	N/mm^2
Required Thickness	0.552	mm
Thikness	0.237	mm
Number of Plies	3	-

Bonding Layers		
Shear Force	51.9E+3	N
Shear Length	320	mm
τ	51.4	N/mm^2
Required Thickness	1.577	mm
Thikness	0.414	mm
Number of Plies	4	-

Foil Case		
Tension	1.8E+3	N
Length	320	mm
σ_{UT}	414.9	N/mm^2
Required Thickness	0.068	mm
Thikness	0.414	mm
Number of Plies	1	-

Gurit SE 70 Pre-Preg		
ρ_F	1.8	g/cm^3
ρ_R	1.28	g/cm^3
ψ	63.0%	W_F
φ	54.8%	V_F
w	200	g/m^2
σ_{UT}	2524	N/mm^2

Laminate Properties		
E_X	92.4E+3	N/mm^2
E_Y	6.6E+3	N/mm^2
G_{XY}	3.8E+3	N/mm^2
ν_{xy}	0.3	-
Thickness	1.58	mm

Shell Properties		
I_{XX}	120.4E+3	mm^4
I_{YY}	4.2E+6	mm^4
EI_{XX}	11.1	$GNmm^2$
EI_{YY}	389.7	$GNmm^2$
Area	801.55	mm^2

Keel Deflection		
δ_{max}	0.03	m
δ_{max}	28.5	mm

Keel Fin Mass		
m_{Fin}	2.53	kg/m

Stress Analysis		
$Lift_{CFX}$	1.9E+3	N
BM_{CFX}	2050.3	Nm
L_{FOIL}	1.10	m
σ_{MAX}	710	N/mm^2
Passing Ratio	3.55	-

Shell

Ply	φ	1-φ	E_F (Pa)	E_R (Pa)	ν_F	ν_R	G_F (Pa)	G_R (Pa)	E_1 (Pa)	E_2 (Pa)	G_{12} (Pa)	ν_{12}	ν_{21}	θ (Degs)	θ (Rad)	sin(θ)	cos(θ)	E_X (Pa)	E_Y (Pa)	G_{XY} (Pa)	ν_{xy}	t (mm)	ρ (g/cm^3)
1	0.55	0.452	235.0E+9	3.5E+9	0.3	0.3	52.0E+9	2.3E+9	130E+9	8E+9	5E+9	0.3	0.02	45	0.8	0.71	0.7	12E+9	12E+9	7E+9	0.23	0.197	1.56
2	0.55	0.452	235.0E+9	3.5E+9	0.3	0.3	52.0E+9	2.3E+9	130E+9	8E+9	5E+9	0.3	0.02	0	0.0	0.0	1.0	130E+9	8E+9	5E+9	0.30	0.197	1.56
3	0.55	0.452	235.0E+9	3.5E+9	0.3	0.3	52.0E+9	2.3E+9	130E+9	8E+9	5E+9	0.3	0.02	0	0.0	0.0	1.0	130E+9	8E+9	5E+9	0.30	0.197	1.56
4	0.55	0.452	235.0E+9	3.5E+9	0.3	0.3	52.0E+9	2.3E+9	130E+9	8E+9	5E+9	0.3	0.02	0	0.0	0.0	1.0	130E+9	8E+9	5E+9	0.30	0.197	1.56
7	0.55	0.452	235.0E+9	3.5E+9	0.3	0.3	52.0E+9	2.3E+9	130E+9	8E+9	5E+9	0.3	0.02	0	0.0	0.0	1.0	130E+9	8E+9	5E+9	0.30	0.197	1.56
8	0.55	0.452	235.0E+9	3.5E+9	0.3	0.3	52.0E+9	2.3E+9	130E+9	8E+9	5E+9	0.3	0.02	0	0.0	0.0	1.0	130E+9	8E+9	5E+9	0.30	0.197	1.56
9	0.55	0.452	235.0E+9	3.5E+9	0.3	0.3	52.0E+9	2.3E+9	130E+9	8E+9	5E+9	0.3	0.02	0	0.0	0.0	1.0	130E+9	8E+9	5E+9	0.30	0.197	1.56
10	0.55	0.452	235.0E+9	3.5E+9	0.3	0.3	52.0E+9	2.3E+9	130E+9	8E+9	5E+9	0.3	0.02	0	0.0	0.0	1.0	130E+9	8E+9	5E+9	0.30	0.197	1.56

Gurit SE 70 Pre-Preg		
ρ_F	1.8	g/cm^3
ρ_R	1.28	g/cm^3
ψ	63.0%	W_F
φ	54.8%	V_F
w	200	g/m^2
σ_{UT}	2524	N/mm^2

Laminate Properties		
E_X	11.7E+3	N/mm^2
E_Y	11.7E+3	N/mm^2
G_{XY}	7.1E+3	N/mm^2
ν_{xy}	0.2	-
Thickness	2.76	mm

Shear Box		
I_{XX}	109.8E+3	mm^4
I_{YY}	777.9E+3	mm^4
EI_{XX}	1.3	$GNmm^2$
EI_{YY}	9.1	$GNmm^2$
Area	818.35	mm^2

Shear Analysis		
Shear Force	1867.5	N
τ_U	205.6	N/mm^2
Shear Area	45.42	mm^2
Passing Ratio	18.0	-

Torsion Analysis		
GJ_Z	23.0E+0	$GNmm^2$
T	402.5E+0	Nm
L	1.23	m
Twist Angle	1.23	°

Shear Box

Ply	φ	1-φ	E_F (Pa)	E_R (Pa)	ν_F	ν_R	G_F (Pa)	G_R (Pa)	E_1 (Pa)	E_2 (Pa)	G_{12} (Pa)	ν_{12}	ν_{21}	θ (Degs)	θ (Rad)	sin(θ)	cos(θ)	E_X (Pa)	E_Y (Pa)	G_{XY} (Pa)	ν_{xy}	t (mm)	ρ (g/cm^3)
1	0.55	0.452	235.0E+9	3.5E+9	0.3	0.3	52.0E+9	2.3E+9	130E+9	8E+9	5E+9	0.3	0.02	45	0.8	0.71	0.7	12E+9	12E+9	7E+9	0.23	0.197	1.56
2	0.55	0.452	235.0E+9	3.5E+9	0.3	0.3	52.0E+9	2.3E+9	130E+9	8E+9	5E+9	0.3	0.02	45	0.8	0.7	0.7	12E+9	12E+9	7E+9	0.23	0.197	1.56
3	0.55	0.452	235.0E+9	3.5E+9	0.3	0.3	52.0E+9	2.3E+9	130E+9	8E+9	5E+9	0.3	0.02	45	0.8	0.7	0.7	12E+9	12E+9	7E+9	0.23	0.197	1.56
4	0.55	0.452	235.0E+9	3.5E+9	0.3	0.3	52.0E+9	2.3E+9	130E+9	8E+9	5E+9	0.3	0.02	45	0.8	0.7	0.7	12E+9	12E+9	7E+9	0.23	0.197	1.56
5	0.55	0.452	235.0E+9	3.5E+9	0.3	0.3	52.0E+9	2.3E+9	130E+9	8E+9	5E+9	0.3	0.02	45	0.8	0.7	0.7	12E+9	12E+9	7E+9	0.23	0.197	1.56
6	0.55	0.452	235.0E+9	3.5E+9	0.3	0.3	52.0E+9	2.3E+9	130E+9	8E+9	5E+9	0.3	0.02	45	0.8	0.7	0.7	12E+9	12E+9	7E+9	0.23	0.197	1.56
7	0.55	0.452	235.0E+9	3.5E+9	0.3	0.3	52.0E+9	2.3E+9	130E+9	8E+9	5E+9	0.3	0.02	45	0.8	0.7	0.7	12E+9	12E+9	7E+9	0.23	0.197	1.56
8	0.55	0.452	235.0E+9	3.5E+9	0.3	0.3	52.0E+9	2.3E+9	130E+9	8E+9	5E+9	0.3	0.02	45	0.8	0.7	0.7	12E+9	12E+9	7E+9	0.23	0.197	1.56
9	0.55	0.452	235.0E+9	3.5E+9	0.3	0.3	52.0E+9	2.3E+9	130E+9	8E+9	5E+9	0.3	0.02	45	0.8	0.7	0.7	12E+9	12E+9	7E+9	0.23	0.197	1.56
10	0.55	0.452	235.0E+9	3.5E+9	0.3	0.3	52.0E+9	2.3E+9	130E+9	8E+9	5E+9	0.3	0.02	45	0.8	0.7	0.7	12E+9	12E+9	7E+9	0.23	0.197	1.56
11	0.55	0.452	235.0E+9	3.5E+9	0.3	0.3	52.0E+9	2.3E+9	130E+9	8E+9	5E+9	0.3	0.02	45	0.8	0.7	0.7	12E+9	12E+9	7E+9	0.23	0.197	1.56
12	0.55	0.452	235.0E+9	3.5E+9	0.3	0.3	52.0E+9	2.3E+9	130E+9	8E+9	5E+9	0.3	0.02	45	0.8	0.7	0.7	12E+9	12E+9	7E+9	0.23	0.197	1.56
13	0.55	0.452	235.0E+9	3.5E+9	0.3	0.3	52.0E+9	2.3E+9	130E+9	8E+9	5E+9	0.3	0.02	45	0.8	0.7	0.7	12E+9	12E+9	7E+9	0.23	0.197	1.56
14	0.55	0.452	235.0E+9	3.5E+9	0.3	0.3	52.0E+9	2.3E+9	130E+9	8E+9	5E+9	0.3	0.02	45	0.8	0.7	0.7	12E+9	12E+9	7E+9	0.23	0.197	1.56

Appendix W: Hotel Load

Eletronic	Reference	Weight	Consumption (mA)		Usage per 24h		Consumption (mAh)		Total Consumption (mAh)
		kg	Light off	Light on	Light off	Light on	Light off	Light on	
Multigraphic	90-60-130	0.75	90	150	12	12	1080	1800	2880
Gyropilot Graphic	90-60-348	0.74	30	50	12	12	360	600	960
NKE Mechanical Ram	90-60-524	3	850	850	0	18	0	15300	15300
Depth Sounder	90-60-456	0.7	35	35	24	0	840	0	840
Masthead Wind Sensor	90-60-105	0.52	25	25	24	0	600	0	600
Fluxgate Compas	90-60-452	0.27	25	25	24	0	600	0	600
Ultrasonic speed sensor	90-60-479-2	0.16	35	35	24	0	840	0	840
Dual Log/Sounder interface	90-60-451	0.16	60	60	24	0	1440	0	1440
Rudder angle sensor	90-60-084	0.45	15	15	24	0	360	0	360
Gyropilot Remote control	90-60-247	0.065	0	0	24	0	0	0	0
Universal radio reciever	90-60-250	0.26	25	25	24	0	600	0	600
AIS transponder	90-60-500	0.25	170	170	24	0	4080	0	4080
Gyropilot Processor - with embedded Gyrocompass	90-60-130	1	30	50	0	24	0	1200	1200
Baro HR 100	90-60-358	0.27	25	25	24	0	600	0	600
Icom-M423G 25 W	IC-M423G	1.2	600	5500	23.5	0.5	14100	2750	16850
Nav Lights	3863001000	0.03	0	0.25	12	12	0	3	3
BLU Sangean ATS 909-X (not on circuit)	PG-10510	0.735	0	0	0	0	0	0	0
Total Weight (kg)	-	10.56						mAh	47153
								Ah	47.2

Power Plant	Weight	Nominal Output			Production	Price	uired Run t	Production/Weight	Comments
	kg	Watts	Ampers	Volts	A/Day	£	Hours	A/Day/kg	-
Watt&Sea Hydro generator	7.5	120	10	12	240	3132	5	32	Stated output @ 5 knots
Efoy Comfort 80 Fuel Cell	6	40	3.3	12	80	2200	15	13	Methanol not included
MaxPower Marine Fuel Cell 75	6.4	38	3.1	12	75	Unknown	16	12	Methanol not included
Islanders Solar Panel HD (1155x560mm)	2.5	100	5.68	12	34	380	9	14	Based on 6 hours of exposure
Honda EU1000i Fuel Generator	13	96	8	12	192	760	6	15	Fuel Not Included

19. Drawings

Lines Plan Mini 6.50 v2.6

Lines Plan Mini 6.50 v1.6

Deck Plan

Rig Plan

Sail Wardrobe

Structural Arrangement

Panel and Core Layout

Frames and Bulkheads

Structural Details

Foil Structure

System Arrangement

Structural Render

Profile Render

Profile View

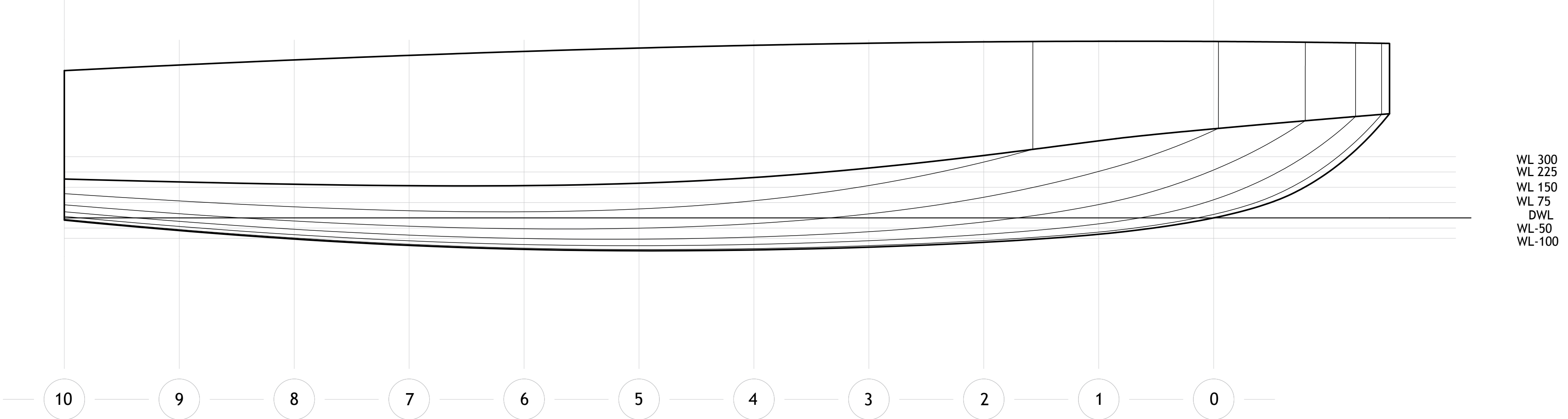

Body Plan

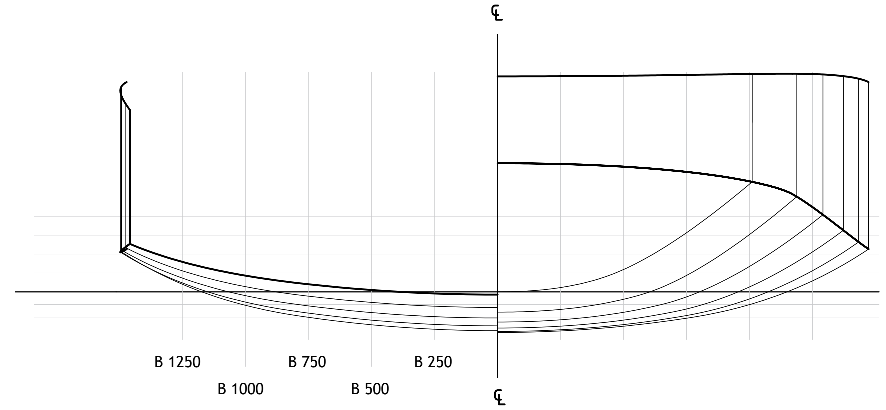

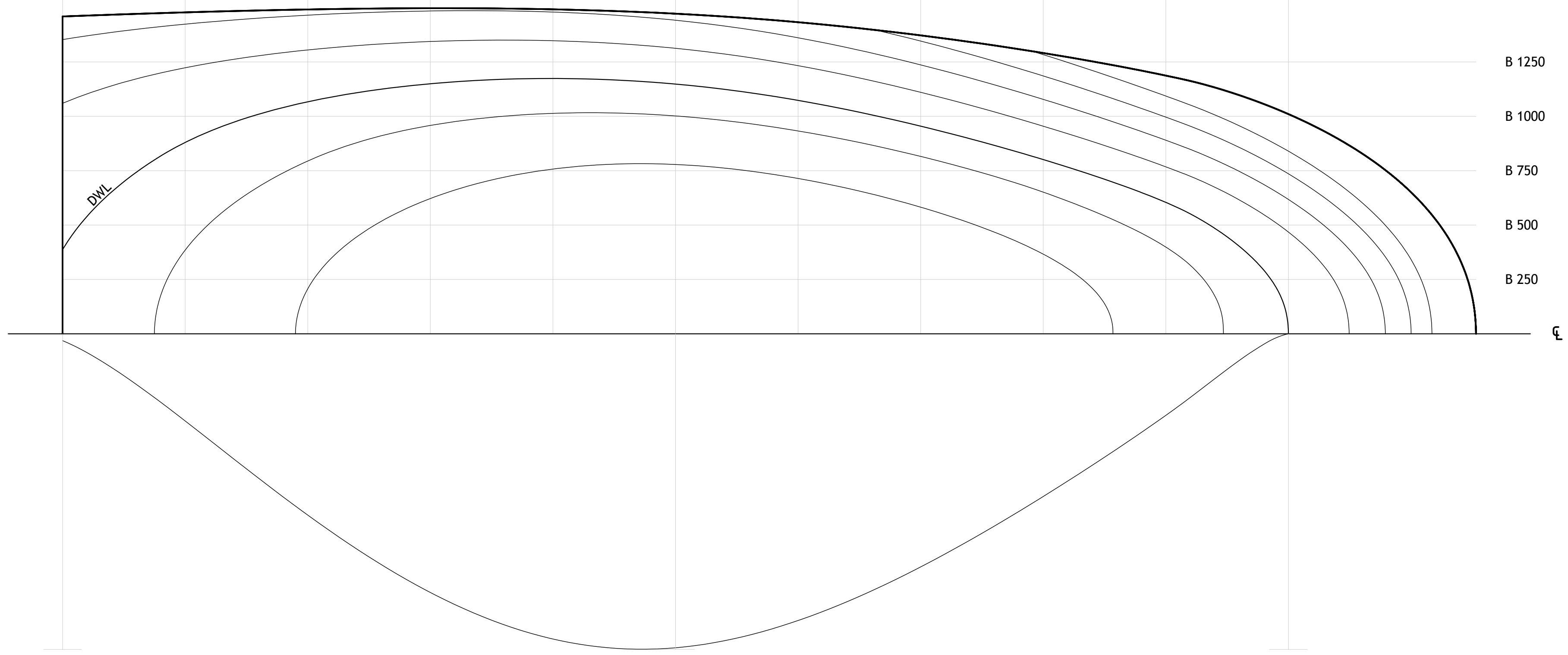

Plan View, Section Area Curve

Yacht Particulars	
L_{OA} (m)	6.5
L_{WL} (m)	5.64
B_{OA} (m)	3
B_{WL} (m)	2.35
T_C (m)	0.16
Displ. (kg)	926
C_P	0.61
C_m	0.71
LCB (%L_{WL} from FP)	-50.88
LCF (%L_{WL} from FP)	-53.25
BM_T	3.9

NOTES:

1. STATION SPACING: 563 mm

Project: Mini 6.50 N°934 Preliminary Design		
Drawing Title: Lines Plan v2.6		Drawn by: Marin Lauber
Issue date: 27.04.2017	Units: mm	Scale: 1:30 @ A3

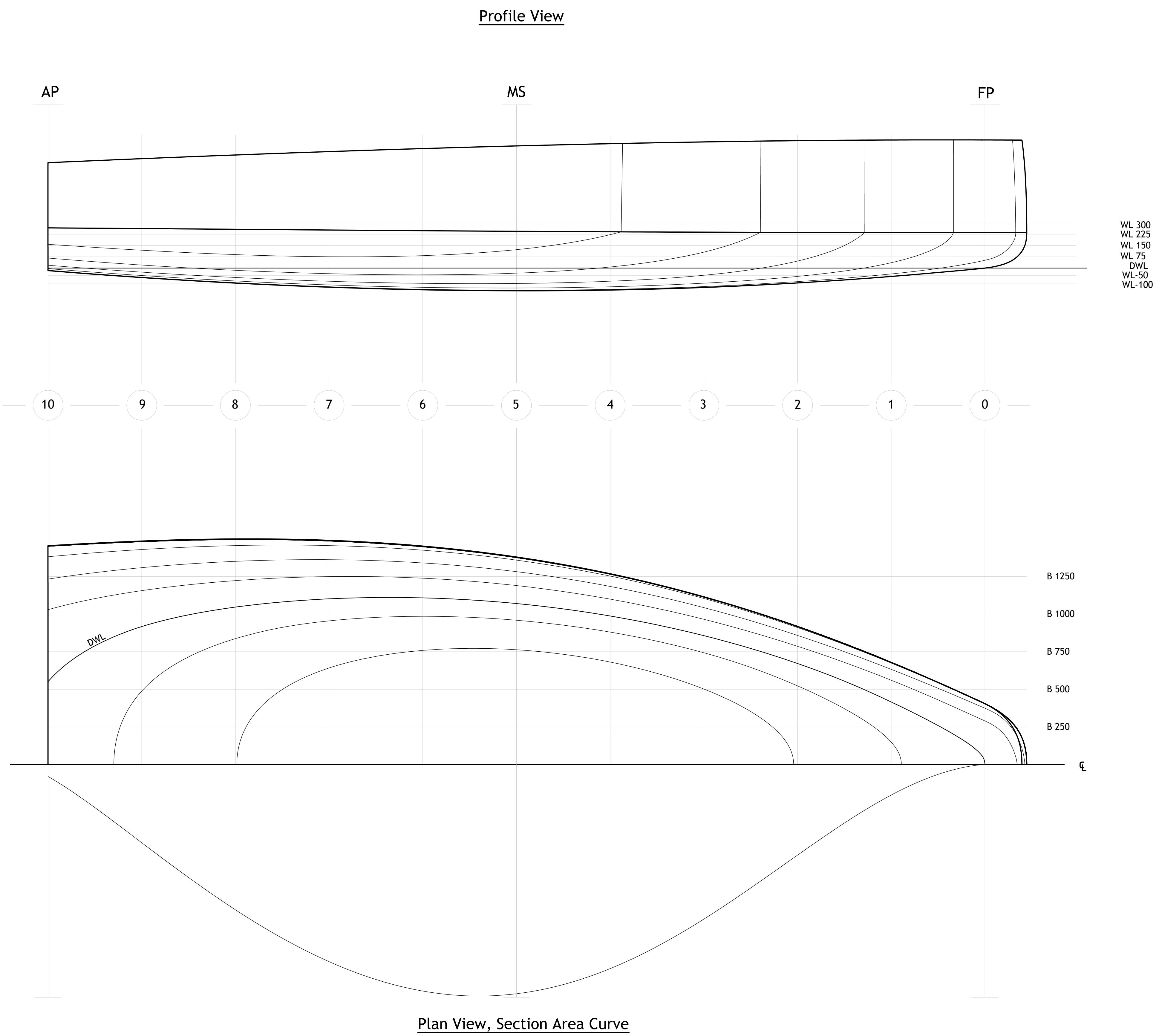

Yacht Particulars	
L_{OA} (m)	6.5
L_{WL} (m)	6.22
B_{OA} (m)	3
B_{WL} (m)	2.22
T_C (m)	0.15
Displ. (kg)	926
C_P	0.59
C_m	0.75
LCB (%L_{WL} from FP)	-53.7
LCF (%L_{WL} from FP)	-55.8
BM_T	3.64

NOTES:

1. STATION SPACING: 622 mm

Project: Mini 6.50 N°934 Preliminary Design		
Drawing Title: Lines Plan v1.6		Drawn by: Marin Lauber
Issue date: 27.04.2017	Units: mm	Scale: 1:30 @ A3

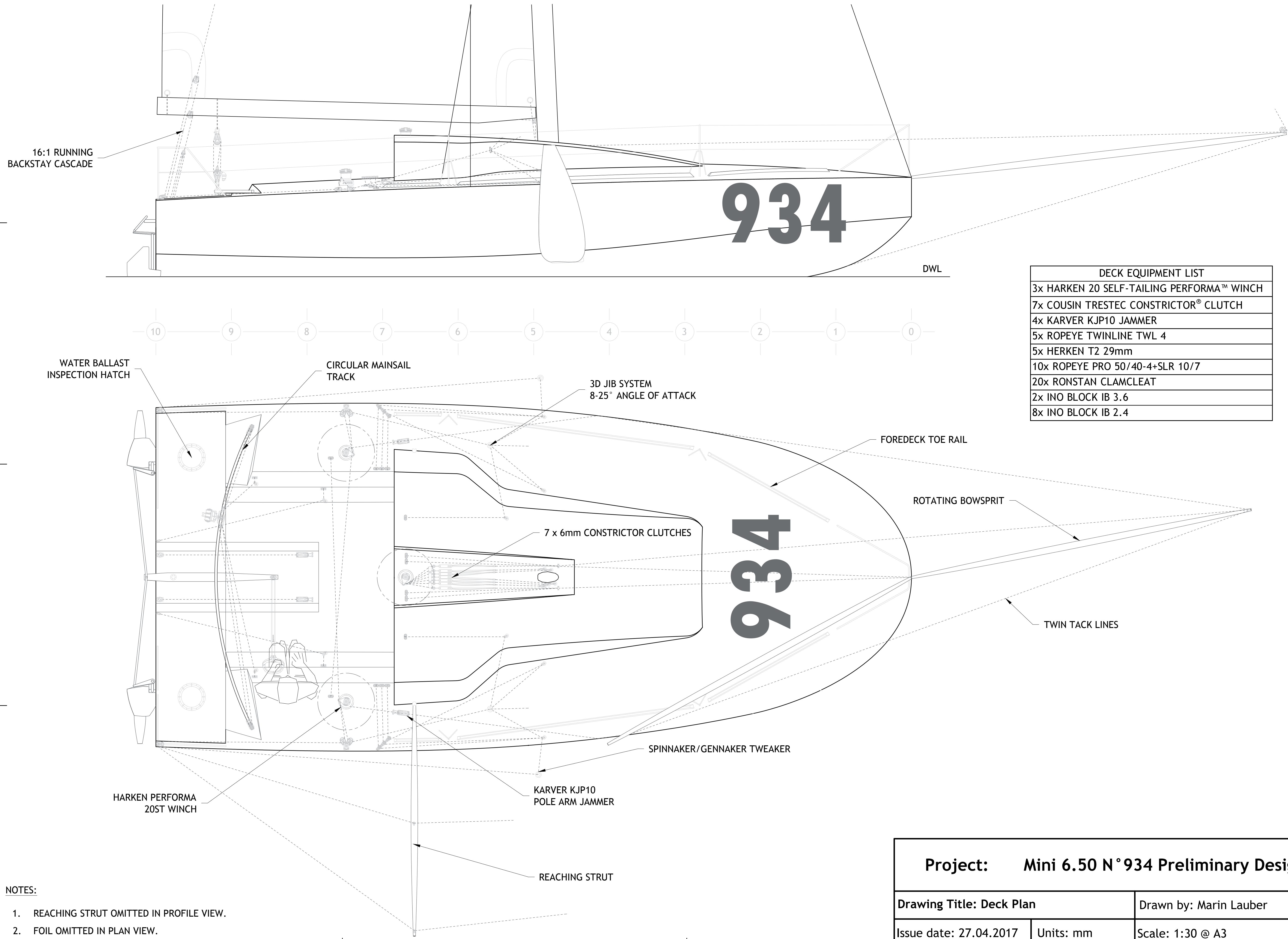

DECK EQUIPMENT LIST
3x HARKEN 20 SELF-TAILING PERFORMA™ WINCH
7x COUSIN TRESTEC CONSTRICTOR® CLUTCH
4x KARVER KJP10 JAMMER
5x ROPEYE TWINLINE TWL 4
5x HERKEN T2 29mm
10x ROPEYE PRO 50/40-4+SLR 10/7
20x RONSTAN CLAMCLEAT
2x INO BLOCK IB 3.6
8x INO BLOCK IB 2.4

NOTES:

1. REACHING STRUT OMITTED IN PROFILE VIEW.
2. FOIL OMITTED IN PLAN VIEW.

Project: Mini 6.50 N°934 Preliminary Design		
Drawing Title: Deck Plan		Drawn by: Marin Lauber
Issue date: 27.04.2017	Units: mm	Scale: 1:30 @ A3

RIGGING DIAMETER UHMWPE DM20		
V1	5.0	mm
D1	6.0	mm
D2	5.0	mm
D3	5.0	mm
D4	5.0	mm

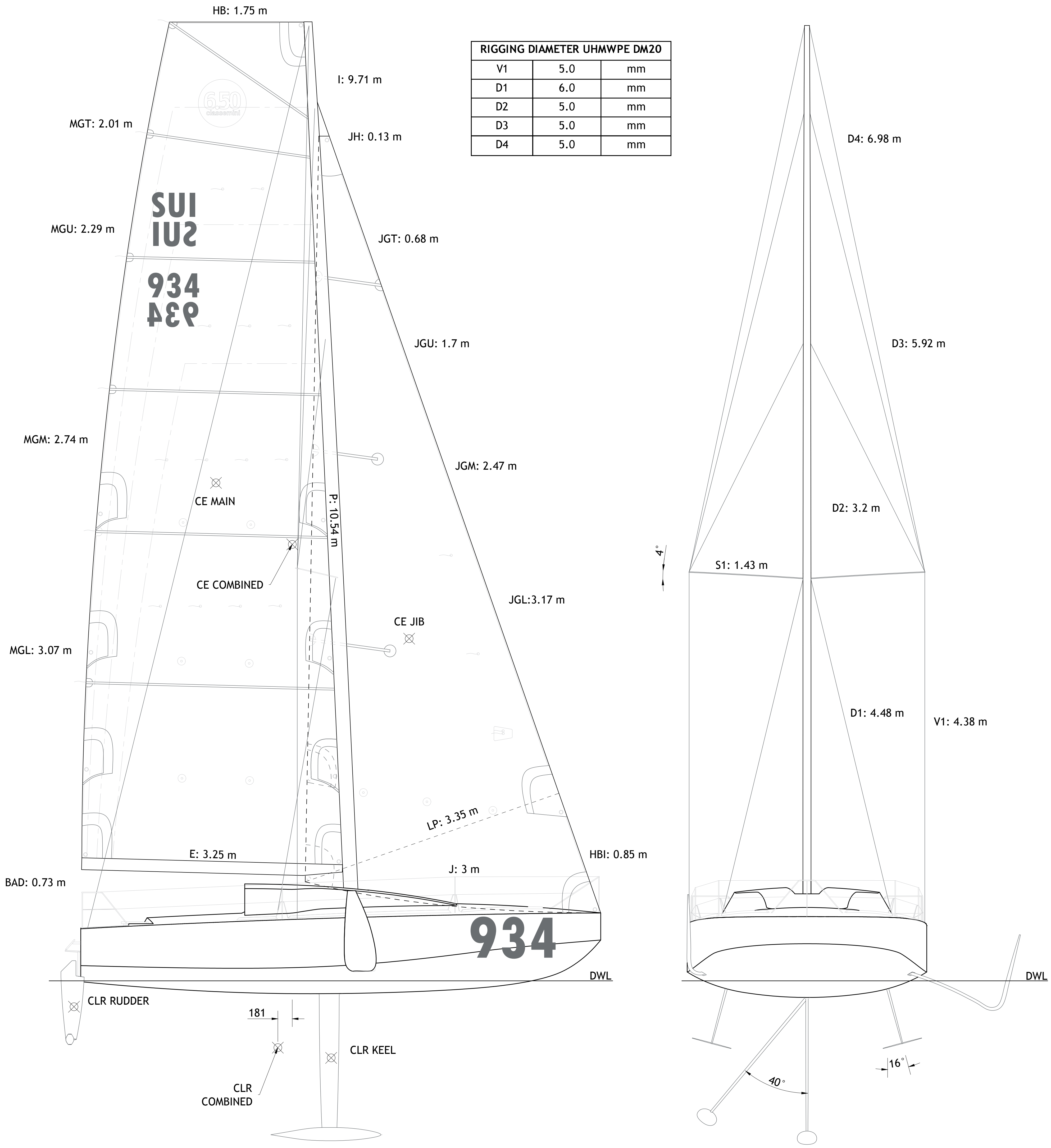

RIG SECTION:
SCALE 1:2

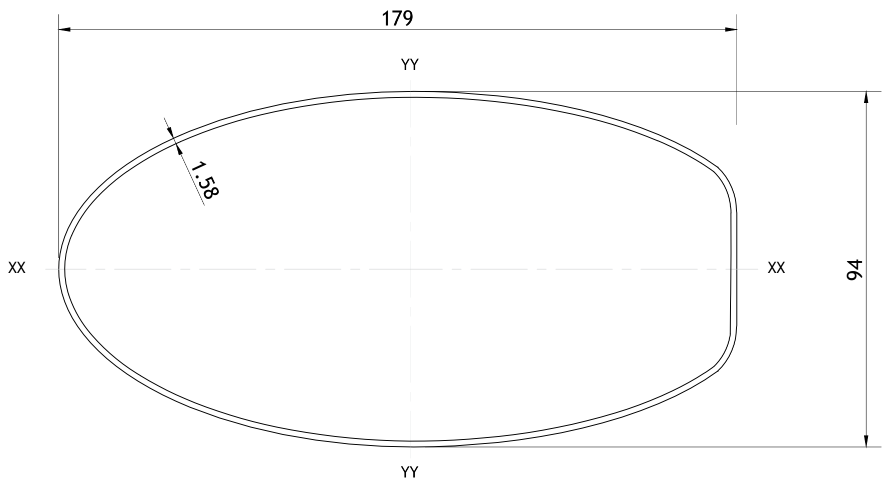

MAST BASIC LAMINATE			
MATERIAL	ORIENTATION	WEIGHT (g/m^2)	No° PLY
SE 70	±45°	200	1
SE 70	90°	200	1
SE 70	0°	200	6

RIG PROPERTIES		
I_{XX}	1.2E+6	mm^4
I_{YY}	3.6E+6	mm^4
EI_{XX}	119	GNmm^2
EI_{YY}	365	GNmm^2
AREA	797	mm^2

NOTES:

1. FORSTAY OMITTED FOR CLARITY.
2. DISPLAYED DISTANCE ARE 3D DISTANCE.
3. SPREADERS TO BE SPECIFIED BY RIG MANUFACTURER.
4. MAST TRACK TO BE SPECIFIED BY RIG MANUFACTURER.
5. SAIL DIMENSIONS ACCORDING TO EQUIPMENT RULES OF SAILING.

Project: Mini 6.50 N°934 Preliminary Design		
Drawing Title: Rig Plan		Drawn by: Marin Lauber
Issue date: 27.04.2017	Units: mm	Scale: 1:50 @ A3 unless otherwise stated

FULL MAIN, FULL JIB

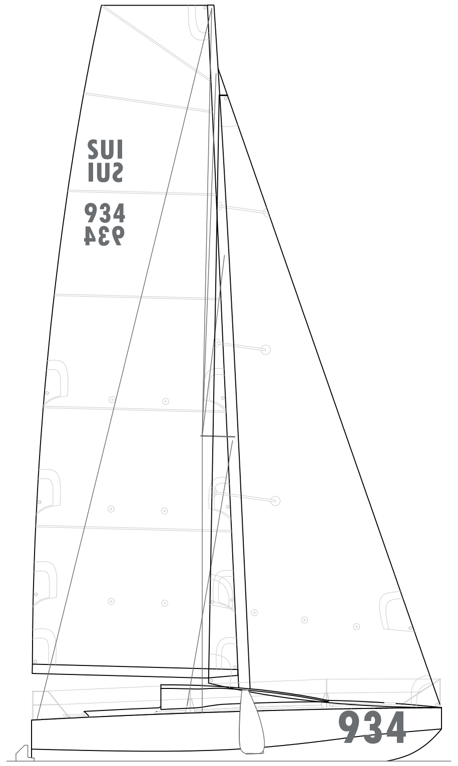

FULL MAIN, GENNAKER

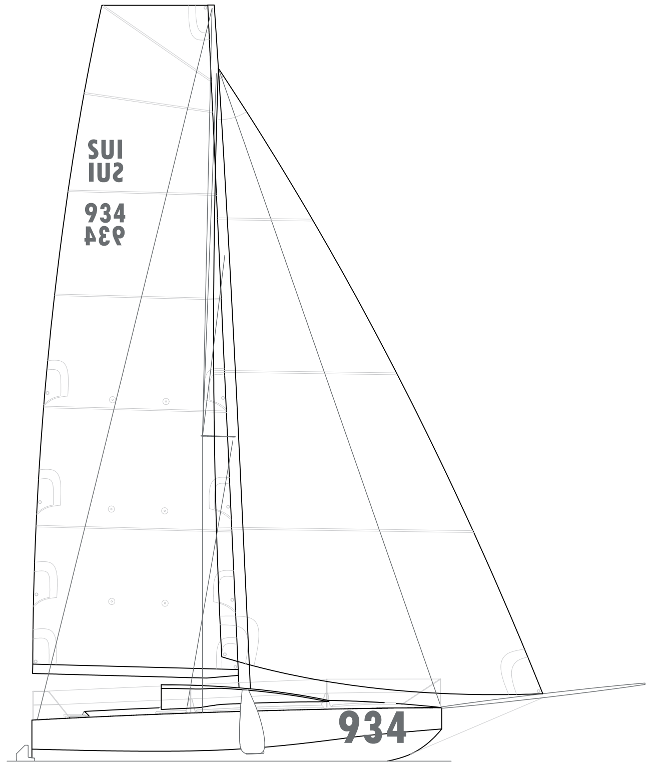

MAIN 1 REEF, JIB 1 REEF

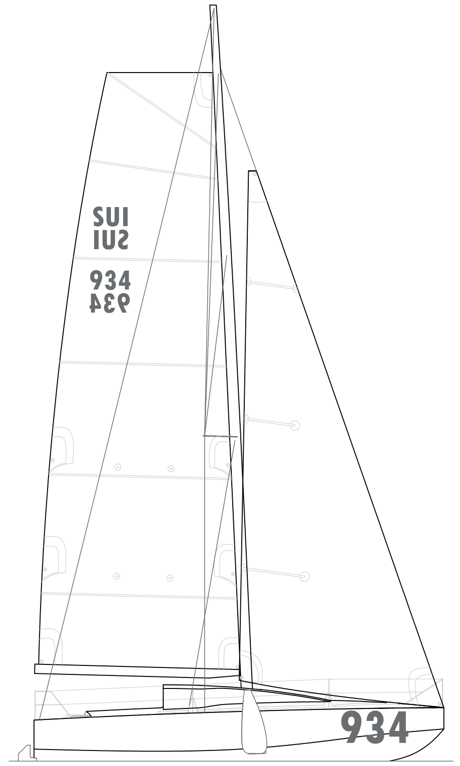

MINI N°934 SAIL WARDROBE			
SAIL	AREA (m^2)	MATERIALS	WIND RANGE (knots)
MAIN	29	POLYESTER 7.5 Oz	0-35
JIB	19.3-13.8	POLYESTER 4.6 Oz	0-25
STROM JIB	4-2.5	POLYESTER 9.8 Oz	25+
GENNAKER	30	POLYESTER 1.5 Oz	0-12
A2	90	POLYESTER .75 Oz	0-16
A4	75	POLYESTER .9 Oz	16-25
CODE 5	55-45	POLYESTER 1.5 Oz	25+

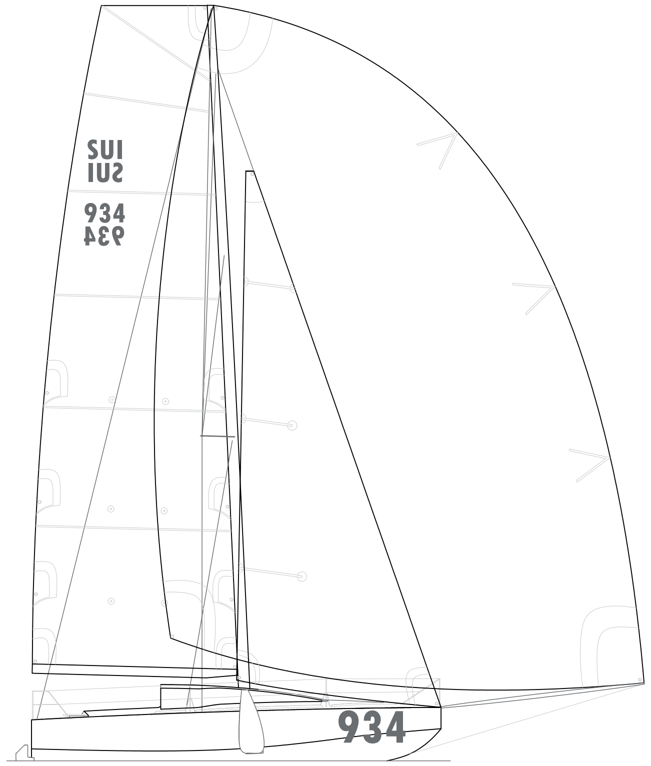

FULL MAIN, JIB 1 REEF, A2

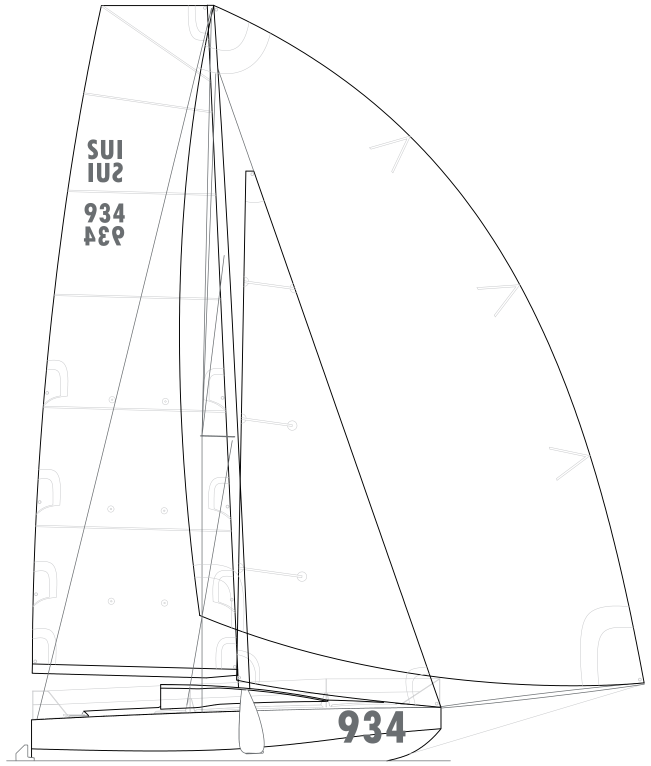

FULL MAIN, JIB 1 REEF, A4

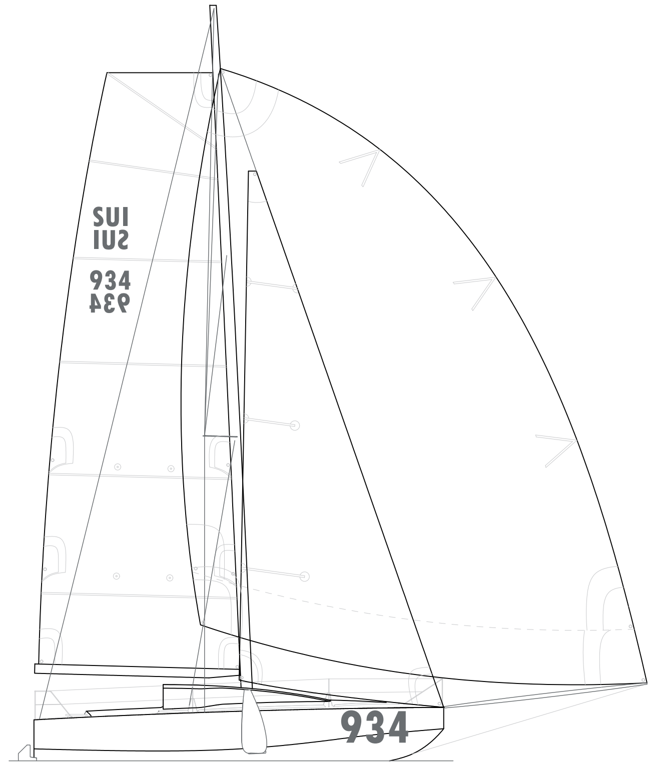

MAIN 1 REEF, JIB 1 REEF, CODE 5

MAIN 2 REEF, JIB 1 REEF, CODE 5 1 REEF

NOTES:

1. STORM JIB NOT SHOWN.
2. PRELIMINARY SAIL WARDROBE, SUBJECT TO CHANGES.

Project: Mini 6.50 N°934 Preliminary Design		
Drawing Title: Sail Wardrobe		Drawn by: Marin Lauber
Issue date: 27.04.2017	Units: mm	Scale: 1:50 @ A3

CENTERLINE STIFFENERS

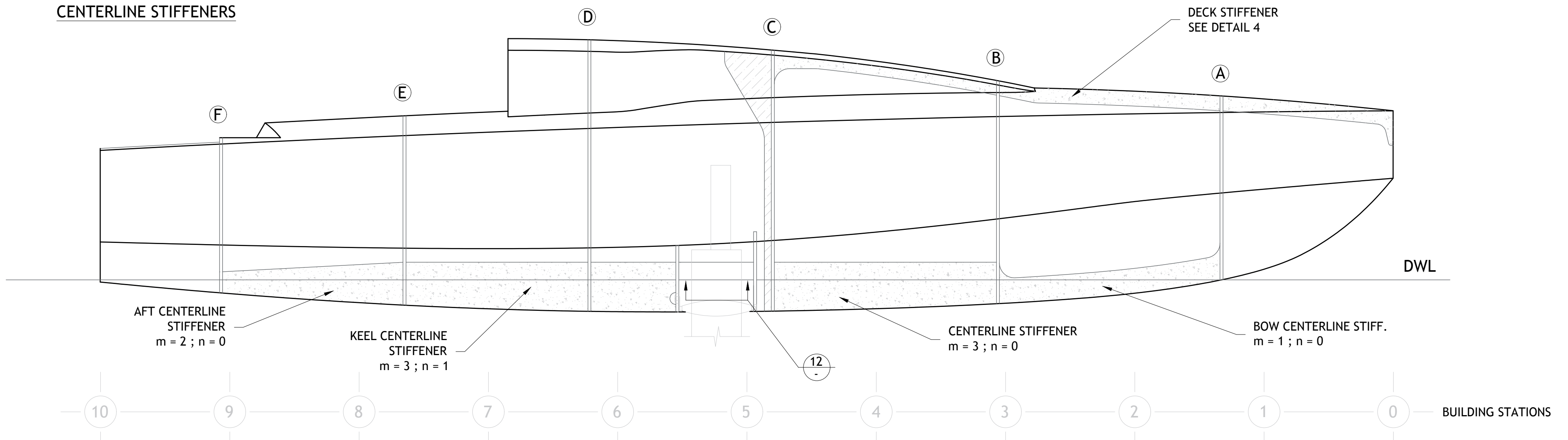

SIDE STIFFENERS

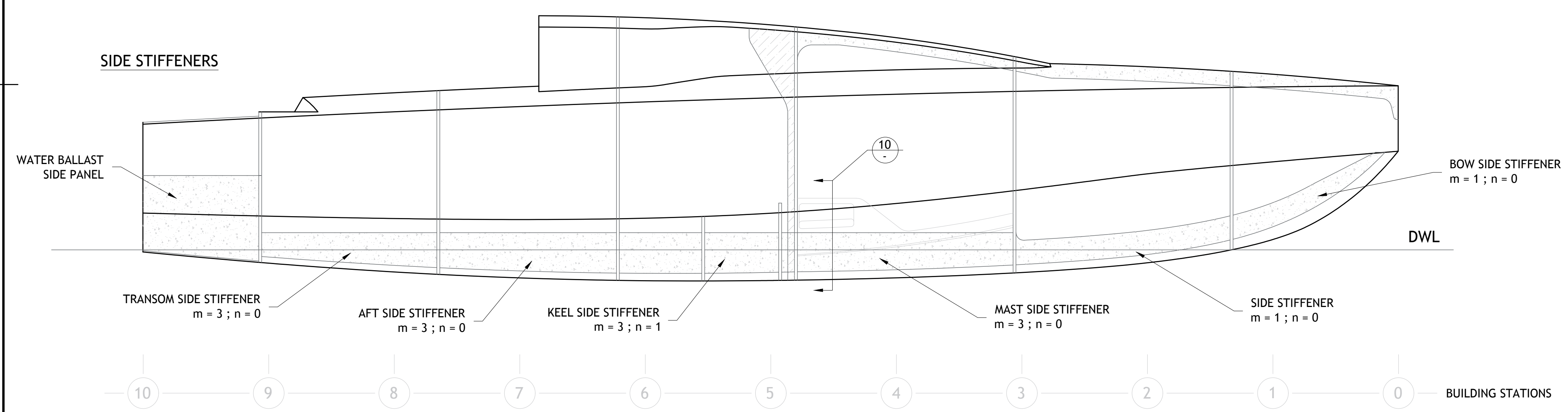

STRUCTURAL ARRANGEMENT AND
LOCAL REINFORCEMENTS

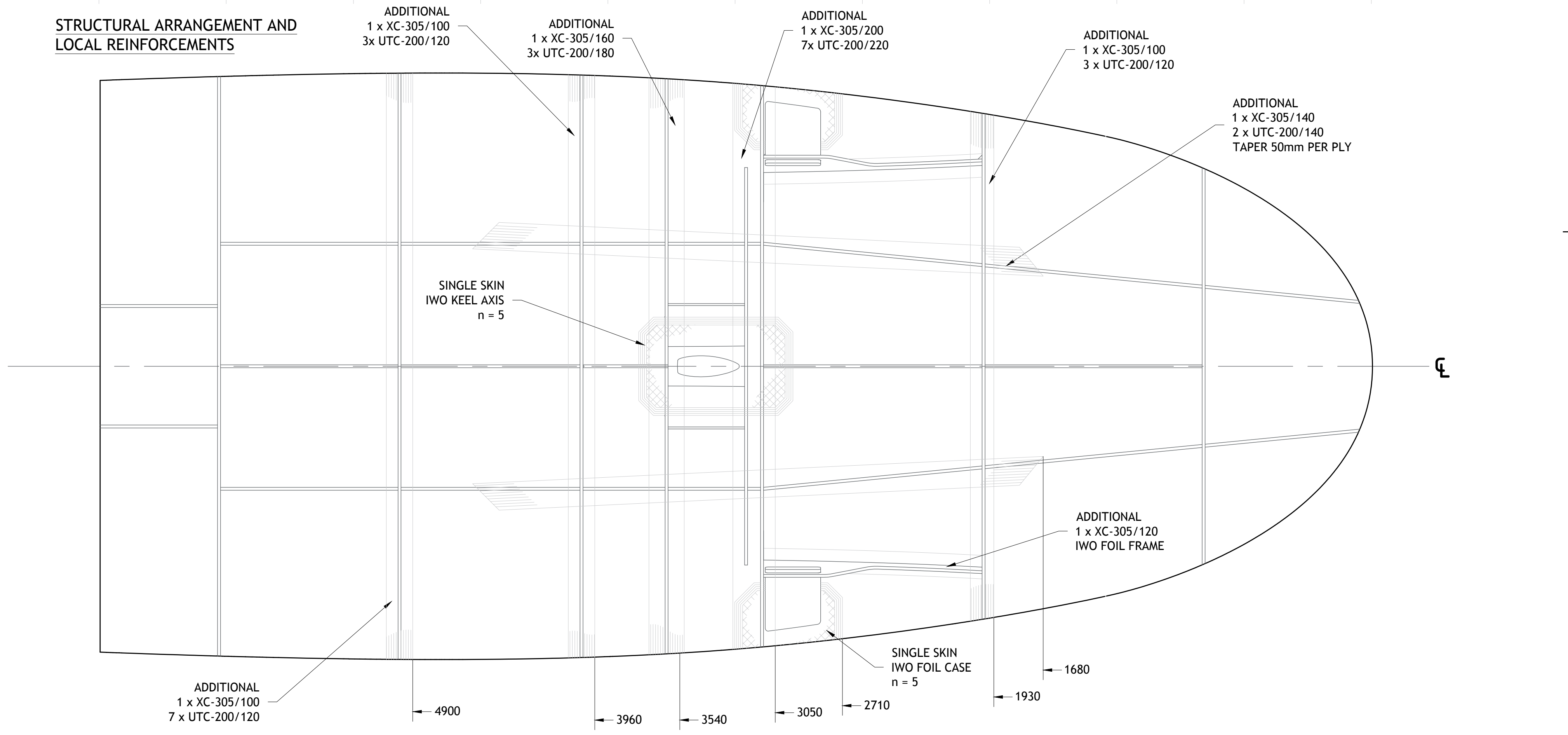

HULL/DECK/COACHROOF LAMINATE **TOTAL S.A.= 43.5 m^2**

MALE MOULDING VACUUM CONSOLIDATED HAND LAMINATION

DESCRIPTION	PLY No.	MATERIAL	FIBRE ANGLE	COVERAGE	EDGE OVERLAP (mm)	CL OVERLAP (TOTAL) (mm)	MATERIAL WIDTH (mm)	THICKNESS/ PLY (mm)	CURED WEIGHT/ PLY (kg/m^2)	SUFACE AREA (m^2)	CURED PLY AREA (m^2)	WEIGHT (kg)	
INNER SKIN	1	RC-200T/1000	±45	TOTAL	50	50	1000	0.271	0.408	39.8	39.8	16.2	
(AGAINST MOULD)	2	UTC-200/500	0	BOTTOM ONLY	0	0	500	0.237	0.351	39.8	39.8	14.0	30
CORE BONDING SYSTEM		SPABOND 345		TOTAL	-	-	-	0.2	1.146	30	30	34.38	
CORE		SAN FOAM 85 kg/m^3 15mm	-	FWD STN. 6	-	-	-	15	1.275	9.8	9.8	12.5	
		SAN FOAM 65 kg/m^3 15mm	-	AFT STN. 6/TOPSIDE/DECK	-	-	-	15	0.975	19.7	19.7	19.2	
		SAN FOAM 65 kg/m^3 10mm	-	COACHROOF	-	-	-	10	0.65	3.6	3.6	2.3	
CORE BONDING SYSTEM		SPABOND 345		TOTAL	-	-	-	0.2	1.146	30	30	34.38	103
OUTER SKIN	3	UTC-200/500	0	TOTAL	0	0	500	0.237	0.351	17.8	17.8	6.2	
(UPPERMOST)	4	RC-200T/1000	±45	TOTAL	50	50	1000	0.271	0.408	40.5	40.5	16.5	23
					BASIC 15mm CORE PANEL THICKNESS			16.016		**TOTAL WEIGHT**		156	
										Av. Panel Weight		3.58	

NOTES:

1. PRELIMINARY STRUCTURAL DESIGN IN ACCORDANCE WITH ISO 12215-5.
2. REFER TO STRUCTURAL DETAIL DRAWING FOR TYPICAL STIFFENER DETAIL.
3. MINOR LOCAL REINFORCEMENT OMITTED FOR CLARITY.

Project:	**Mini 6.50 N°934 Preliminary Design**	
Drawing Title: Structural Arrangement		Drawn by: Marin Lauber
Issue date: 27.04.2017	Units: mm	Scale: 1:30 @ A3

DECK AND BOTTOM
CENTERLINE VIEW

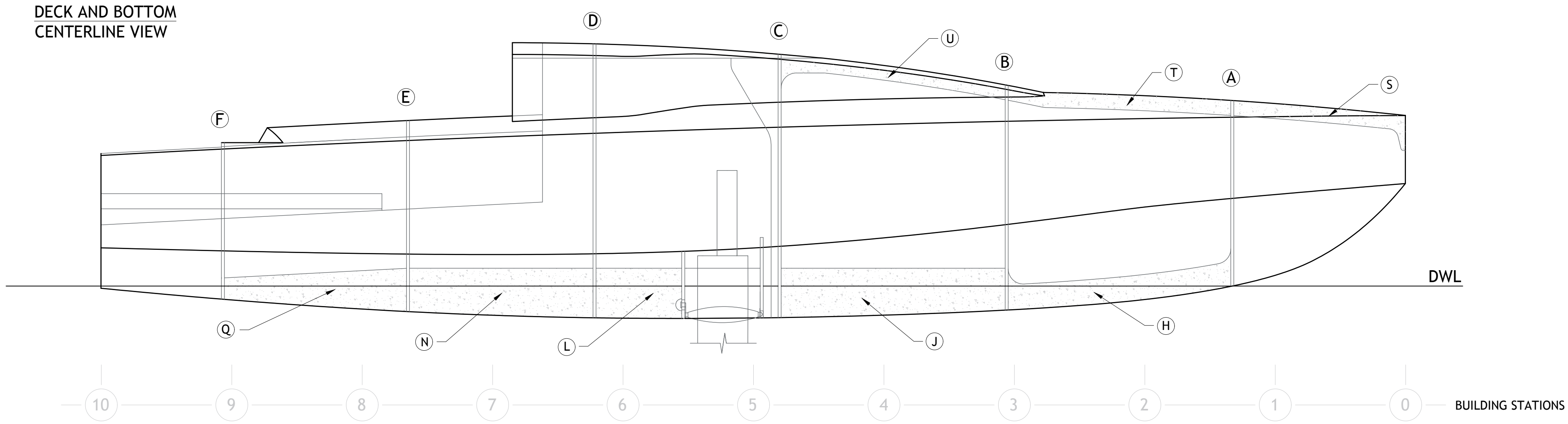

SECTION AT STIFFENERS

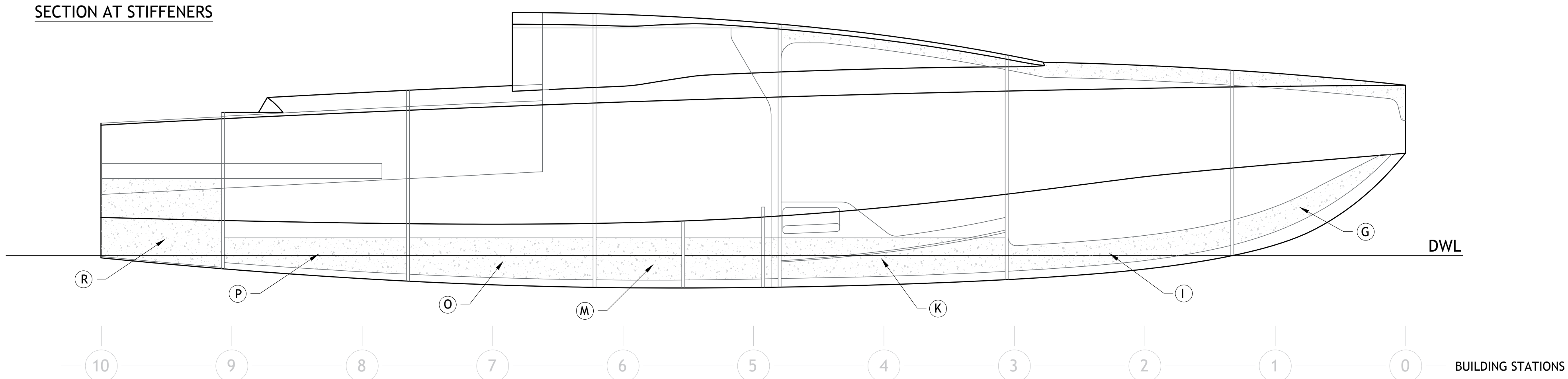

CORE TRANSITION AND PANELS

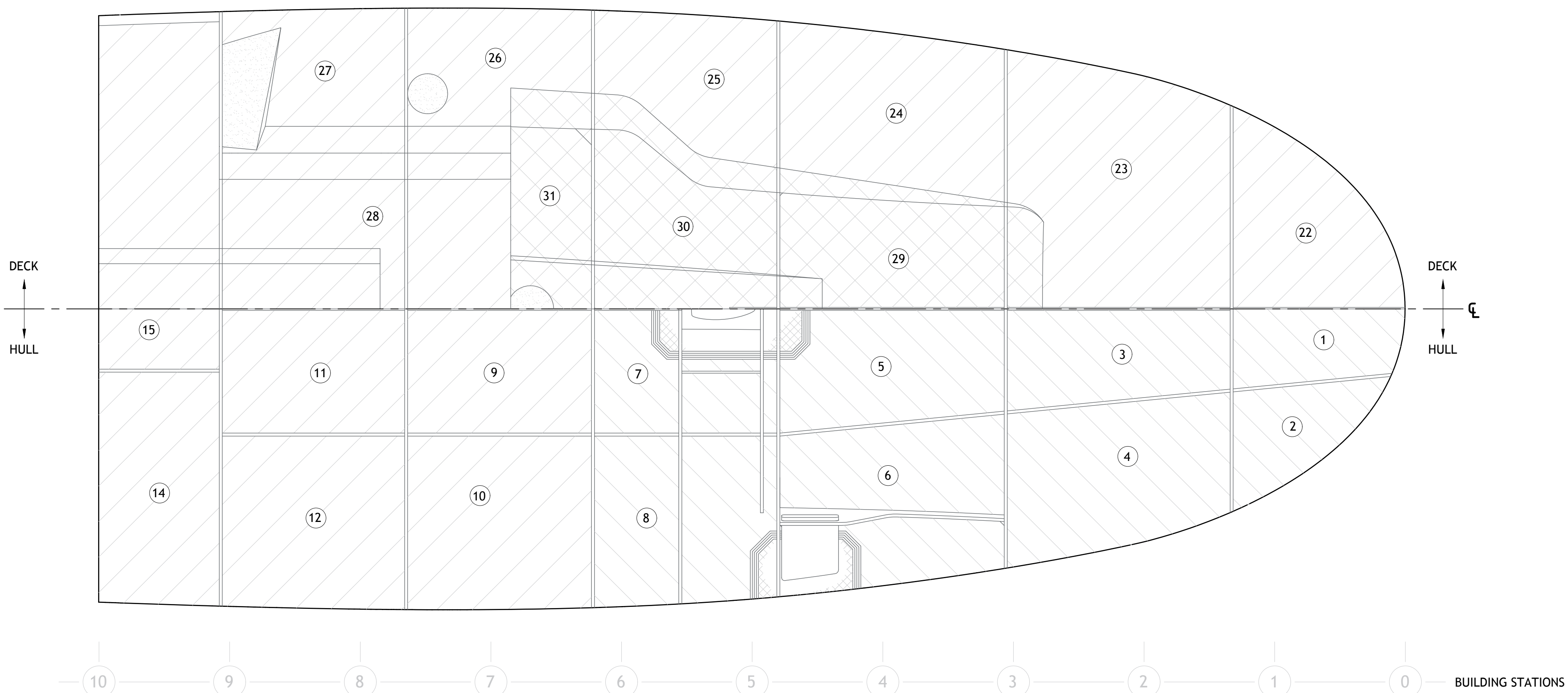

CORE TRANSITION AND PANELS

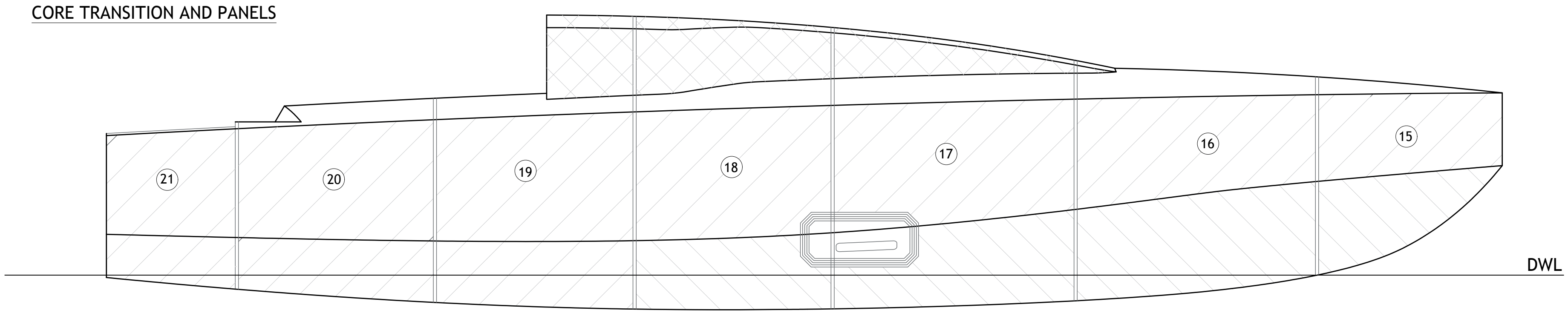

CORE KEY:

- 85 kg/m³ CORCELL M: 15mm
- 65 kg/m³ CORCELL M: 15mm
- 65 kg/m³ CORCELL M: 10mm
- HIGH DENSITY CORE INSERT

NOTES:

1. PRELIMINARY STRUCTURAL DESIGN IN ACCORDANCE WITH ISO 12215-5.
2. LETTERS REFER TO STIFFENERS, NUMBERS REFER TO PANELS OF ISO 12215-5 SCANTLING RESULTS.
3. MINOR LOCAL REINFORCEMENT OMITTED FOR CLARITY.

Project: Mini 6.50 N°934 Preliminary Design		
Drawing Title: Panels and Core Layout		Drawn by: Marin Lauber
Issue date: 27.04.2017	Units: mm	Scale: 1:30 @ A3

LOCAL FIBRE DIRECTION

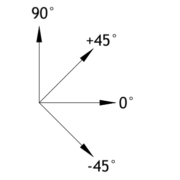

BULKHEAD A:

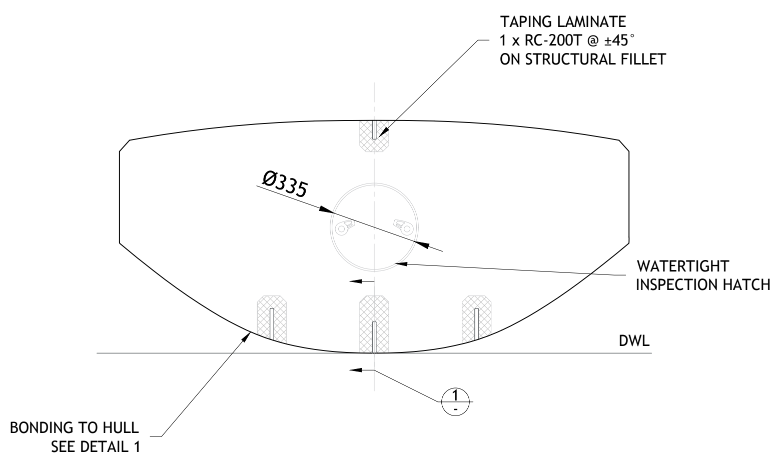

FRAME B:

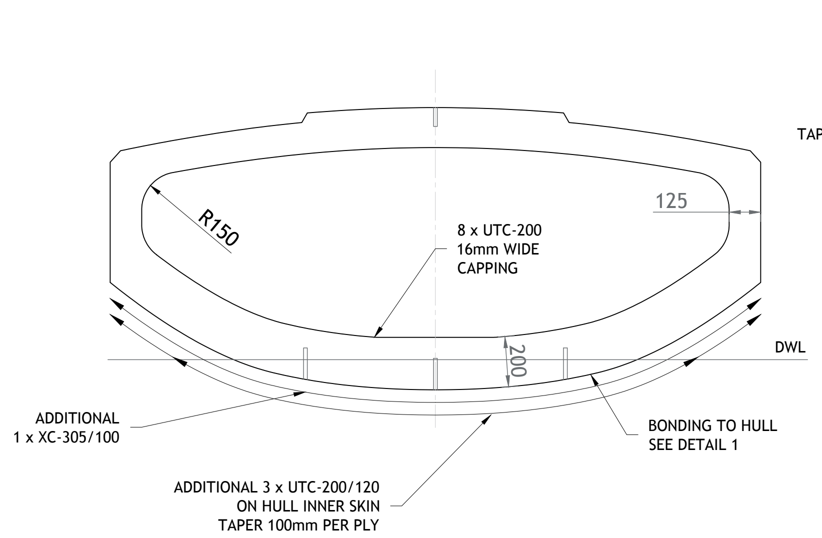

FRAME C:

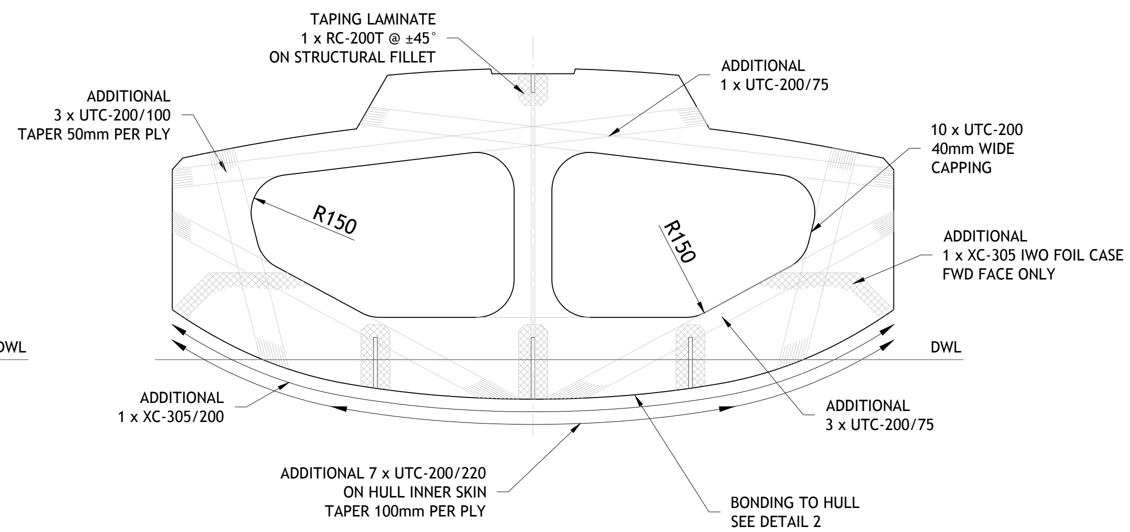

FRAME D:

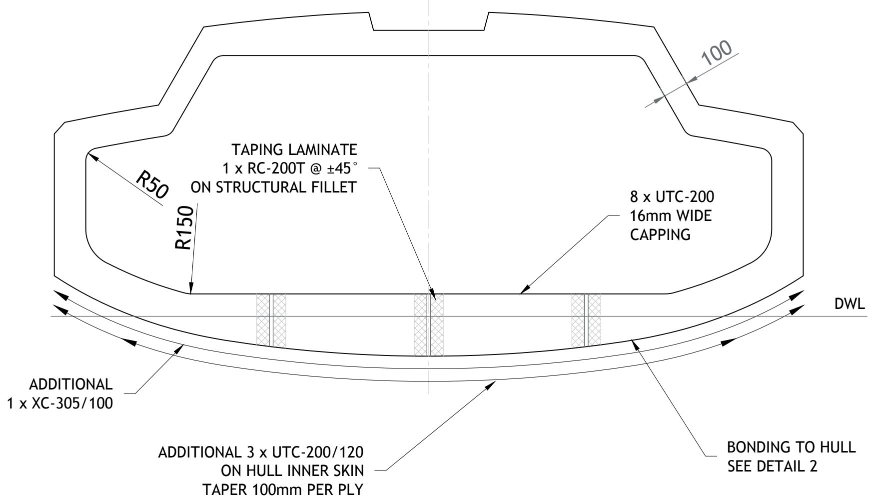

FRAME E:

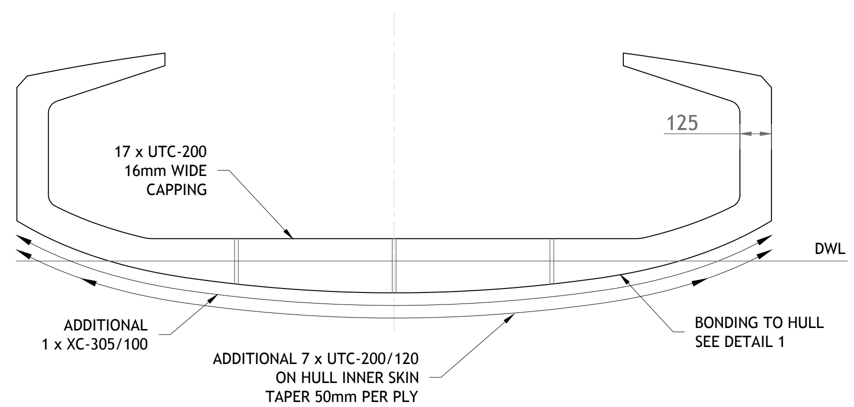

FRAME F:

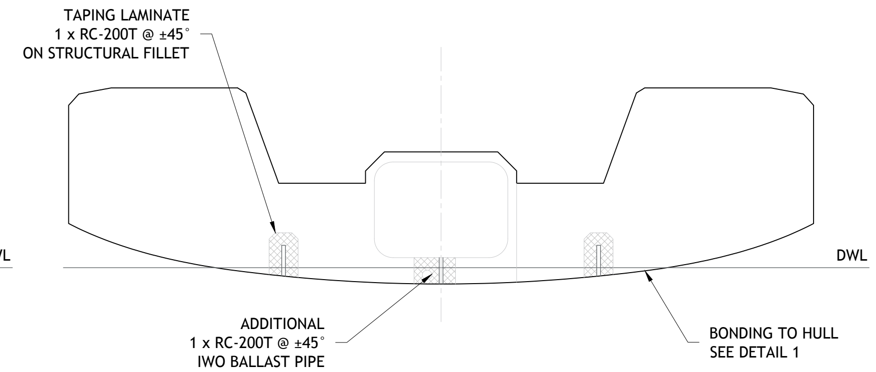

AFT KEEL FLOOR:

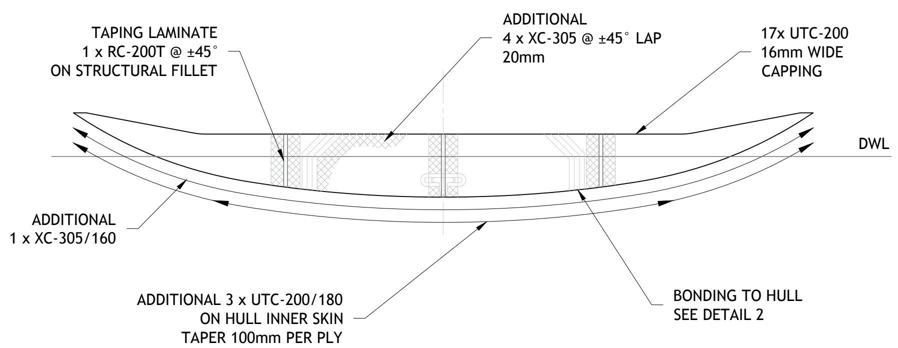

FORWARD KEEL FLOOR:

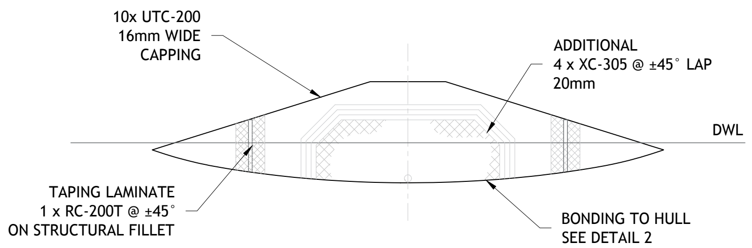

FRAME BASIC LAMINATE			
LAYER	WEIGHT (g/m^2)	ORIENTATION	THICKNESS (mm)
XC-305	305	±45°	0.414
65 kg/m^3 SAN FOAM	975	-	15
XC-305	305	±45°	0.414
TOTAL CURED	2.171	-	15.828

NOTES:

1. PRELIMINARY STRUCTURAL DESIGN IN ACCORDANCE WITH ISO 12215-5.
2. STRUCTURAL JOIN TO BE R10mm SPABOND 345 STRUCTURAL FILLET UNLESS OTHERWISE STATED.
3. ALL TAPES ON BOTH FACES UNLESS OTHERWISE STATED.

Project:	**Mini 6.50 N°934 Preliminary Design**
Drawing Title: Bulkheads and Frames	Drawn by: Marin Lauber
Issue date: 27.04.2017	Units: mm
Scale: 1:30 @ A3	

1 GIRDER TO FRAME JOINT
SCALE 1:2

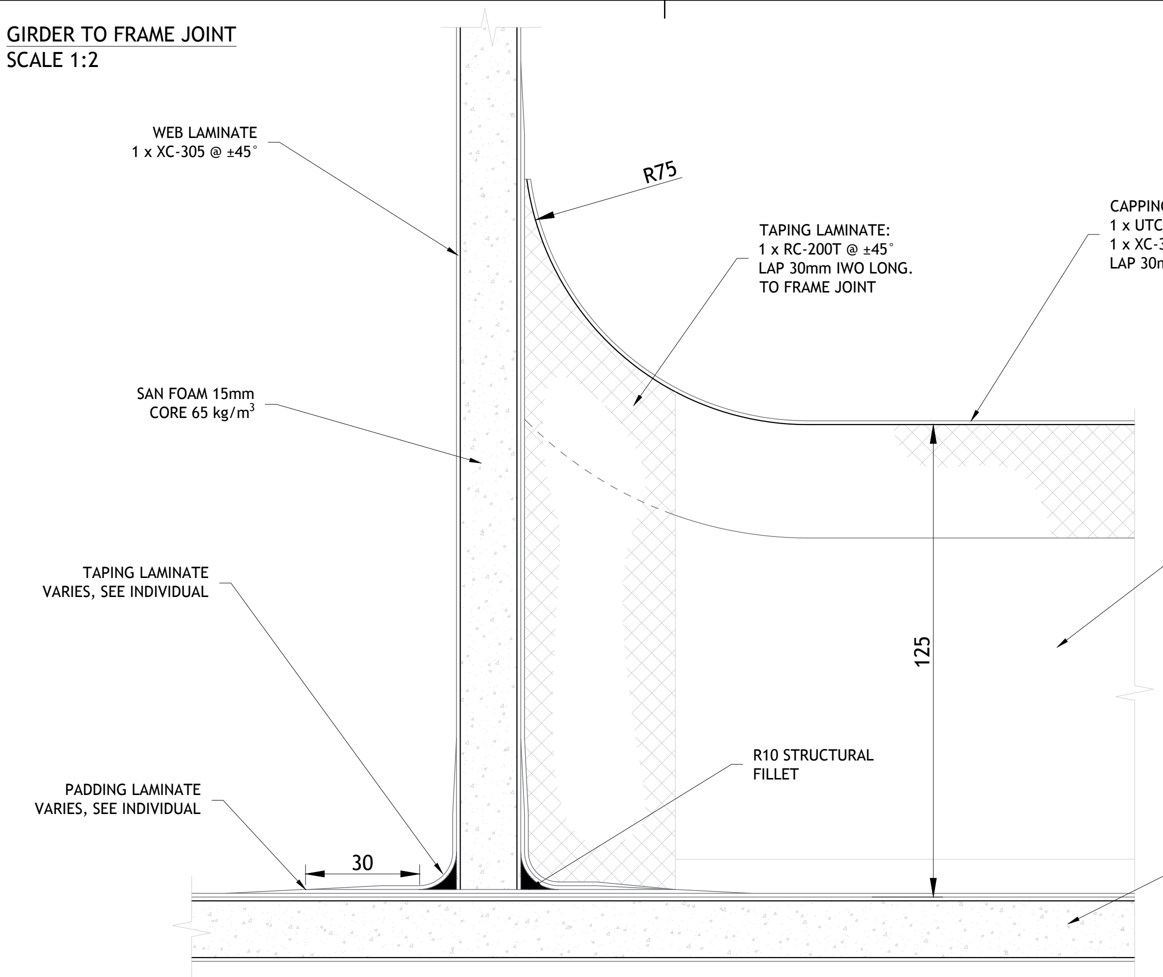

2 TYPE 1 STRUCTURAL FILLET
SCALE 1:2

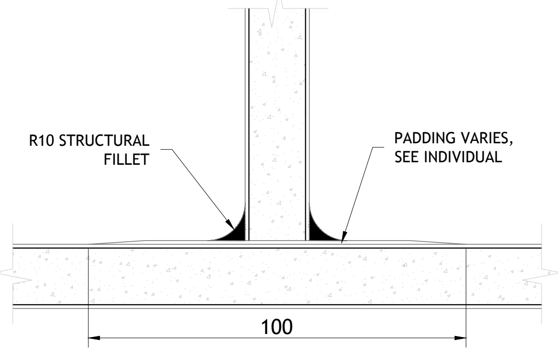

3 TYPE 2 STRUCTURAL FILLET
SCALE 1:2

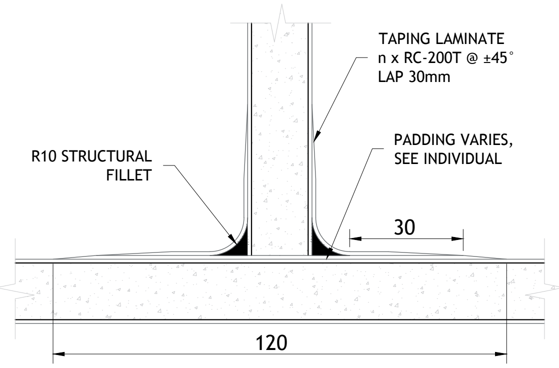

4 DECK STIFFENER
SCALE 1:2

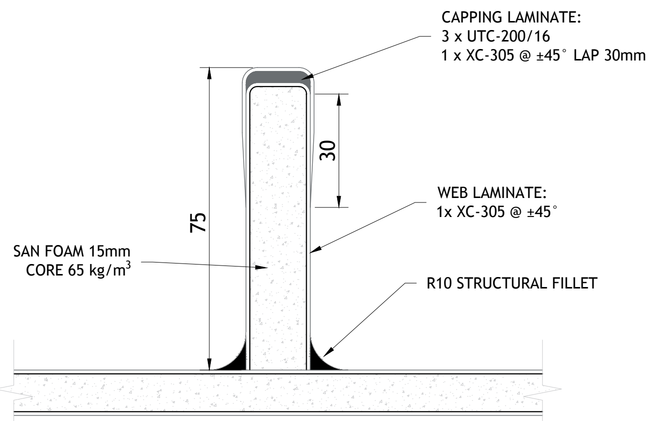

5 SINGLE SKIN TRANSITION
SCALE 1:2

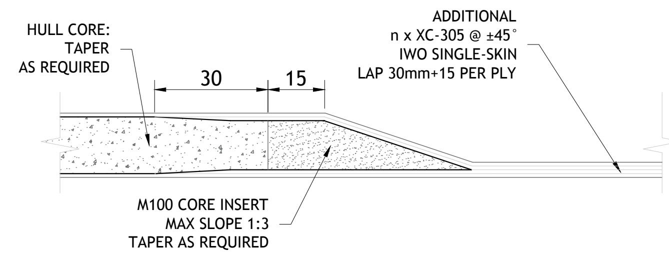

6 MAST BULKHEAD
SCALE 1:4

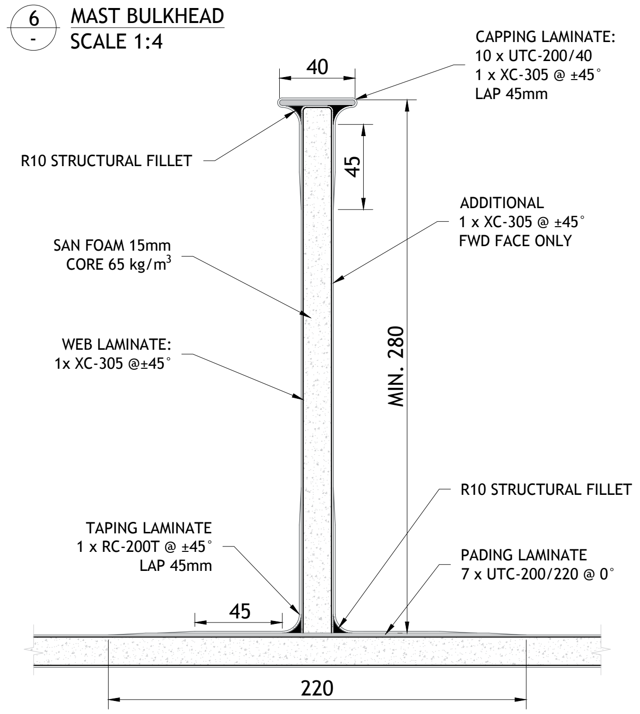

7 AFT KEEL FLOOR
SCALE 1:4

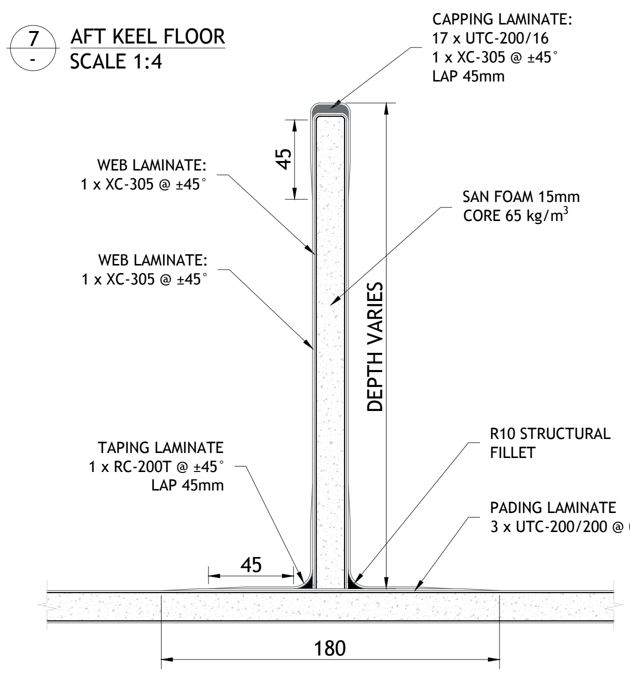

8 TYPICAL STIFFENER
SCALE 1:4

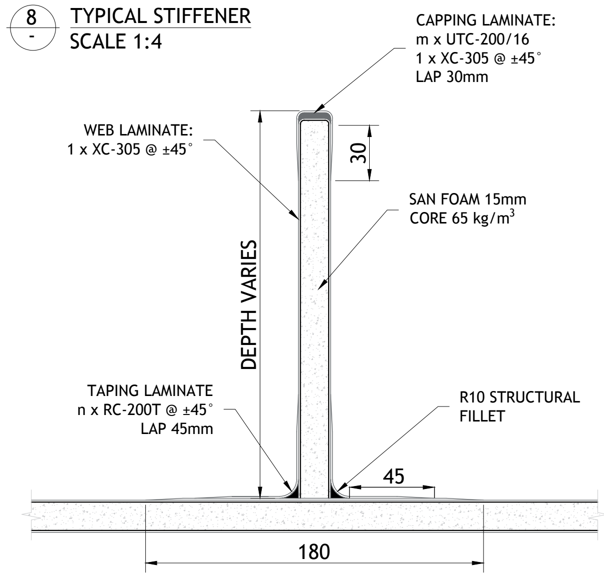

NOTES:

1. PRELIMINARY STRUCTURAL DESIGN IN ACCORDANCE WITH ISO 12215-5.
2. STRUCTURAL ADHESIVE TO BE SPECIFIED BY BUILDER.

Project: Mini 6.50 N°934 Preliminary Design		
Drawing Title: Structural Details		Drawn by: Marin Lauber
Issue date: 27.04.2017	Units: mm	Scale: varies, see individual

9 FOIL SECTION LAMINATE
SCALE 1:1
EPPLER 214 12.5%

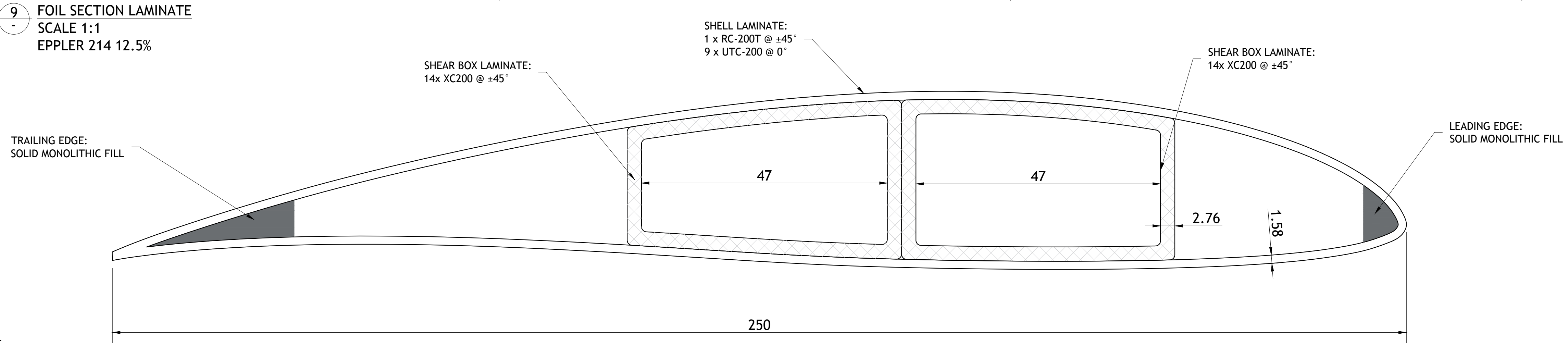

LAMINATE PROPERTIES			
PART	E_X (GPa)	E_Y (GPa)	THICKNESS (mm)
SHELL	92.4	6.6	1.58
SHEAR BOX	11.7	11.7	2.76

FOIL PROPERIES		
I_{XX}	230.2E+3	mm^4
I_{YY}	5.0E+6	mm^4
EI_{XX}	20.2	$GNmm^2$
EI_{YY}	398.8	$GNmm^2$
AREA	1619.9	mm^2

10 FOIL BOX LAMINATE
SCALE 1:4

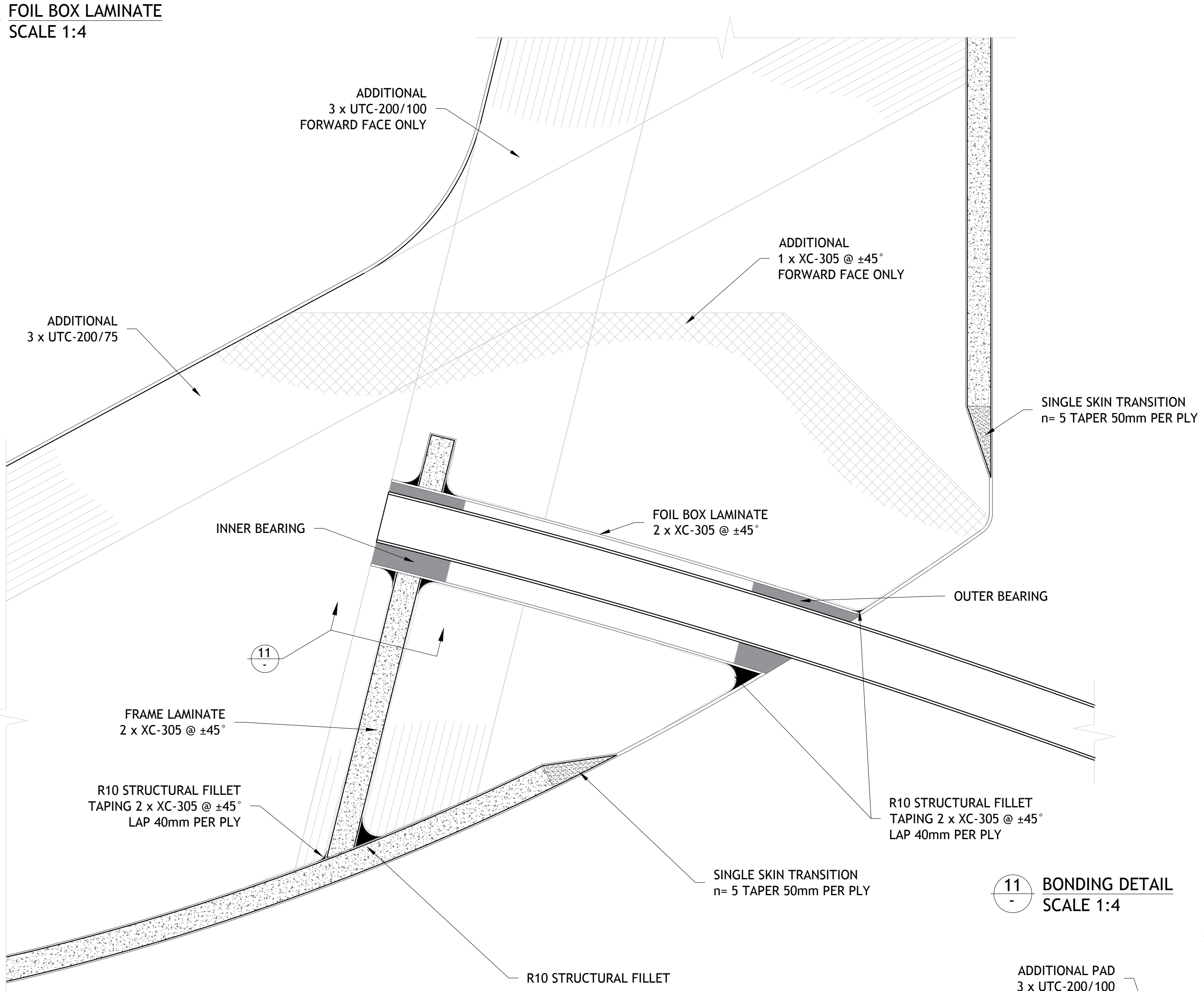

12 KEEL BEARING DETAILS
SCALE 1:3

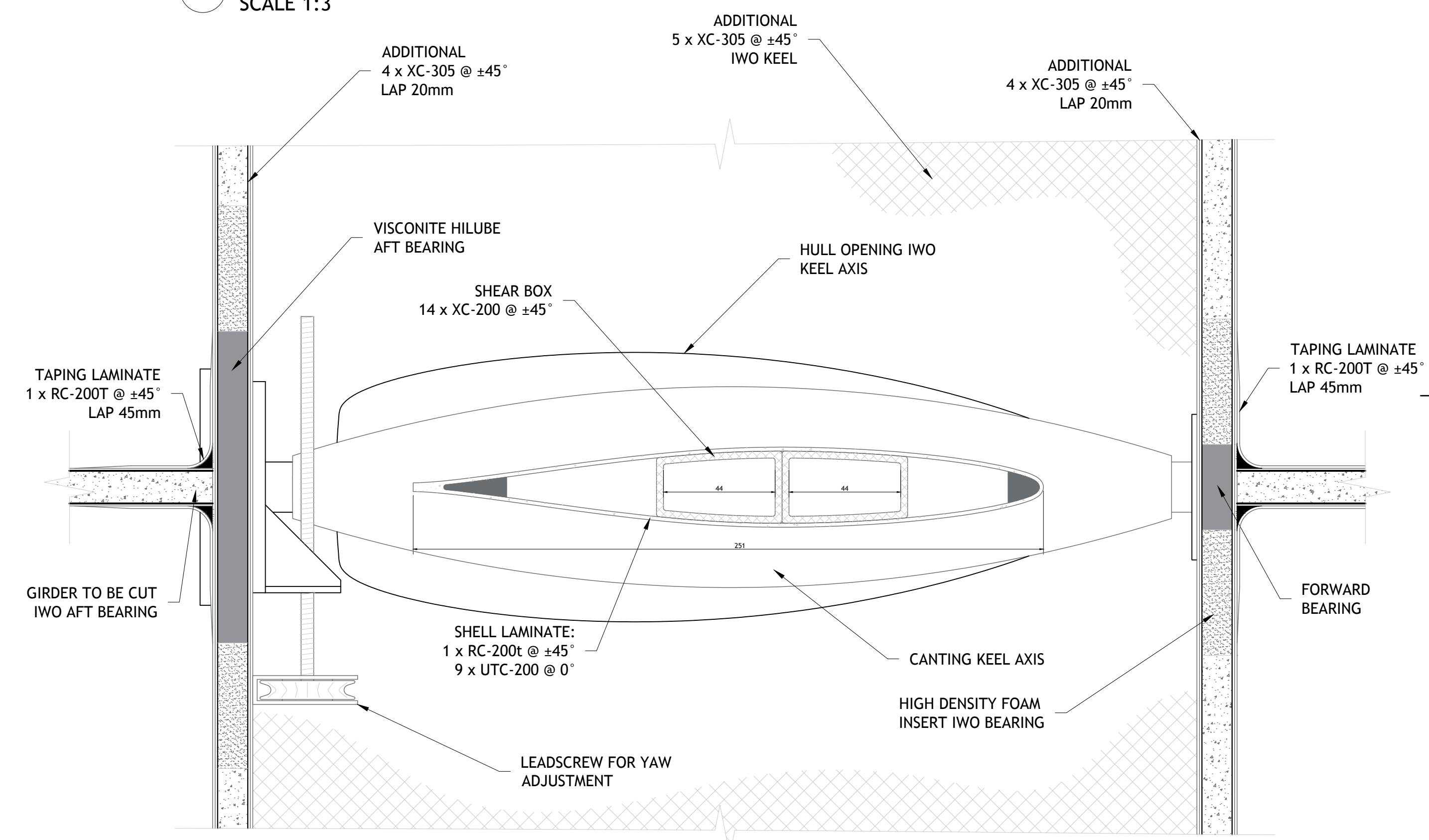

11 BONDING DETAIL
SCALE 1:4

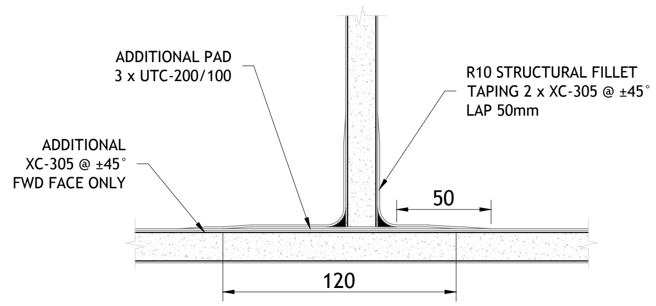

NOTES:

1. PRELIMINARY STRUCTURAL DESIGN IN ACCORDANCE WITH ISO 12215-5.
2. WATERTAIGHTNESS OF KEEL TO BE ACHIEVED WITH AN ADDITIONAL PLATE BETWEEN KEEL AXIS AND SKIN.
3. OUTER BEARING TO BE MOUNTED FROM OUTSIDE.

Project: Mini 6.50 N°934 Preliminary Design		
Drawing Title: Foil Structure		Drawn by: Marin Lauber
Issue date: 27.04.2017	Units: mm	Scale: Varies, See Individual

SYSTEMS INSTALLATION SCHEMATIC
SCALE N-A

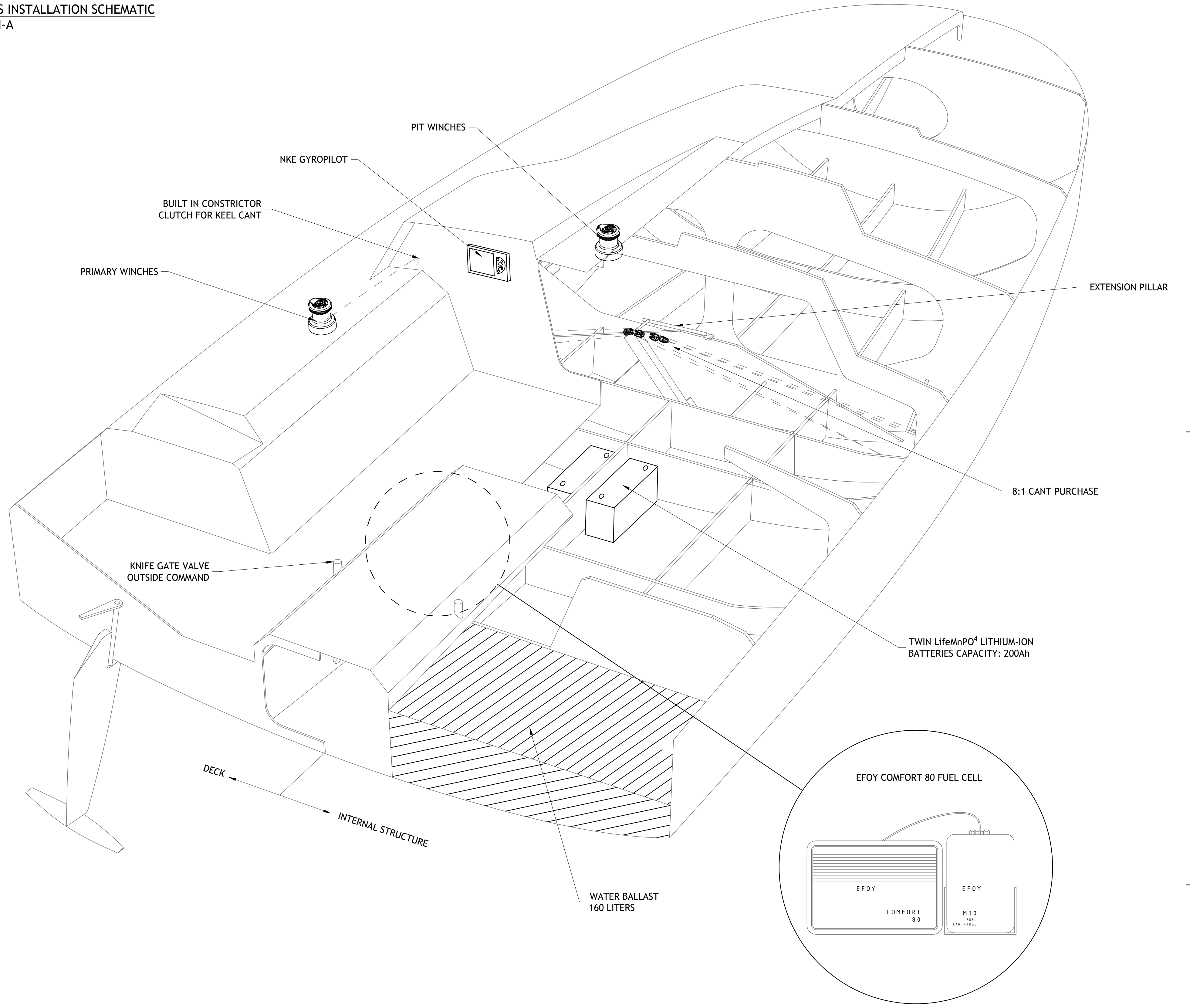

ELECTRONIC INSTALLATION SCHEMATIC
SCALE N-A

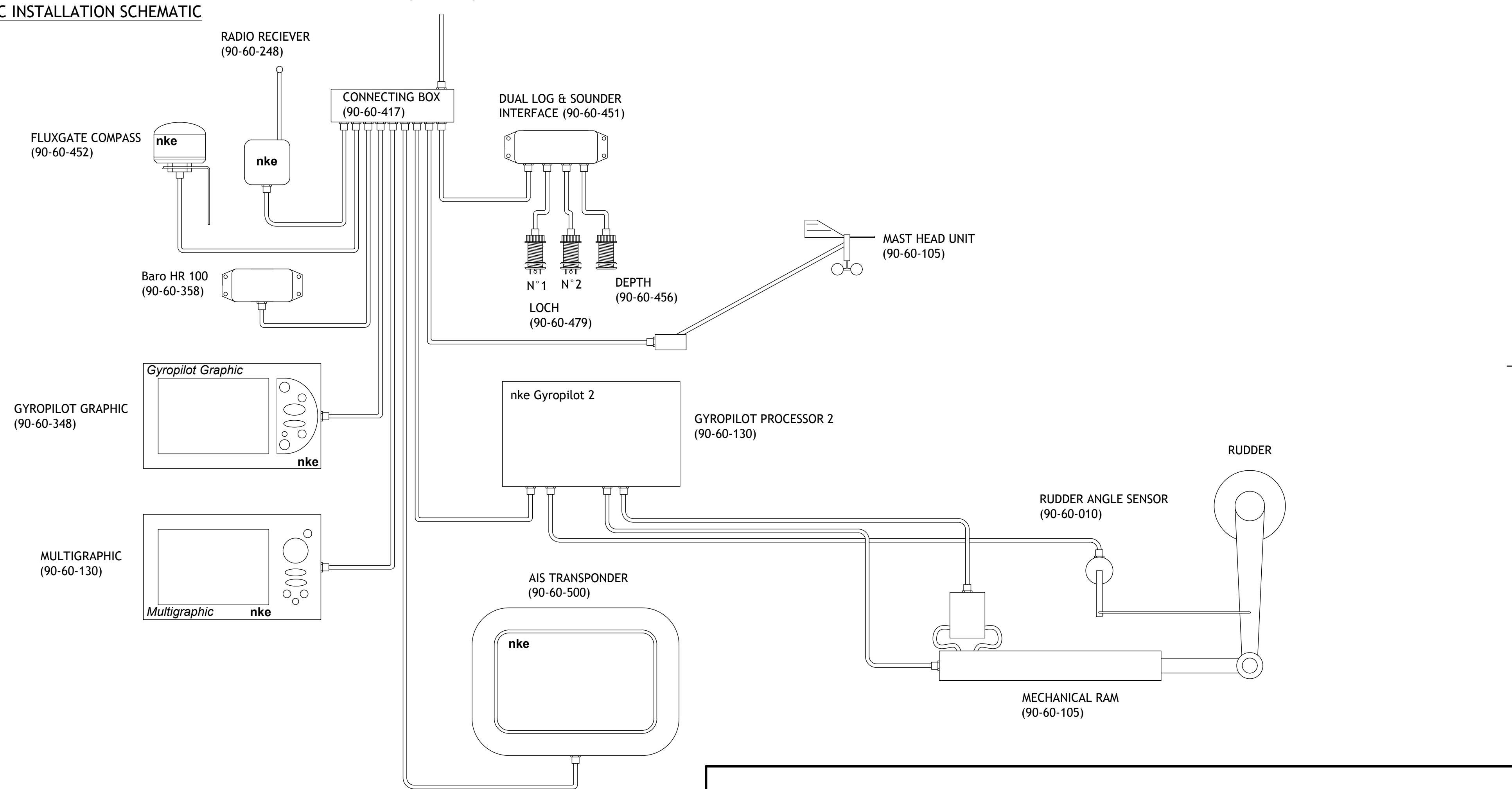

Project:	**Mini 6.50 N°934 Preliminary Design**

Drawing Title: System Arrangement		Drawn by: Marin Lauber
Issue date: 27.04.2017	Units: mm	Scale: N-A

NOTES:

1. ALL NKE CONNECTION: NMEA 2000.
2. PRELIMINARY ELECTRONIC SYSTEM ARRANGEMENT, NO FOR INSTALLATION.

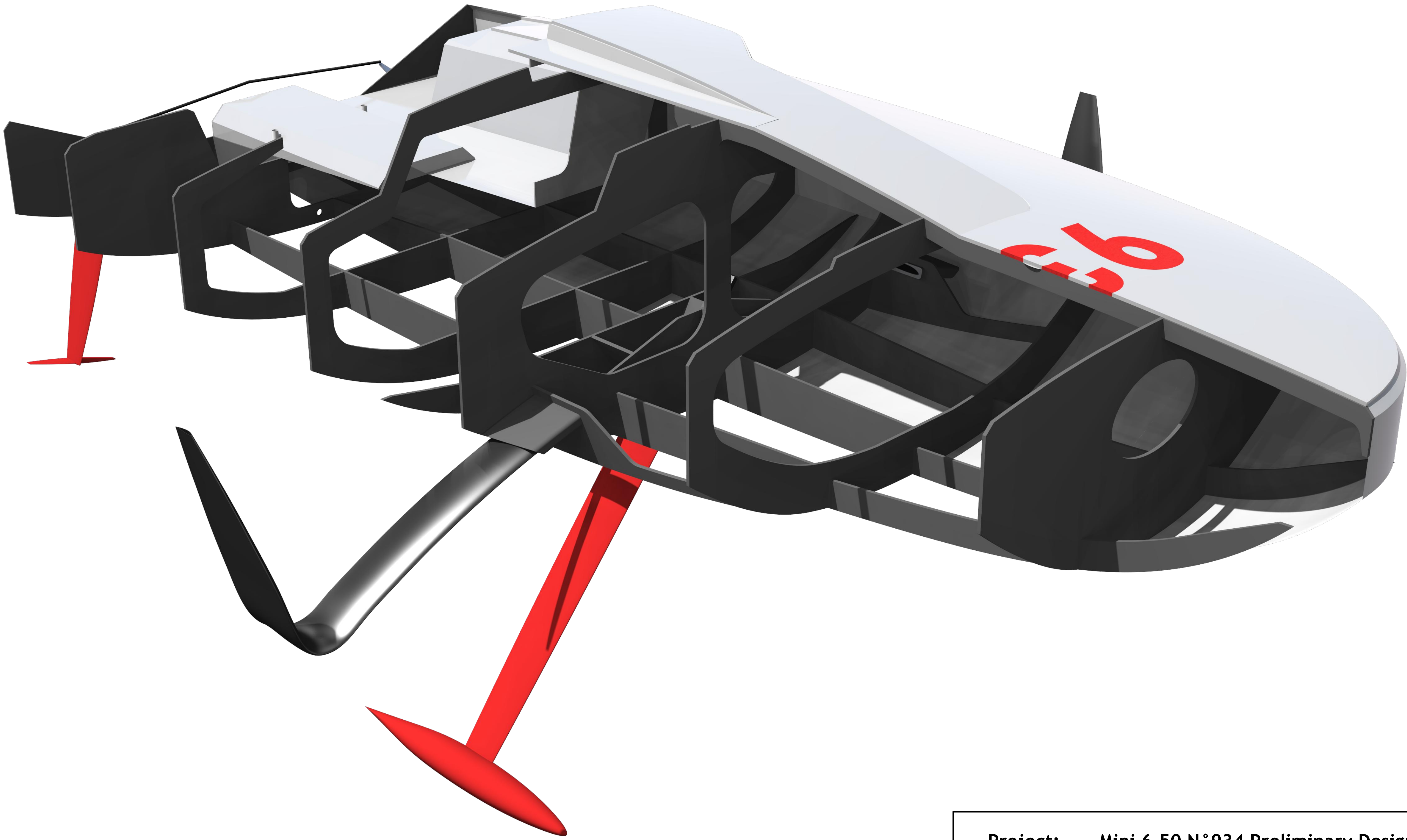

Project: Mini 6.50 N°934 Preliminary Design		
Drawing Title: Structural Render		Drawn by: Marin Lauber
Issue date: 27.04.2017	Units: mm	Scale: n-a

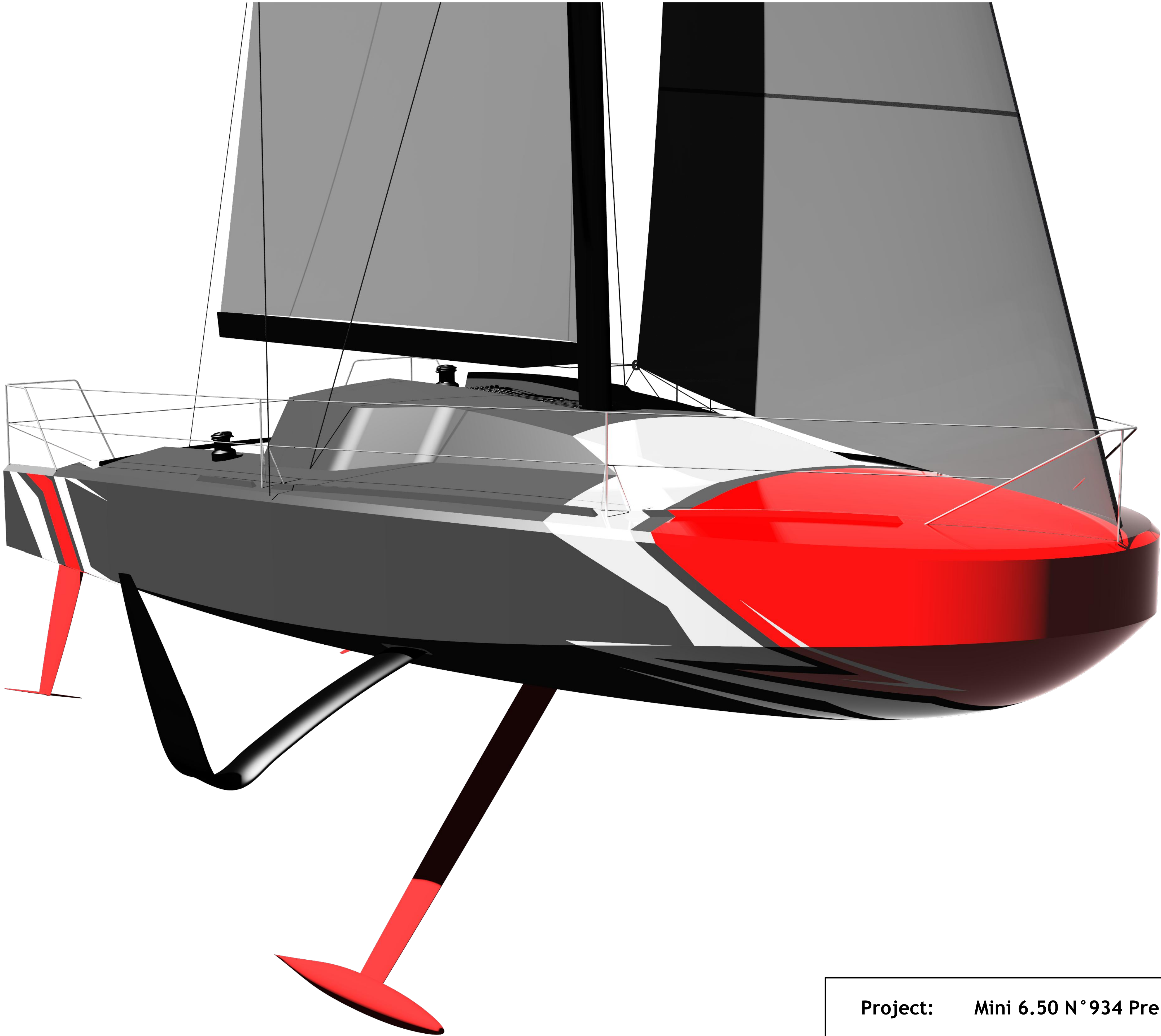

Project:	**Mini 6.50 N°934 Preliminary Design**

Drawing Title: Profile Render		Drawn by: Marin Lauber
Issue date: 27.04.2017	Units: mm	Scale: n-a